1985

Stochastic modeling of water movement in the saturated-unsaturated zone

Sang-Ok Chung
Iowa State University

Chung, Sang-Oh

STOCHASTIC MODELING OF WATER MOVEMENT IN THE SATURATED-UNSATURATED ZONE

Iowa State University PH.D. 1985

Stochastic modeling of water movement in the saturated-unsaturated zone

by

Sang-Ok Chung

A Dissertation Submitted to the
Graduate Faculty in Partial Fulfillment of the
Requirements for the Degree of
DOCTOR OF PHILOSOPHY

Department: Civil Engineering
Major: Water Resources

Approved:

Signature was redacted for privacy.

In Charge of Major Work

Signature was redacted for privacy.

For the Major Department

Signature was redacted for privacy.

For the Graduate College

Iowa State University
Ames, Iowa

1985

TABLE OF CONTENTS

LIST OF TABLES

LIST OF FIGURES

NOMENCLATURE

A	a soil parameter in the modified Holtan's infiltration equation
a	a nonlinear regression parameter in the Van Genuchten's retention equation
C	generalized specific water capacity
CLAI	crop leaf area index
F	accumulated infiltration
f	average infiltration capacity during a time period in the modified Holtan's infiltration equation
f_c	wet soil infiltration capacity in the modified Holtan's infiltration equation
g	gravitational acceleration
h	soil water pressure (suction) head
h_a	soil water pressure head at the air entry
K	hydraulic conductivity
K_s	saturated hydraulic conductivity
K_r	relative hydraulic conductivity
k	intrinsic permeability
m	1 - 1/N in the Van Genuchten's retention equation
N	a nonlinear regression parameter in the Van Genuchten's retention equation
n	porosity
P	a soil parameter in the modified Holtan's infiltration equation
P_ℓ	fluid pressure

P_c	water pressure just beneath air-water interface
pF	base 10 logarithm of absolute value of pressure (suction) head
q	flow rate across a unit cross section
R	a parameter defined by a constant divided by pressure head in hysteresis model
R_{no}	net solar radiation above the crop canopy
R_{ns}	net solar radiation at the soil surface
r	radius of pore opening
$\bar{r}$	normalized radius of pore opening
r_h	harmonic mean radius of curvature of the air-water interface
S	soil water storage potential above any impeding strata in the modified Holtan's infiltration equation
S(z,t)	source or sink term in the flow equation
$S_e(h)$	effective saturation as a function of pressure head
S_s	specific storage of an aquifer
S_w	degree of saturation
T	total pore volume above any impeding strata in the modified Holtan's infiltration equation
t	time
V	flow velocity of a fluid
v	total plant root zone depth
W(z)	plant root extraction rate
Y	base 10 logarithm of hydraulic conductivity
z	gravitational head

α	autoregressive parameter in the nearest neighbor model
β	coefficient in the governing flow equation
γ	specific gravity of liquid water
Δt	size of time step
Δz	size of space step in the z-direction
ε_i	normally distributed random numbers
η	a factor multiplied to ε_i to yield σ_y
$\Theta(h)$	effective water content at pressure head h
$\Theta_w(h)$	effective water content at pressure head h on the main wetting curve
$\Theta_d(h)$	effective water content at pressure head h on the main drying curve
$\Theta_w(h_1)$	effective water content at the wetting reversal point h_1 on the main wetting curve
$\Theta_d(h_1)$	effective water content at the wetting reversal point h_1 on the main drying curve
$\Theta(h_1)$	effective water content at the wetting reversal point h_1
Θ_u	effective water content at saturation
$\theta(h)$	water content at pressure head h
$\theta_w(h)$	water content at pressure head h on the main wetting curve
$\theta_d(h)$	water content at pressure head h on the main drying curve
$\theta_w(h_1)$	water content at the wetting reversal point h_1 on the main wetting curve
θ_r	residual water content
θ_s	saturation water content

θ_u	ultimate (saturation) water content
λ	fitted parameter in Brook and Corey's retention equation
μ	viscosity of fluid
μ_y	mean of Y
ρ	radius of pores
$\tilde{\rho}$	normalized radius of pores
$\rho(1)$	lag one spatial autocorrelation coefficient
$\rho(2)$	lag two spatial autocorrelation coefficient
ρ_ℓ	density of fluid
σ	interfacial surface tension
σ_y	standard deviation of Y
Φ	total head
∇	gradient operator
∇^2	Laplacian operator

CHAPTER I. INTRODUCTION

Water resources is one of the most invaluable natural resources for the lives of mankind as well as other living things. Groundwater, which is one of the major water resources in the United States and also all around the world, represents about 22 percent of the total world's fresh water including glaciers and icecaps, and represents about 98 percent of the fresh water excluding glaciers and icecaps (Bouwer, 1978). Adequate management of groundwater is essential in order to keep the groundwater resources usable.

Water movement in the subsurface is probably the most complicated process in the hydrologic cycle. Much research on the saturated flow system has been conducted by hydrologists over past years, but only recently research on unsaturated flow has received significant interest. However, a combined saturated-unsaturated flow study is required to incorporate the nature of the flow system in both zones. Consequently, water movement in soils has been considered with increasing frequency as problems that combine both the saturated and unsaturated flow zones (Babu, 1980).

The understanding of water movement in soils is important in many practical problems. For example, in order

to determine irrigation requirements, wastewater land application rates, pumping rates, groundwater recharge rates, agricultural drainage requirements, and others, it is necessary to understand the flow mechanism in the soils both in the saturated and unsaturated zones.

Soils are very heterogeneous and have stochastic properties even though many previous studies were based on the assumptions such that soils are homogeneous and have deterministic properties. Spatial variability of soil water properties has been introduced in groundwater hydrology and soil physics since the 1960s and more intensively since the late 1970s. Several flow models have been developed treating hydraulic properties as stochastic variables rather than a deterministic function of space (e.g., Freeze, 1975; Dagan, 1979).

For groundwater management purposes, numerical modeling techniques have been extensively used since the 1970s. There are many existing mathematical models in groundwater management that treat both quantity and quality.

In the present study, a stochastic model of one-dimensional saturated-unsaturated flow was developed. In this model, the hysteresis in the soil water retention relationship and the stochastic properties of the hydraulic conductivity were considered. A first order nearest neighbor model was applied to handle the stochastic property

of the saturated hydraulic conductivity. Soil surface boundary condition was determined from the measured precipitation and pan evaporation. Modified Holtan's equation was used in determining infiltration rate. The groundwater flow problem was solved by a finite difference scheme using the Douglas-Jones predictor-corrector method.

Objectives

The overall objective of this research was to develop a stochastic mathematical model to simulate one-dimensional transient water flow through the integrated saturated-unsaturated zone and to predict the variations of the water table elevation and pressure head in the soil considering stochastic soil water properties.

The specific objectives involved in this study were:

1. To develop a mathematical model of soil water movement in the saturated-unsaturated zone using stochastic hydraulic conductivities. The model should be able to simulate the dynamic water table behavior, pressure head and water content profiles in the layered soil using the Monte Carlo method.
2. To verify the model with field data.

CHAPTER II. LITERATURE REVIEW

Introduction

Groundwater flow is a complex phenomenon which is governed by many influencing parameters of soil and water. Groundwater flow systems can be divided into two different domains: saturated flow and unsaturated flow. The flow pattern of the unsaturated zone is generally vertical and that of the saturated zone is more normally horizontal. Many studies on the saturated flow system have been done using either one-, two-, or three-dimensional models. However, a one-dimensional analysis is dominant in the study of unsaturated flow, since there is limited lateral movement of water in unsaturated flow in most cases.

Three different approaches can be considered in analyzing water flow in porous media (Bear, 1972; Sophocleous, 1978). They are molecular, microscopic, and macroscopic approaches. The molecular level transport theory is developed based on the movement of water molecules, the microscopic level transport theory is developed by utilizing the continuum approach, and the macroscopic level transport theory is developed by replacing microscopic variables by their volume averages. In the macroscopic approach, overall macroscopic values of physical properties of a representative volume element are used.

Until the mid-1970s only saturated flow problems had received intense interests from hydrologists. Recently, unsaturated flow problems began to receive interests from hydrologists.

The unsaturated flow system may be as important as the saturated flow system. The unsaturated zone is near the soil surface and plays a critical role in partitioning precipitation into surface runoff, evapotranspiration, and groundwater recharge (Milly, 1982). The reason why the water flow in the unsaturated zone is as important as the flow in the saturated zone is illustrated in the following examples given by Bear (1979). The first example is the infiltration process, which is the downward water movement from ground surface to the water table through the unsaturated zone. It may replenish the water table aquifer by the water from precipitation, irrigation, etc. The second example is related to groundwater quality. Pollutants applied in various forms on the ground surface, for example, fertilizers, pesticides, solid waste land fills, septic tanks, are often dissolved in the water applied on the soil surface. The infiltrating water then carries pollutants as it moves downward towards the water table. Various phenomena, such as dispersion, diffusion, adsorption, and degradation take place during the pollutants transport. However, one cannot study the movement of

pollutants carried by the water without information on the movement of water itself in the unsaturated zone.

In the unsaturated zone, a fraction of the pores' volume is filled with air, which can physically obstruct water movement. Water flows only through the still saturated finer pores or in film around the soil particles. Therefore, unsaturated flow should theoretically be treated as two-phase flow of water and air. However, the usual approach is to analyze only the flow of water and consider the air as part of solid phase (Bouwer, 1978).

Liquid flux in the soil can be separated into three components, that due to temperature gradients, that due to water potential gradients, and that due to gravity (Philip and De Vries, 1957). However, analyses of soil water movement have been largely based on theories of isothermal water movement which neglect movement induced by temperature gradients. Philip and De Vries (1957) proposed a theory to predict water movement as a consequence of temperature and soil water potential gradients. Sophocleous (1978, 1979), by modifying the Philip and De Vries equation for heat and water transport in porous media, showed the effects of temperature gradient on water flow were negligible at high moisture contents, but were significant at very low moisture contents. On the other hand, Higuchi (1984) found that water flow induced by a temperature gradient was negligible

below a depth of 30 cm where diurnal soil temperature variations were quickly damped.

Numerical methods, using high speed computers, are used in the solution of the groundwater flow problems, which are governed by a nonlinear parabolic partial differential equation that is very difficult to solve analytically. Finite difference schemes have been used primarily for such flow problems. Finite element schemes, which are a relatively new technique, have been used in flow problems since the last two decades. In the present study, a finite difference scheme was used since it was sufficient for the one-dimensional flow problems.

Theories on Saturated-Unsaturated Flow

For describing transient one-dimensional flow through saturated-unsaturated porous media there are two different theories (Fujioka and Kitamura, 1964). One theory admits a fundamental difference between flow in the saturated zone and flow in the unsaturated zone. In this theory, water in the unsaturated zone is assumed to have compressibility, while water in the saturated zone is assumed to be incompressible. Therefore, the propagation of pore pressure should suddenly change at the boundary between the saturated and unsaturated soil profile and consequently the law of movement of soil water above and below the water table is

distinctly different. Accepting this theory of discontinuity, the transient saturated-unsaturated interface constitutes an internal moving boundary.

For the transient one-dimensional saturated-unsaturated flow study with the water table as a lower boundary, a moving boundary approach has been applied since the solution domain fluctuates from the soil surface to the water table (Hornberger and Remson, 1970; Gilding, 1983). This method was originally introduced by Landau (1950) and followed by Lotkin (1960) to study the heat flow within a melting rod. In this approach, a transformation of the vertical coordinates was made such that the moving boundary problem can be converted to a problem with a fixed nodal spacing.

The second theory proposes that the flow exhibits sufficient continuity across the water table. The water flows continuously irrespective of whether it is above or below the water table in the whole soil-water-air system (Freeze, 1969). Therefore, it is mathematically unnecessary to differentiate between the saturated and unsaturated zones.

Fujioka and Kitamura (1964), studying the vertical drainage problem using a laboratory column, found no sudden change of pressure at the boundary between the saturated zone and unsaturated zone of soil water. They concluded that the soil water near the water table may be in a

continuous and rather unsaturated system, so that we cannot consider the soil water of positive pressure to be completely saturated.

In the present study, the theory of continuity of pressure across the saturated-unsaturated interface is adopted.

Governing Equation

A physically based analysis of water flow in the soil must begin with a derivation of the governing equation and accompanying boundary and initial conditions from established principles. The general flow equation for the saturated-unsaturated zone can be derived from the Darcy's law and the principle of continuity of mass.

Here, it is shown that the Darcy's equation can be derived from the principle of momentum conservation. For an isothermal, Newtonian incompressible fluid, for which the fluid viscosity and density are constant, the momentum equation leads to the Navier-Stokes equation (White, 1979; Bear, 1972). The Navier-Stokes equation is given by:

$$\rho_\ell \frac{dV}{dt} = \rho_\ell g - \nabla p_\ell + \mu \nabla^2 V \qquad (2.1)$$

where ρ_ℓ = density of fluid,

V = velocity of fluid,

t = time,

g = gravitational acceleration

P_ℓ = fluid pressure,

μ = viscosity of fluid,

∇ = gradient operator, and

∇^2 = Laplacian operator.

The left hand side term represents inertial force, and the right hand side terms represent gravity force, pressure force, and viscous force per unit volume. The microscopic equation (2.1) must be transformed to a more useful macroscopic equation using average values of velocity and pressure. Averaging the Navier-Stokes equation is discussed by Bear (1972). In addition, it is assumed that in a porous medium the inertial forces are negligible, which is the case with a steady, laminar flow and that the viscous forces are proportional to the mean velocity of fluid with an opposite direction. Then, if the z-coordinate is positive upward, Eq. (2.1) reduces to:

$$0 = -\rho_\ell g - \nabla P_\ell - \frac{\mu}{k} V \qquad (2.2)$$

where P_ℓ = macroscopic average fluid pressure,

V = macroscopic average flow velocity, and

k = intrinsic permeability.

Solving Eq. (2.2) for V we will get:

$$V = - \frac{k\rho_\ell g}{\mu} \nabla(h + z) = - K \nabla\phi \qquad (2.3)$$

where h = pressure head,

z = gravitational head,

K = hydraulic conductivity, and

ϕ = total head.

Eq. (2.3) is the Darcy's equation for the steady-isothermal solute free of water in an isotropic saturated porous media. In the above equation, the statistical requirement that the medium must be sufficiently homogeneous on the scale of averaging volume should be satisfied. Darcy's equation can be applied to unsaturated media when the hydraulic conductivity is allowed to vary as a function of pressure head h or volumetric water content θ. For the unsaturated flow, Eq. (2.3) can be expressed as:

$$V = - K(\theta) \nabla\phi, \text{ or } V = - K(h) \nabla\phi \qquad (2.4)$$

Derivation of the continuity equation is given in Hillel (1980a). Consider a volume element of soil in the shape of a rectangular parallelepiped inside a space shown in Figure 1. Assume the sides of the volume element are Δx, Δy, and Δz, and no source or sink exists inside the volume. The continuity principle is defined by:

Mass inflow rate - mass outflow rate

= rate of mass change in the volume

That is, considering only x-direction to simplify the derivation:

$$\rho_\ell q \Delta y \Delta z - \left(\rho_\ell q + \frac{\partial \rho_\ell q}{\partial x} \Delta x \right) \Delta y \Delta z = \frac{\partial \rho_\ell (n S_w)}{\partial t} \Delta x \Delta y \Delta z \qquad (2.5)$$

where q = flow rate across a unit cross section in the x-direction

n = porosity, and

S_w = degree of saturation.

In Eq. (2.5), the product of porosity and degree of saturation is equal to water content. The mass outflow rate is derived from truncated Taylor series. Eq. (2.5) can be rearranged assuming constant soil water density:

$$\frac{\partial(nS_w)}{\partial t} = -\frac{\partial q}{\partial x} \tag{2.6}$$

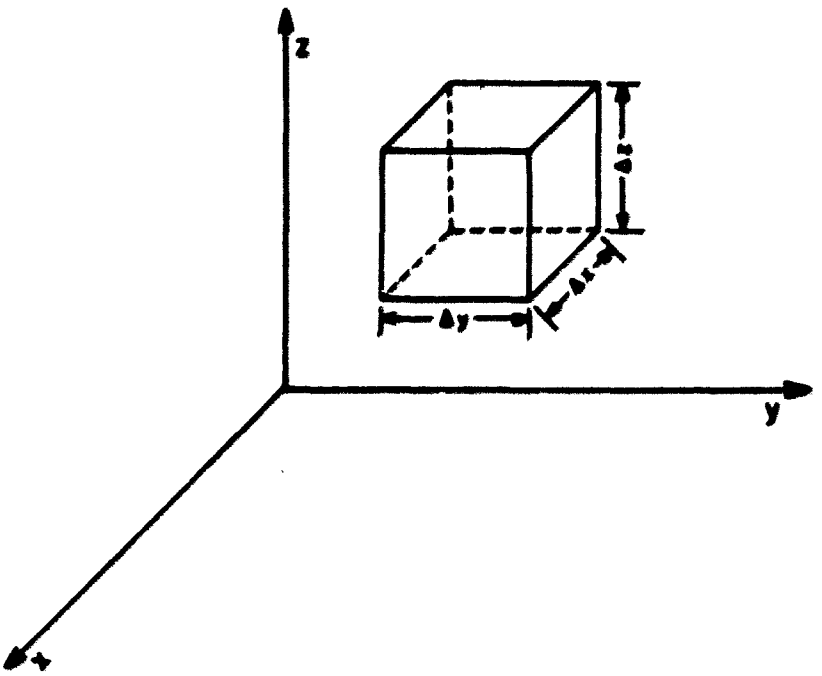

Figure 1. An element volume in a Cartesian coordinate system

By substituting Eq. (2.4) into Eq. (2.6) since V=q, the general one-dimensional flow equation follows:

$$\frac{\partial (nS_w)}{\partial t} = \frac{\partial}{\partial x} \left[K(\theta) \frac{\partial \phi}{\partial x} \right] \tag{2.7}$$

Now, the left hand side term of Eq. (2.7) can be modified to further simplify the equation. By expanding the left hand side:

$$\frac{\partial (nS_w)}{\partial t} = n \frac{\partial S_w}{\partial t} + S_w \frac{\partial n}{\partial t} \tag{2.8}$$

But $\frac{\partial n}{\partial t}$ can be replaced by $S_s \frac{\partial h}{\partial t}$, where S_s is the specific storage, which is specific yield divided by the aquifer thickness. Then,

$$\frac{\partial (nS_w)}{\partial t} = n \frac{\partial S_w}{\partial t} + S_w S_s \frac{\partial h}{\partial t} \tag{2.9}$$

For practical purposes, it is convenient to express Eq. (2.9) in terms of the pressure head and the volumetric water content rather than in terms of pressure head and degree of saturation. Then, Eq. (2.9) becomes:

$$\frac{\partial (nS_w)}{\partial t} = \frac{\partial \theta}{\partial t} + \frac{\theta}{n} S_s \frac{\partial h}{\partial t} \tag{2.10}$$

Applying the chain rule to Eq. (2.10) and substituting into Eq. (2.7) we obtain:

$$\left(\frac{\partial \theta}{\partial h} + \frac{\theta}{n} S_s \right) \frac{\partial h}{\partial t} = \frac{\partial}{\partial x} \left[K(\theta) \frac{\partial \phi}{\partial x} \right] \tag{2.11}$$

This equation can be modified by replacing $\frac{\theta}{n}$ with β (Neuman

et al., 1974; Van Genuchten, 1982):

$$\left(\frac{\partial \theta}{\partial h} + \beta S_s \right) \frac{\partial h}{\partial t} = \frac{\partial}{\partial x} \left[K(\theta) \frac{\partial \phi}{\partial x} \right] \qquad (2.12)$$

The first term of the left hand side of Eq. (2.12) is the slope of the water content-moisture tension curve and is zero for fully saturated flow. For the second term, it is assumed that S_s can be disregarded in the unsaturated flow because the effect of compressibility on the storage of water is very small in comparison to the effect of changes in the moisture content (Neuman, 1973). Therefore, $\beta = 1$ in the saturated zone and $\beta = 0$ in the unsaturated zone. Eq. (2.12) is the general governing equation for the one-dimensional saturated-unsaturated flow. For two- or three-dimensional flow systems, the governing equation can be derived as the same manner. For one-dimensional vertical flow with axis positive upward, the hydraulic head is expressed as the sum of pressure head and elevation head. Then, Eq. (2.12) with a source or sink term will be changed to:

$$C \frac{\partial h}{\partial t} = \frac{\partial}{\partial z} \left[K(\theta) \left(\frac{\partial h}{\partial z} + 1 \right) \right] + S(z,t) \qquad (2.13)$$

where $C = \frac{\partial \theta}{\partial h} + \beta S_s$, the generalized specific water capacity,

$S(z,t)$ = source or sink, showing rate of supply or extraction from a differential volume of

soil.

S(z,t) is positive for a source and negative for a sink. Eq. (2.13) was used in the present study.

In this section, the governing equation was derived using the h-based instead of θ-based. Milly and Eagleson (1980) discussed the differences between the two approaches. The advantages of the h-based equation are: (1) it is applicable in both the unsaturated and saturated zones, and (2) the flux expression is simpler.

Boundary Conditions

Boundary conditions and initial conditions are necessary in order to solve the soil water flow equation. Two boundary conditions, top and bottom, are required in a vertical one-dimensional flow system if the flow domain is finite. The top boundary is an atmospheric boundary which is along the soil-air interface on the top of the soil and the bottom boundary is at the lower end of flow domain which may be either saturated or unsaturated. Either pressure head or flux can be used to specify the boundary conditions. However, the flux boundary condition is easier to determine and consequently is the most widely used method in previous studies.

Along the soil-air interface, moisture can come into or leave from the soil water system by infiltration or

evaporation, respectively. When the potential rate of infiltration exceeds the infiltration capacity of the soil, a portion of the water may be lost by runoff. The potential infiltration rate from a given soil depends only on atmospheric conditions, while the actual infiltration rate is limited by the ability of the soil medium to infiltrate. The same thing happens for potential and actual evaporation. The actual evaporation rate across the top boundary is therefore governed by soil water conditions such as antecedent moisture content, while the potential rate is controlled by atmospheric or other external conditions. Therefore, the exact top boundary condition at the soil surface cannot be predicted a priori. The boundary flux obtained by solving the flow equation should be checked against the potential rates.

Generally, the lower boundary flux condition cannot be determined from direct measurement, but must be determined from other indirect ways. The water budget approach or weighing lysimeter method is the best method to use. The hydraulic gradient between two different vertical points can be used to calculate the flux or through model calibration to a set of field data the lower boundary flux can be determined.

Infiltration

The infiltration process is a complex phenomenon which has several influencing parameters such as soil properties, rainfall intensity, initial water content, depth of groundwater level, etc. Infiltration has the largest influence in the runoff volume on a watershed (Mein and Larson, 1973). Research on this topic has been conducted for several decades since Green and Ampt (1911) developed a physically based infiltration equation.

There are several infiltration equations, either empirical or theoretical, found in the current literature. Empirical equations include the Kostiakov equation, Horton equation, and Holtan equation. Theoretical equations include the Green-Ampt equation and Philip equation. These equations cannot be used directly for soils with different antecedent moisture contents without some modifications. Huggins and Monke (1968) modified Holtan's equation, and Skaggs (1978) modified the Green-Ampt equation. Huber et al. (1982) modified both the Horton's and Green-Ampt equations. Mein and Larson (1973) and Chu (1978) modified the Green-Ampt equation for the two stages of infiltration, before and after surface ponding. Mein and Larson (1973) used only steady rainfall, and Chu (1978) extended Mein and Larson's study for unsteady rainfall.

Rawls and Brakensiek (1983) presented a procedure with

tables and graphs for estimating the Green-Ampt equation parameters, such as effective porosity, capillary pressure head, and saturated hydraulic conductivity, based on readily available soils and agronomic data.

Holtan et al. (1967) developed an iterative computational procedure for the modified Holtan's equation to determine the incremental infiltration for a time period. This computational procedure has been used in several later studies (e.g., DeBoer, 1969; Anderson, 1975; Shahghasemi, 1980).

Table 1 shows various infiltration equations. All the original infiltration equations in Table 1 were discussed in detail by Hillel (1980b).

Evapotranspiration

Potential evapotranspiration depends on climatological factors such as solar radiation, air temperature, humidity and wind velocity. Actual evapotranspiration can be measured directly by weighing lysimeters. However, such measurements are costly and are rarely available. Most potential evapotranspiration (PET) values are obtained from climatological data using one of the many predictor models. A summary of the models for PET including required input data is given in Skaggs (1978). Perhaps the most reliable model is the Penman equation. The input data required for

Table 1. Infiltration equations

Name	Equation	
Green and Ampt	$i = i_c + A/I$	theoretical
Philip	$i = i_c + (s/2)\, t^{-\frac{1}{2}}$	theoretical
Kostiakov	$i = Bt^{-m}$	empirical
Horton	$i = i_c + (i_o - i_c)\, e^{-kt}$	empirical
Holtan	$i = i_c + a(M - I)^n$	empirical
Modified Holtan	$i = i_c + a(\frac{S - I}{T})^P$	empirical
Modified G-A	$i = A + B/I$	theoretical
Modified G-A	$i = K\,(1 + \frac{M_d\, S_h}{I})$	theoretical

A, B, a, k, m, n, p = parameters depending on soil properties.

I = accumulated infiltration.

i = infiltration rate.

i_c = steady state infiltration rate.

i_o = initial infiltration rate.

K = hydraulic conductivity.

M = water storage capacity of soil.

M_d = initial soil moisture deficit.

S = water storage potential above any impedint strata.

S_h = average suction head at the wetting front.

s = sorptivity.

T = total pore volume above any impeding strata.

t = time from the beginning of the infiltration.

the Penman equation include air temperature, wind velocity, humidity, and solar radiation. However, these climatological input data are all available at only very few locations. Saxton et al. (1974a) developed a linear regression equation to predict PET for brome grass from the pan evaporation data which are relatively easy to obtain. Skaggs (1978) used the Thornthwaite model which requires only mean daily temperature as an input. Selection of the prediction model depends upon the availability of the climatological data and the precision requirement of the simulation model. Actual evapotranspiration rates depend upon moisture availability in the top soil layer as well as soil cover, plant leaf and root system development. Saxton et al. (1974b) developed an ET model based on energy distribution which included crop canopy and root system.

Ritchie (1972) fitted an exponential equation to describe the relationship between the fractional net radiation reaching the soil surface and the leaf area index for several different row crops. Molz and Remson (1970) introduced a simple equation to determine the root extraction term for plant transpiration which approximates the pattern of plant transpiration such that 40%, 30%, 20%, and 10% of the total transpiration comes from each successively deeper root zone.

Deep percolation and lateral flow

Deep percolation, which is used to represent the flux across the bottom boundary whether it is saturated or not, is not easy to measure directly. It can be measured using a weighing lysimeter or can be calculated by the water budget approach. It also can be calculated from the hydraulic gradient obtained from piezometers at different depths.

Lateral flow, important in the saturated zone, can be calculated from the horizontal hydraulic gradient. It also can be predicted from the assumption that the groundwater table is nearly parallel to the ground surface. From this assumption, the lateral flow can be neglected if the ground surface has a small or no slope.

Both deep percolation and lateral flow can be determined from the model calibration procedure when field determination is not possible.

Soil Properties

Soil has various parameters of interest in determining moisture movement. Porosity, water content, pressure head, hydraulic conductivity, texture, and others are some of those parameters. Many of these parameters exhibit a hysteretic property. In this section, some concepts of soil water properties as well as some methods of determining them are discussed.

Measurement of soil water pressure and water content

The variable amount of water contained in a unit volume of soil is known as volumetric water content. Many soil properties, such as moisture tension and unsaturated hydraulic conductivity, depend very strongly upon water content (Hillel, 1980a). There are both direct and indirect methods of measuring water content including: gravimetric, electrical resistance block, neutron scattering, and gamma ray methods. The gravimetric method, which is the only direct method, consists of soil sampling, weighing and drying. This method is laborious and needs a long time to oven dry the soil samples. The electrical resistance block method is based upon the theory that the electrical resistance of a porous block placed in the soil depends upon the soil water suction. This method is accurate only when the soil undergoes no wetting reversal during the period of measurement. The neutron moisture meter consists of two main parts: a probe, which is lowered into an access tube inserted vertically into the soil, and a scaler, which monitors the flux of slow neutrons scattered by the soil. This method has gained widespread acceptance as an efficient and reliable technique for monitoring soil moisture in the field. The major disadvantage of this method is the poor resolution quality. The sphere of influence of the measurement has a radius of approximately 30 cm (Bouwer,

1978).

The gamma ray scanner consists of two spatially separated probes, a source and a detector. Gamma rays are emitted from the source and detected by the detector after being absorbed in soil water. This method is used in the laboratory under controlled conditions.

Soil water pressure (tension) can be measured by a tensiometer. The tensiometer is a practical device for in situ measurement of pressure head in the soil. It consists of three parts: a porous cup, a connecting tube, and a manometer. A pressure transducer can be used instead of a manometer. The effective range of tensiometer measurements is 0 to 0.8 atmosphere.

Soil water retention

The pressure or matric potential, h, is a variable to describe the energy level of soil solution within an unsaturated porous medium. The quantity 'gh', where g is gravitational acceleration, is the amount of energy required to move a unit mass of water, isothermally and reversibly, from a porous medium to the free water surface. When soil water is at hydrostatic pressure greater than atmospheric, its pressure potential is considered positive. When it is at a pressure lower than atmospheric, the pressure potential is considered negative. This negative pressure potential

has been termed capillary potential or matric potential.

The forces ordinarily considered to be the determinants of h in unsaturated media are capillary attraction and adsorption. These forces attract and bind water in the soil and lower its potential energy below that of bulk water. Capillarity is evidenced in the pressure differences across curved air-water interfaces under surface tension. Adsorption involves the relatively short distance interaction of water with the surface of the solid phase of the medium and forms hydration envelopes over the particle surfaces. These two mechanisms of soil water interaction are illustrated in Figure 2.

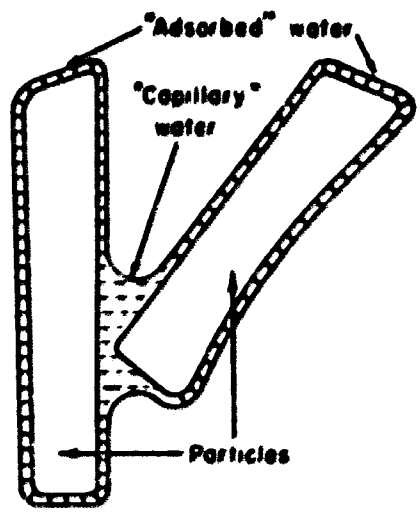

Figure 2. Water in an unsaturated zone under capillarity and adsorption (after Hillel, 1980a)

The magnitude of these forces are determined by the microscopic distribution of water in the medium, by temperature, and by the nature of the medium itself (Milly and Eagleson, 1980). In relatively moist media, the effect of capillarity is dominant in determining h. Only the largest pores are air filled, and the air-water interface has relatively small curvature. Bear (1979) expressed the pressure in the water just beneath the air-water interface as:

$$P_c = 2\sigma/r_h \tag{2.14}$$

where P_c = pressure in water, just beneath the air-water interface,

σ = interfacial surface tension,

r_h = harmonic mean radius of curvature of the interface, negative for concave water surface.

Then, the pressure head, h, is given by:

$$h = P_c/\gamma = 2\sigma/\gamma r_h \tag{2.15}$$

where γ = specific gravity of liquid water.

The amount of water retained at a given level of h in the capillary regime is thus determined by the distribution of the larger pore sizes. It follows that the soil structure is a strong factor in determining the relation between h and water content, θ, for large θ.

As water is removed from the medium, the remaining

water becomes increasingly closer to the soil particle surface. The effect of adsorption becomes predominant at low values of θ. In the adsorption regime, the moisture content at fixed h for any soil is correlated with the specific surface of the medium and can therefore be considered a function of soil texture and mineralogy.

The value of h at the boundary between the capillary and adsorption regimes, if such a boundary can be defined, has not been clearly determined. Miller and Miller (1955) suggest that the capillary theory of soil water is valid at least in the coarse silt to sand range. Buckman and Brady (1969) divided between capillary and adsorbed water at about pF = 4.5, where pF is defined by:

$$pF = \log_{10}(-h) \qquad (2.16)$$

where h = negative pressure (suction) head in cm. Hillel (1980a) says that below pF = 3 the capillary effect is dominant and as pF increases importance of adsorption is increased.

McQueen and Miller (1974) studied the relationship between pF and θ for pF up to 7. They concluded that pF can be represented empirically as a piecewise linear function of θ for values of θ not near saturation. The three segments are:

pF 5.0 - 7.0 tightly adsorbed segment,

pF 2.5 - 5.0 adsorbed film segment, and

pF 0.0 - 3.0 capillary segment.

So far there is no distinct division between the capillary and adsorption range. The closer the water molecule to the soil particle, the stronger the adsorptive force. Care should be exercised in assuming the range of pF that may be treated using capillary theory.

There are several empirical equations for the soil water retention. Brooks and Corey (1964) analyzed drying curves for many consolidated rock samples and found the relationship between h and θ as:

$$h = h_a \left(\frac{\theta - \theta_r}{\theta_s - \theta_r} \right)^{-\frac{1}{\lambda}} \qquad \theta > \theta_r \qquad (2.17)$$

where h_a = air entry value,

θ_r = the residual water content, which is the minimum water content value at which $d\theta/dh$ approaches zero on a retention curve,

θ_s = the saturated water content, and

λ = a fitted parameter.

The pressure potential h_a is the value of h at which air is first drawn through the soil sample during dewatering in the laboratory.

Mualem (1976) fitted the published data for 45 soils to the Brooks and Corey model. Residual water contents ranged

from 0.01 to 0.28, but were mostly less than 0.10. The λ ranged from 0.19 to 11.67, but were mostly less than 3.0.

Hysteresis

The relationship between pressure head and water content can be obtained in two ways: (1) by gradually drying an initially saturated soil, and (2) by gradually wetting an initially dry soil. Each yields a continuous curve, but the curves are not identical. The equilibrium water content at a given pressure is greater in drying than in wetting as illustrated in Figure 3. This nonunique characteristic of the functions h and θ for a particular soil at a fixed temperature is known as hysteresis.

Complete drying and wetting proceed along the cycle of curves A and B in Figure 3. They are called the main wetting and drying curves, respectively. When wetting reversals occur anywhere other than at the common end points of curves A and B, scanning curves, C to F in Figure 3 result. Curves C and D are primary wetting and drying scanning curves, while E and F are secondary wetting and drying scanning curves. It is apparent that the relation between h and θ at any time is dependent on the wetting history of the medium.

The hysteresis effect may be attributed to several causes (Hillel, 1980a). They are:

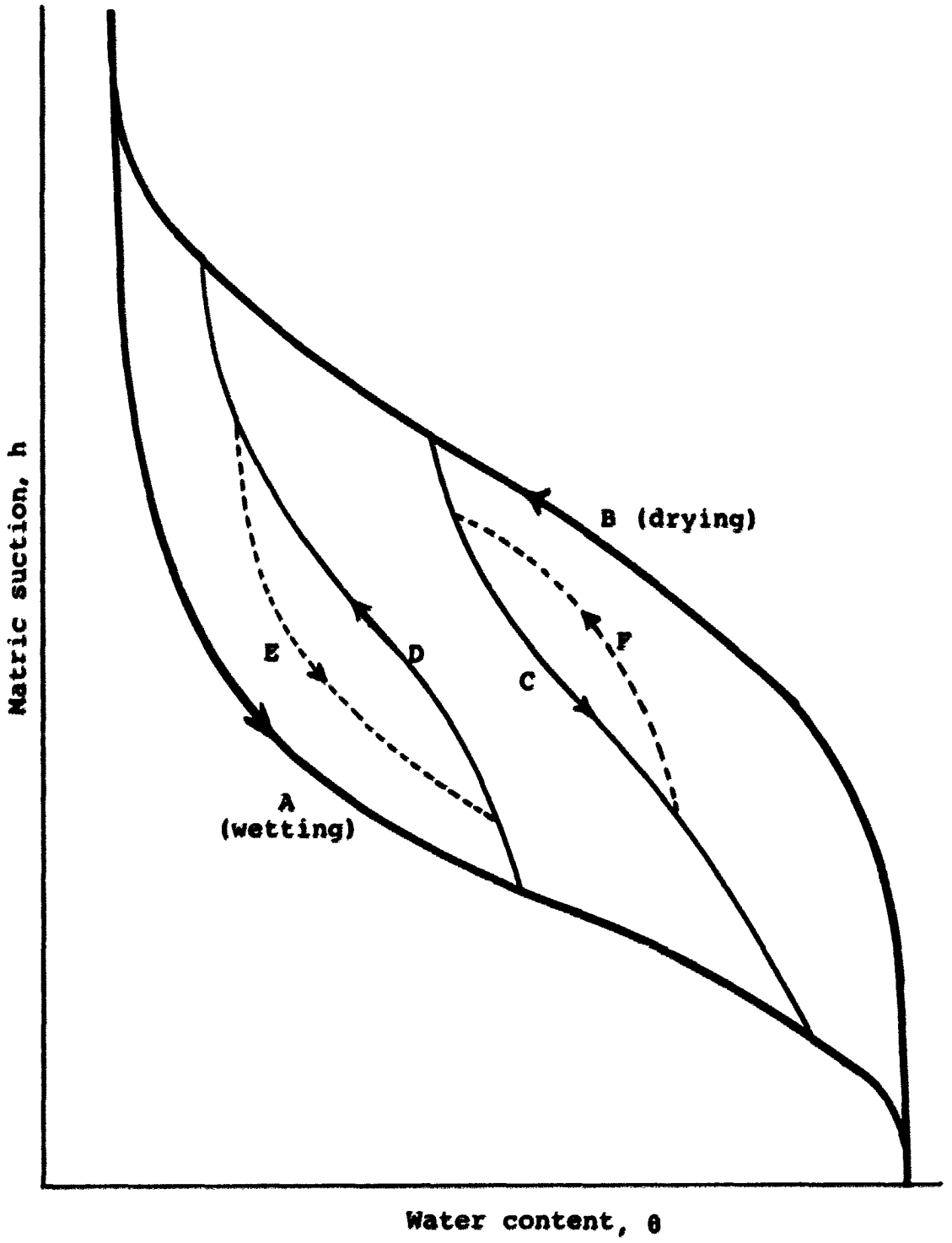

Figure 3. The hysteretic soil water retention curves

(1) the ink bottle effect,

(2) the contact angle effect,

(3) the entrapped air effect, and

(4) the swelling, shrinking, or aging effect.

Among them the ink bottle effect has been quite successful in explaining the hysteresis. The ink bottle effect is that at least some pores drain and refill at different capillary pressures. Miller and Miller (1956) recognized this effect as a natural implication of the capillary theory of moisture relation.

Figure 4 shows the concept of the ink bottle pore and

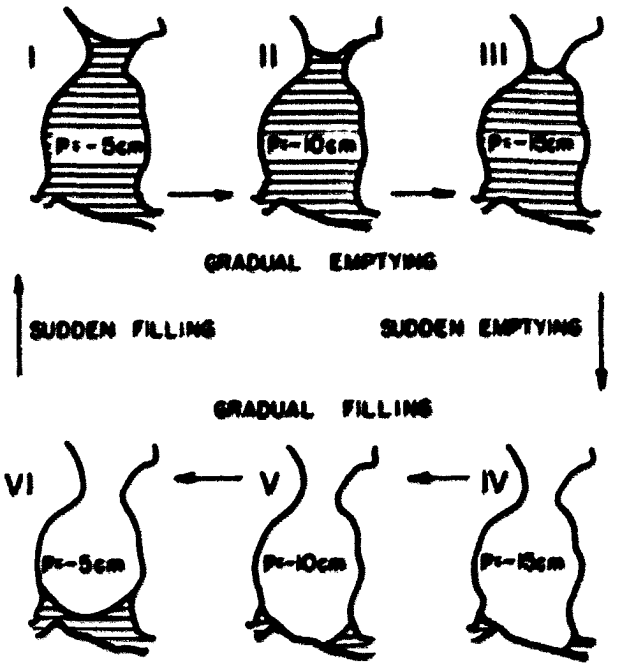

Figure 4. Ink bottle hysteresis in a single bottle (after Miller and Miller, 1956)

how hysteresis in a single pore could occur. Anywhere between p = -5 cm and p = -15 cm there are two possible solutions of Eq. (2.15); one a full state, the other an empty state. At -5 cm, the empty state becomes unstable and executes a sudden and irreversible "Haines jump" to the full state at p = -5 cm. Conversely, at -15 cm the full state "Haines jump" occurs to the empty state. In practice, these jumps occur in milliseconds, so the pressure at which they occur is independent of the time rate of approach to that pressure.

Determination of hydraulic conductivity

Knowledge of the relationship of unsaturated hydraulic conductivity with either water content or pressure head is required to solve for unsaturated flow problems. However, reliable estimates of the unsaturated hydraulic conductivity are especially difficult to obtain, partly because of its extensive variability in the field, and partly because measuring this parameter is time consuming and expensive (Van Genuchten, 1980).

Values of hydraulic conductivity are sensitive to small changes in water content (Nielsen et al., 1973). Characteristically, hydraulic conductivity values decrease an order of magnitude for only a small decrease in water content. It is not unusual for hydraulic conductivity to

range over five orders of magnitude for water contents measured in the field. In addition, unsaturated hydraulic conductivity shows hysteretic effects, especially as functions of pressure head, which makes this problem more difficult.

There are several methods of measuring hydraulic conductivity either in the field or in the laboratory. These methods are discussed in detail by Hillel (1980a). In situ methods include the sprinkling infiltration method, impeding layer method, and redistribution method. Laboratory methods include the steady state method and transient state method.

However, estimating the hydraulic conductivity of a soil as a function of its water content in the field or by taking soil samples to the laboratory for analysis is laborious and time consuming (Libardi et al., 1980). Consequently, empirical and theoretical relationships between unsaturated conductivity and either water content or pressure head have been proposed. Several empirical relationships have been developed from soil water retention curves (e.g., Brooks and Corey, 1964; Campbell, 1974, and referenced therein). All of these empirical equations are power or exponential functions of pressure head or water content as shown in Table 2. Bresler and Green (1982) suggested, based on their experience, that if one is

Table 2. Empirical equations relating hydraulic conductivity to water content or pressure head

No.	Equation	Independent variable	Fitting parameters
(1)	$K(h) = a/h^n$	h	a, n
(2)	$K(h) = a/(b + h^n)$	h	a, b, n
(3)	$K(\theta) = a\theta^m$	θ	a, m
(4)	$K(h) = K_s (h_a/h)^n$	h	n
(5)	$K(h) = K_s /[1 + (h/h_w)^m]$	h	m
(6)	$K(h) = K_s \exp[a(h - h_a)]$	h	a
(7)	$K(\theta) = K_s \left(\frac{\theta - \theta_r}{\theta_s - \theta_r} \right)^\gamma$	θ	γ, θ_r

h = soil water pressure (suction) head.

θ = volumetric water content.

h_a = air entry value.

h_w = water entry value.

K_s = saturated hydraulic conductivity.

θ_s = saturated water content.

θ_r = residual water content.

a, b, m, n, and γ = parameters to be determined.

interested in the whole range of $K(\theta)$, then the power function equations (4) and (7) in Table 2 were superior.

Mualem (1976) developed a new model for predicting the relative hydraulic conductivity from a soil water retention curve:

$$K_r(\theta) = S_e^{\frac{1}{2}} \left[\int_{\theta_r}^{\theta} \frac{1}{h(x)}\, dx \Big/ \int_{\theta_r}^{\theta_s} \frac{1}{h(x)}\, dx \right]^2 \qquad (2.18)$$

where K_r = $K(\theta)/K_s$, relative hydraulic conductivity,

K_s = saturated hydraulic conductivity,

$h(x)$= soil water pressure head as a function of water content,

$S_e = \frac{\theta - \theta_r}{\theta_s - \theta_r}$, effective saturation where subscripts s and r represent saturated and residual values of the soil water content, respectively.

Van Genuchten (1980) developed a closed form equation for predicting the hydraulic conductivity of unsaturated soil based upon Mualem's equation with the general retention equation of the form:

$$S_e(h) = \left[\frac{1}{1 + (ah)^N} \right]^m \qquad (2.19)$$

where h = absolute value of the pressure head,

a, N = nonlinear regression parameters to be determined,

$m = 1 - 1/N$.

The relative hydraulic conductivity is expressed as a function of pressure head as:

$$K_r(h) = \frac{\{ 1 - (ah)^{N-1} [1 + (ah)^N]^{-m} \}^2}{[1 + (ah)^N]^{\frac{m}{2}}} \qquad (2.20)$$

Eqs. (2.19) and (2.20) do not consider hysteresis. Consequently, for a hysteretic model two or more sets of parameter values for drying and wetting conditions must be determined.

Stochastic Analysis

Unlike small laboratory soil columns, field soils are heterogeneous, hence the development of water and solute transport models as well as the technique for sampling field soils must account for spatial variability. Studies on heterogeneity of agricultural and watershed lands indicate that soils exhibit appreciable field variability in properties which affect soil water movement. Nielsen et al. (1973) reported a wide range (four orders of magnitude) of steady state hydraulic conductivity in a 150-hectare experimental site. They also reported the steady state hydraulic conductivities were log normally distributed (Nielsen et al., 1973). Willardson and Hurst (1965) found a log normal distribution of hydraulic conductivity based on 254 auger hole measurements in 12 fields in Australia and on

1498 samples from soils in California.

In order to account for the variability in soil water properties, a stochastic approach has been introduced in groundwater studies during the last two decades. All the soil water properties have spatial variability. However, the field variability is simplified by assuming that only the saturated hydraulic conductivity is spatially variable, while the other properties such as porosity, residual water content, and air entry value, are constant over the field (Dagan and Bresler, 1983). The justification of this assumption is that the saturated hydraulic conductivity changes considerably over the field, while the other parameters vary in much narrower limits. Previous analysis by Russo and Bresler (1982) showed that the impact of the variability of these parameters is indeed limited.

There are several approaches to provide stochastic prediction in groundwater flow problems. McMillan (1966), Freeze (1975), and Smith and Freeze (1979a,b) used the Monte Carlo method for modeling the stochastic nature of the saturated flow problems. Bennion and Hope (1974), Gelhar (1976) and Bakr et al. (1978) used spectral analysis technique for steady saturated flow studies. Tang and Pinder (1977) used perturbation theory for solving transient saturated flow problems. Andersson and Shapiro (1983) compared the perturbation method with the Monte Carlo method

for one-dimensional steady state unsaturated flow. Dagan and Bresler (1983) and Bresler and Dagan (1983) studied one-dimensional unsaturated stochastic flow problems using a statistical averaging procedure and probability density function of saturated hydraulic conductivity.

The Monte Carlo method and the spectral analysis method are considered the most promising techniques in the stochastic analysis of the groundwater flow problems. In both methods, the integral scale, which characterizes the average distance over which point values of hydraulic conductivity are positively correlated, is an important parameter. The integral scale is the upper limit on discretization in a medium. The Monte Carlo method and the spectral analysis method are discussed further.

Monte Carlo method

The Monte Carlo method is a method of solving mathematical and physical problems approximately by simulation using random quantities or input variables. Prior to the appearance of electronic computers, this method was not widely applicable since the simulation of random quantities by hand is a very laborious process.

The Monte Carlo method makes possible the simulation of any process influenced by random factors. It can even be used to solve many mathematical problems involving no chance

by artificially devising a probabilistic model. For these reasons, the Monte Carlo method can be considered a universal method for solving mathematical problems (Sobol, 1974).

The random variable in a Monte Carlo model can be either discrete or continuous. Random numbers can be classified by pure random, pseudorandom, and quasirandom numbers. A detailed description of random numbers can be found in Hammersley and Handscomb (1964). Generation of random numbers and transformation into a specific probabilistic distribution are discussed in detail elsewhere (Hammersley and Handscomb, 1964; Sobol, 1974).

The use of the Monte Carlo method in stochastic groundwater problems involves repetitive simulations using a mathematical model coupled with a statistical analysis of the results. Freeze (1975) used the Monte Carlo method for stochastic saturated flow studies without considering spatial correlation of soil properties. Later, Smith (1978), and Smith and Freeze (1979a,b) considered spatial correlation in saturated hydraulic conductivity using a first order nearest neighbor model, which will be discussed in detail in the next chapter. They predicted the mean and variance of hydraulic head from the spatially varying hydraulic conductivity input. Smith and Hebbert (1979) applied the Monte Carlo method in studying hydrologic

effects of spatial variability on infiltration and Warrick et al. (1977) applied the Monte Carlo method in their unsaturated flow study.

Spectral analysis

This technique is an analytical approach to determine the stochastic variability in soil properties. This technique has been used by Bennion and Hope (1974) to analyze one-dimensional variability of porosity and permeability from oil reservoirs. Gelhar (1976) and Bakr et al. (1978) applied this method to study spatial variability of steady flows in a saturated aquifer. In spectral analysis, two basic assumptions must be made: (1) the medium and flow system are considered to be continuous and (2) there is a spatial correlation structure of the medium properties. Variation of hydraulic conductivity can be thought of in the continuum sense as a random field which is characterized by a spatial covariance function and spectral density function.

The procedure for the spectral analysis as shown by Bakr et al. (1978) can be summarized as follows:

1. Develop the governing partial differential flow equation.
2. Express two variables, hydraulic head and hydraulic conductivity, in the equation in terms of a mean and a

perturbation neglecting the product of perturbations.

3. Solve the fluctuation of hydraulic head in the perturbation equation in terms of fluctuation of hydraulic conductivity following stochastic Fourier-Stieltjes integral.
4. Find the spectral density function of fluctuation of hydraulic head by using the inverse Fourier transform.
5. Find the autocovariance of head fluctuation by Fourier transform of spectral density function of hydraulic head.

Comparison

Smith (1978), and Smith and Freeze (1979a) discussed the differences and the advantages of the two techniques of stochastic analysis. The major difference in these techniques is that the conductivity field is represented by a series of discrete blocks in the Monte Carlo method, while it is represented by a continuum in spectral analysis. They pointed out that the disadvantages of the spectral analysis method are that they are apparently inappropriate for problems in which the input variables have a large variance and for problems of bounded domains. Of course, the advantage of the spectral analysis method is that it gives an analytical solution. On the other hand, the Monte Carlo method can handle problems with both large variance in the

input variables and bounded domains, but it requires larger amounts of computer time for solution.

In this study, the transient saturated-unsaturated bounded domain flow problem was considered, and the Monte Carlo method was used.

Analytical and Numerical Solutions

The governing equation of saturated-unsaturated flow is a nonlinear partial differential equation with variable coefficients and cannot be solved by the usual methods. Nonlinearity greatly complicates the mathematics of unsaturated flow problems. Kirkham and Powers (1972) showed a technique to solve the nonlinear partial differential flow equation analytically. They used Boltzmann's transformation applied to the nonlinear partial differential equation to obtain an ordinary differential equation which can be solved analytically.

Numerical methods are the principal approach to the solution of unsaturated flow problems. Either finite difference or finite element method can be used for the saturated-unsaturated flow. Each one has its own advantages and disadvantages, and it is hard to say that one is always better than the other. It depends on the problem being modeled and other conditions. One of the major reasons in choosing the finite element method over a more simple finite

difference method is the stability of the resulting nonlinear equation system (Cooley, 1983). Although the recently introduced finite element method may be advantageous for two or three dimensional problems, especially with complex geometries, they show little or no advantage over the finite difference method for transient one-dimensional problems (Emery and Carson, 1971).

The fundamental idea in the finite difference technique is to replace all derivatives by finite differences and thus reduce the original continuous boundary value problem to a discrete set of simultaneous algebraic equations. There are several different solution formations for finite difference models, but these can be grouped as either implicit or explicit methods. Although explicit methods for solving differential equations are simple and straightforward, the restriction on mesh size and time steps in order to meet stability requirements is severe. This sometimes make explicit methods unsuitable for practical applications. On the other hand, the implicit method is less restrictive in mesh size and time steps but they are numerically more complicated because they involve the solution of a system of equations at each time step. Detailed descriptions of these schemes can be found elsewhere (e.g., Richtmyer and Morton, 1967; Remson et al., 1971; Lapidus and Pinder, 1982).

Haverkamp et al. (1977), in a comparison among six

different finite difference schemes applied to a one-dimensional infiltration problem, found that: (1) the explicit methods used between 5 to 10 times more computer time than the implicit methods, (2) results using the Kirchhoff integral transformation were no better than those obtained with the implicit model with no transformation, and (3) considering computer time and numerical stability, the implicit finite difference approximation has the widest range of applicability for predicting water movement in the soil both in the saturated and unsaturated zones.

Based upon the above discussions, the implicit finite difference method was considered better than the explicit method for the subsurface flow problems. The Crank-Nicolson method and the Douglas-Jones predictor-corrector method are the most successful solution methods applied to the one-dimensional subsurface flow studies. These two implicit methods received much attention from researchers owing to their numerical stability and simplicity. These methods result in a tridiagonal set of simultaneous equations which can be solved rapidly using the Thomas algorithm (Remson et al., 1971) by a digital computer.

Douglas and Jones (1963) developed an implicit predictor-corrector method for solution of nonlinear parabolic differential equations. The predictor and corrector difference equations are modified form of the

Crank-Nicolson equation. In the predictor stage, the equation solves for the values of pressure head at a half time step. The intermediate values of pressure head are used to update the coefficients which in turn are used in the corrector stage to obtain a solution at the full time step. This scheme is nonconditionally stable and has relatively high accuracy with a uniform rate of convergence $O(h^2 + k^{3/2})$ where h and k are step sizes of space coordinate and time, respectively (Remson et al., 1971; Gilding, 1983). A particular advantage of this method is that this scheme is noniterative and leads to a tridiagonal system of equations which can be solved efficiently. Several researchers (e.g., Afshar and Marino, 1978; Hornung and Messing, 1980; Gilding, 1983) successfully applied the Douglas-Jones predictor-corrector method in their one-dimensional flow studies.

Dane and Mathis (1981) introduced an adaptive finite difference scheme in which both the spatial and temporal step sizes were allowed to be changed during the flow problem solution process. This approach might give better results but is more complicated.

CHAPTER III. MODEL DEVELOPMENT

Introduction

Mathematical models are extensively used in the science of hydrology. Groundwater management has relied heavily on the simulation model study. A model is defined as a simplified representation of the real system for some purposes. A model includes those features of the real system that are essential for the purpose of the model and it leaves out those that are not essential. Simulation is a technique of constructing and running a model of a real system in order to study its behaviors. A deterministic model has no random variables and for a given input it always produces the same output. A stochastic model has random variables which may be represented by some probability distribution. For a given input, a stochastic model will produce different outputs.

In this study, a stochastic model has been developed to predict the variation of pressure head, water content, and water table elevation under transient field conditions in a saturated-unsaturated soil. The Monte Carlo method is used to simulate a large number of equally probable and spatially correlated values of saturated hydraulic conductivity that can be used as inputs to the flow model. The results from the Monte Carlo simulations can be analyzed using standard

statistical routines.

In developing this model, several criteria were considered. First, the hysteretic property of the soil water retention relationship and the stochastic properties of soil water parameters were to be considered. Secondly, the model was to be designed to require data that were generally available for a watershed. Thirdly, the model was developed in a way that it can be easily modified by inserting or changing any component without major revision of the entire model.

Model objective

The major objective of the development of this model was to solve the equation of moisture flow in the unsaturated-saturated zone. The model should be able to predict the mean and variance of the outputs, namely, water table elevation and pressure head. The model should also allow consideration of nonhomogeneous layered geologic formations, and should analyze transient flow conditions with the model upper boundary at the ground surface.

Assumptions

Assumptions underlying the development of any model are very important in understanding and applying that model. The following were major assumptions underlying the

development of the present stochastic water transport model.

1. The flow system was considered continuous throughout the saturated-unsaturated zone;

2. The porous medium was comprised of nondeformable particles;

3. Water flow could be described by Darcy's law, that is, the flow was laminar;

4. No water quality variable or electrochemical effects were considered;

5. The effects of temperature gradients, osmotic gradients and other minor gradients on water flow were neglected;

6. Water vapor transport was not considered;

7. The effect of temperature on the hydraulic conductivity was ignored, that is, the effect of temperature on the density and viscosity of water was neglected; and

8. The hydraulic conductivity of the soil water was considered significantly stochastic, while the other soil water properties were considered nonsignificantly stochastic.

Finite Difference Equation

The governing flow equation (2.13) and the boundary conditions must be changed into the form of a finite difference equation in order to apply the solution scheme. The governing equation (2.13) can be rewritten by simply

expanding the right hand side.

$$C \frac{\partial h}{\partial t} = \frac{\partial K}{\partial z} \left(\frac{\partial h}{\partial z} + 1 \right) + K \frac{\partial^2 h}{\partial z^2} + S(z,t) \qquad (3.1)$$

An implicit finite difference solution method, known as Douglas-Jones predictor-corrector method, was selected for use to solve Eq. (3.1) numerically. In the predictor stage, the main objective is to estimate the coefficients C and K for the corrector stage. The values of pressure head at the half time step are computed using the values of C and K of the previous time step. The values of C and K for the half time step are determined from the pressure head solution at the half time step. In the corrector stage, the pressure head solution is obtained using the C and K values from the predictor step or the half time step.

The finite difference equation for the predictor step takes the form:

$$C_j^n \frac{h_j^{n+\frac{1}{2}} - h_j^n}{\frac{1}{2}\Delta t} = \left(\frac{K_{j+1}^n - K_{j-1}^n}{2\Delta z} \right)\left(\frac{h_{j+1}^n - h_{j-1}^n}{2\Delta z} + 1 \right) + K_j^n \left(\frac{h_{j-1}^{n+\frac{1}{2}} - 2h_j^{n+\frac{1}{2}} + h_{j+1}^{n+\frac{1}{2}}}{(\Delta z)^2} \right) + S(z,t) \qquad (3.2)$$

The corrector follows the predictor with the form:

$$C_j^{n+\frac{1}{2}} \frac{h_j^{n+1} - h_j^n}{t} = \left(\frac{K_{j+1}^{n+\frac{1}{2}} - K_{j-1}^{n+\frac{1}{2}}}{2\Delta z} \right) \left(\frac{h_{j+1}^{n+\frac{1}{2}} - h_{j-1}^{n+\frac{1}{2}}}{2\Delta z} + 1 \right) + K_j^{n+\frac{1}{2}} \left(\frac{h_{j-1}^{n+1} - 2h_j^{n+1} + h_{j+1}^{n+1}}{2(\Delta z)^2} + \frac{h_{j-1}^n - 2h_j^n + h_{j+1}^n}{2(\Delta z)^2} \right) + S(z,t) \qquad (3.3)$$

where j = space step index,

n = time step index,

Δt = size of time step, and

Δz = size of space step in the z-direction.

The superscripts in Eqs. (3.2) and (3.3) represent the time step and the subscripts represent the spatial location. Eqs. (3.2) and (3.3) are general equations for the intermediate (internal) nodal points. Both Eqs. (3.2) and (3.3) can be reduced to the general form:

$$A_i h_{j-1} + B_i h_j + C_i h_{j+1} = D_i \tag{3.4}$$

Eqs. (3.2) and (3.3) must be modified to incorporate the boundary conditions. To incorporate a flux boundary condition in the finite difference equations, imaginary nodes are introduced at j = 0 and j = n+1 as shown on Figure 5. The flux condition at the bottom boundary (j=1) can be expressed as:

$$q_1^{n+\frac{1}{2}} = -K_1^n \left(\frac{h_2^{n+\frac{1}{2}} - h_0^{n+\frac{1}{2}}}{2\Delta z} + 1 \right) \tag{3.5}$$

for the predictor, and

$$q_1^{n+1} = -K_1^{n+\frac{1}{2}} \left(\frac{h_2^{n+1} - h_0^{n+1}}{2\Delta z} + 1 \right) \tag{3.6}$$

for the corrector, where q_1 is the water flux across the lower boundary. Solving Eqs. (3.5) and (3.6) for the

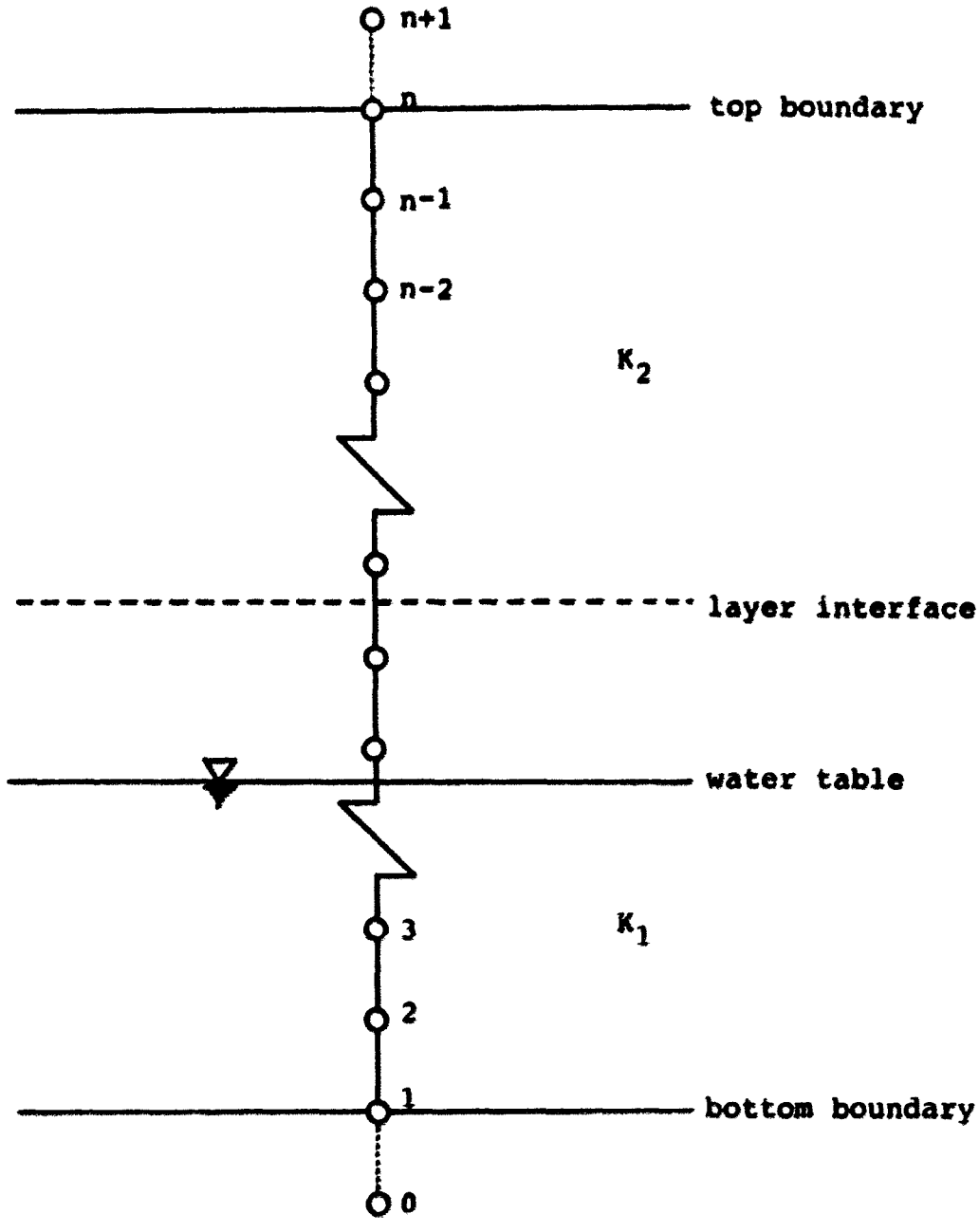

Figure 5. Flow system discretization including imaginary points

imaginary point, h_0, and substituting into Eqs. (3.2) and (3.3), respectively, the following are obtained for node 1 at the lower boundary:

$$C_1^n \frac{h_1^{n+\frac{1}{2}} - h_1^n}{\frac{1}{2}\Delta t} = \left(\frac{K_2^n - K_1^n}{\Delta z} \right) \left(- \frac{q_1^{n+\frac{1}{2}}}{K_1^n} \right)$$

$$+ 2K_1^n \left[\frac{h_2^{n+\frac{1}{2}} - h_1^{n+\frac{1}{2}} + \Delta z + \Delta z \, q_1^{n+\frac{1}{2}}/K_1^n}{(\Delta z)^2} \right] + S(z,t) \quad (3.7)$$

for the predictor, and

$$C_1^{n+\frac{1}{2}} \frac{h_1^{n+1} - h_1^n}{\Delta t} = \left(\frac{K_2^{n+\frac{1}{2}} - K_1^{n+\frac{1}{2}}}{\Delta z} \right) \left(- \frac{q_1^{n+1}}{K_1^{n+\frac{1}{2}}} \right)$$

$$+ K_1^{n+\frac{1}{2}} \left[\frac{h_2^{n+1} - h_1^{n+1} + \Delta z + \Delta z \, q_1^{n+1}/K_1^{n+\frac{1}{2}}}{(\Delta z)^2} \right.$$

$$\left. + \frac{h_2^n - h_1^n + \Delta z + \Delta z \, q_1^{n+\frac{1}{2}}/K_1^n}{(\Delta z)^2} \right] + S(z,t) \quad (3.8)$$

for the corrector.

Equations for the upper boundary can be obtained by following the same procedures. The flux condition at the soil surface boundary can be expressed as:

$$q_n^{n+\frac{1}{2}} = - K_n^n \left(\frac{h_{n+1}^{n+\frac{1}{2}} - h_{n-1}^{n+\frac{1}{2}}}{2\Delta z} + 1 \right) \quad (3.9)$$

for the predictor, and

$$q_n^{n+1} = -K_n^{n+\frac{1}{2}} \left(\frac{h_{n+1}^{n+1} - h_{n-1}^{n+1}}{2\Delta z} + 1 \right) \qquad (3.10)$$

for the corrector. Combining Eqs. (3.2) and (3.9), and Eqs. (3.3) and (3.10), the following were obtained for node n at the soil surface:

$$C_n^n \frac{h_n^{n+\frac{1}{2}} - h_n^n}{\frac{1}{2}\Delta t} = \left(\frac{K_n^n - K_{n-1}^n}{\Delta z} \right) \left(- \frac{q_n^{n+\frac{1}{2}}}{K_n^n} \right)$$

$$+ 2K_n^n \left[\frac{h_{n-1}^{n+\frac{1}{2}} - h_n^{n+\frac{1}{2}} - \Delta z - \Delta z\, q_n^{n+1}/K_n^n}{(\Delta z)^2} \right] + S(z,t) \qquad (3.11)$$

for the predictor, and

$$C_n^{n+\frac{1}{2}} \frac{h_n^{n+1} - h_n^n}{\Delta t} = \left(\frac{K_n^{n+\frac{1}{2}} - K_{n-1}^{n+\frac{1}{2}}}{\Delta z} \right) \left(- \frac{q_n^{n+1}}{K_n^{n+\frac{1}{2}}} \right)$$

$$+ K_n^{n+\frac{1}{2}} \left[\frac{h_{n-1}^{n+1} - h_n^{n+1} - \Delta z - \Delta z\, q_n^{n+1}/K_n^{n+\frac{1}{2}}}{(\Delta z)^2} \right.$$

$$\left. + \frac{h_{n-1}^n - h_n^n - \Delta z - \Delta z\, q_n^{n+1}/K_n^{n+\frac{1}{2}}}{(\Delta z)^2} \right] + S(z,t) \qquad (3.12)$$

for the corrector.

In order to incorporate the upper and lower boundary conditions requires the flux across these boundaries to be known at all time periods. The upper boundary (soil surface) flux can be determined using infiltration equations

(during rainfall events) and soil evaporation estimates. The lower boundary flux is not as easy to determine and is often used as a calibration parameter.

Eqs. (3.2), (3.7) and (3.11) for the predictor stage and Eqs. (3.3), (3.8) and (3.12) for the corrector stage lead in each stage to a set of linear equations of the form:

$$\begin{bmatrix} B_1 & C_1 & & & & \\ A_2 & B_2 & C_2 & & 0 & \\ & A_3 & B_3 & C_3 & & \\ & & \ddots & \ddots & \ddots & \\ & & & \ddots & \ddots & \ddots \\ & 0 & & & A_{n-1} B_{n-1} & C_{n-1} \\ & & & & A_n & B_n \end{bmatrix} \begin{Bmatrix} h_1 \\ h_2 \\ h_3 \\ \vdots \\ \vdots \\ \vdots \\ h_{n-1} \\ h_n \end{Bmatrix} = \begin{Bmatrix} D_1 \\ D_2 \\ D_3 \\ \vdots \\ \vdots \\ \vdots \\ D_{n-1} \\ D_n \end{Bmatrix} \qquad (3.13)$$

where h_i denotes the unknown pressure head and the other variables can be determined from given information. This tridiagonal matrix is diagonally dominant and can be solved by standard numerical techniques. The Thomas algorithm is recognized as being one of the most efficient in this respect (Remson et al., 1971) and was incorporated in this model.

Model Components

The major processes included in this model were soil water movement, infiltration, evapotranspiration, and deep

percolation. The main computer program was designed to control the general sequence and to call each process subprogram in its logical sequence. The computer program was designed using a modular system so as to allow easy modification by changing or inserting any system subprogram without affecting the general flow system. The flowchart of the main program is shown in Figure 6, and the description of subprograms is listed in Table 3.

Solution of flow equation

The major portion of this program is the subroutine FLOW which solves the finite difference equations developed in the previous section. The Douglas-Jones predictor-corrector method was used in this subprogram. FLOW sets up a tridiagonal system of equations with the computed specific water capacity and conductivity values. This tridiagonal matrix is solved by calling TRIDIA and the pressure head solution will be obtained. From the pressure head solution, FLOW determines wetting history, water content, specific water capacity and hydraulic conductivity by calling HYSTER, RETENT, and CONDUC, respectively.

The top boundary condition was not simple to handle. Traditionally, the top boundary condition has been specified as a value of water content or pressure head at the soil surface and iterating until the computed flux was acceptably

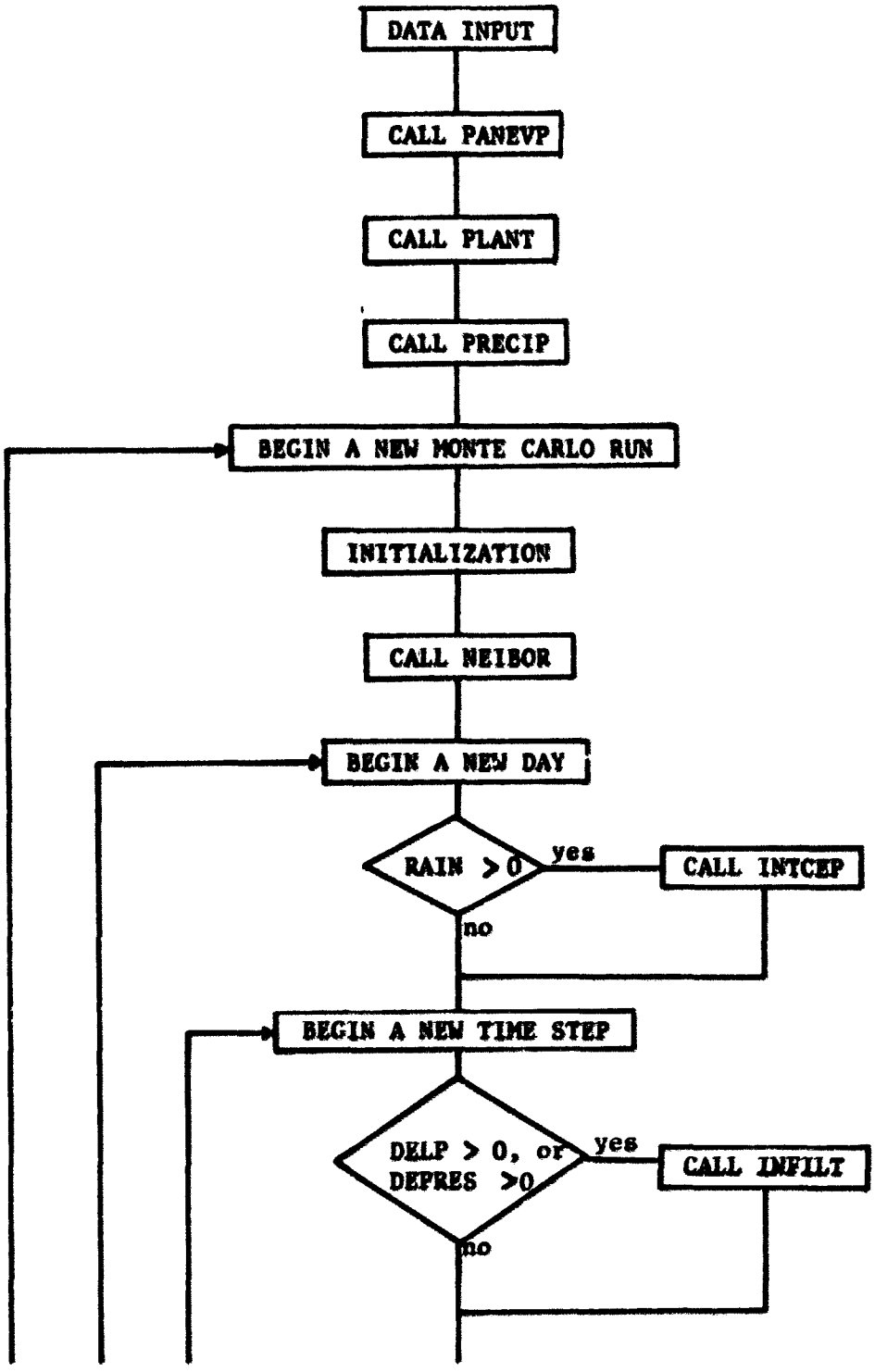

Figure 6. Flowchart of the main computer program

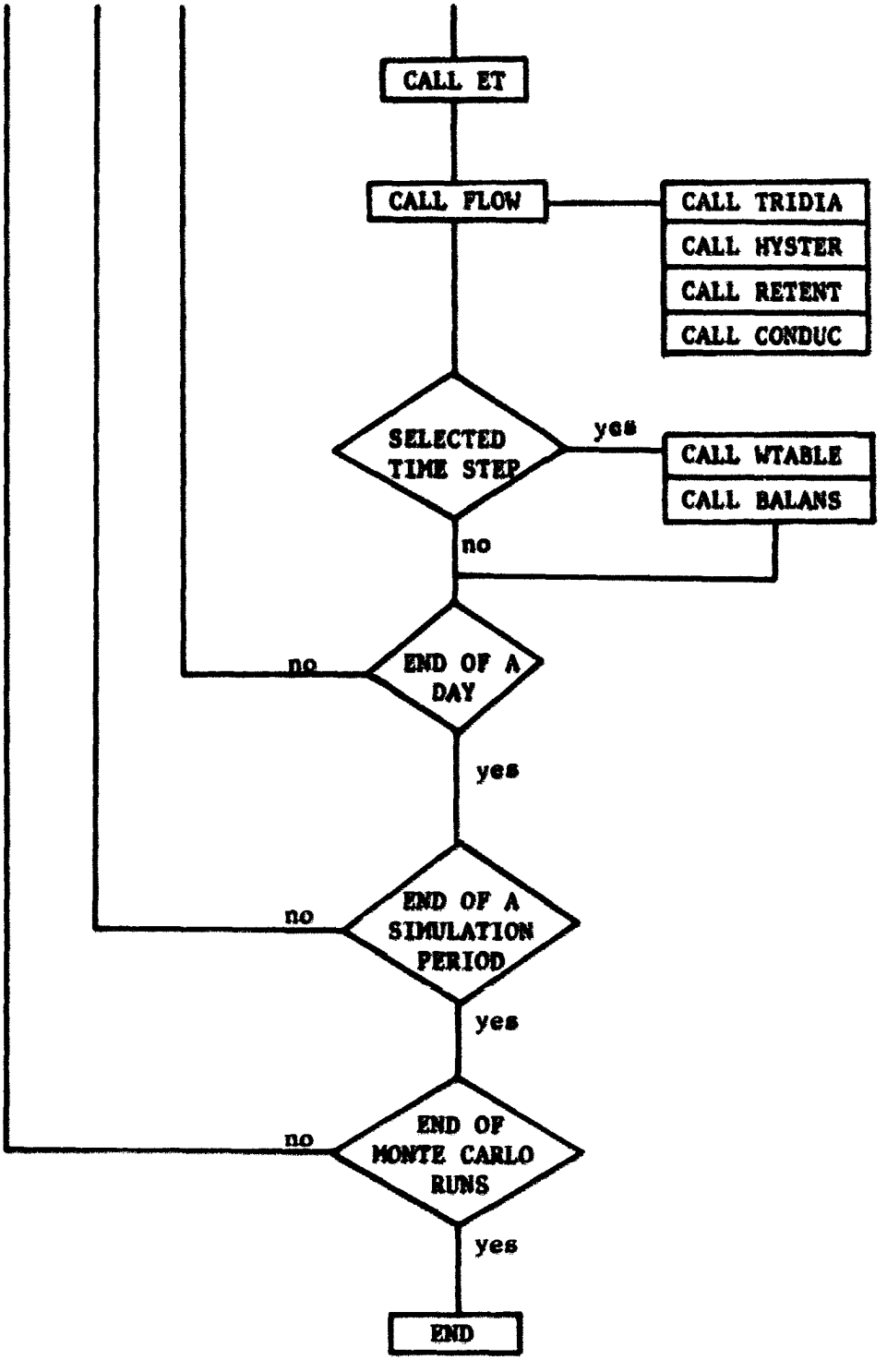

Figure 6 (Continued)

Table 3. Description of subprograms

Name	Description
BALANS	Computes water storage difference in the flow domain between, (1) from initial storage and boundary fluxes, and (2) from current water content in the soil profile
CONDUC	Computes hydraulic conductivity and specific water capacity
ET	Computes actual soil evaporation and plant transpiration
FLOW	Sets up and solves flow equations and computes coefficients of flow equations by calling subprograms
GGNML	IMSL library subroutine which generates normally distributed random numbers with mean zero and standard deviation one
HYSTER	Updates wetting history and computes water content evaluated at the wetting reversal value of pressure head on the main wetting curve
INFILT	Computes infiltration rate using modified Holtan's equation with Bailey's iteration method
INTCEP	Computes initial abstraction of a rainfall and determines amount of rainfall excess during a time step
NEIBOR	Computes stochastic saturated hydraulic conductivity distribution using first order nearest neighbor model
PANEVP	Computes hourly distributed potential evapo-transpiration rates from the daily pan evaporation data
PLANT	Computes plant root density distribution and crop leaf area index

Table 3 (Continued)

Name	Description
PRECIP	Computes average rainfall amount during a time step before initial abstraction
RETENT	Computes water content for a given pressure head and wetting history using Mualem's model
TRIDIA	Solves tridiagonal matrix problems
WTABLE	Computes water table depth from soil surface at a given time

close to the potential flux value. An alternative approach, introduced by Gilding (1983), did not need to iterate. First, the potential flux at the boundary was imposed in the flow equation and the system of equations was solved. Then, a check was made to determine whether or not the computed pressure head at the soil surface lies within the range of the predetermined maximum and minimum pressure head. If it does, this gives the desired solution. If the computed soil surface pressure head was not acceptable, the surface pressure head must take the violating maximum or minimum value, and the required solution is found by imposing this maximum or minimum pressure head as boundary condition. By indexing the nodal points increasing upwards as shown on Figure 5, the computation can be performed without any repetition. Applying the Thomas algorithm to solve the tridiagonal matrix given as Eq. (3.13), the top boundary pressure head solution can be checked immediately before the back substitution stage of the algorithm. Therefore, even if the value is set to the limiting constraint, this change does not affect anything already computed.

The actual surface flux can be computed from Eqs. (3.9) and (3.10) when the surface boundary has the limiting values. Pressure head at the imaginary point in Eqs. (3.9) and (3.10) can be computed from Eqs. (3.2) and (3.3) using the pressure head solutions for the real nodal points.

Hysteretic model

For the purpose of simulation of the flow model, a representation of the hysteretic soil water wetting-drying process is needed. Many empirical based analytical forms for the isothermal soil moisture characteristic have been proposed.

A series of papers (Mualem, 1973, 1974, 1977; Mualem and Dagan, 1975) has described a set of models which may be used to approximate the hysteresis in the soil water retention process. These conceptual models account for the capillary hysteresis effect discussed in the previous chapter. In his papers, Mualem hypothesized that a porous medium could be modeled as a continuous set of pore groups. Each pore group is defined by r, the radius of the pore opening in the group, and ρ, the radius of the pores in the group. The relative value of the medium occupied by a pore group is given by the distribution function $f(r,\rho)$. That is, $f(r,\rho)\, dr\, d\rho$, is the proportion of the bulk medium occupied by the pore group having opening sizes between r and $r+dr$ and having pore radii between ρ and $\rho+d\rho$. Mualem normalized r and ρ by defining:

$$\bar{r} = \frac{r - R_{min}}{R_{max} - R_{min}} \tag{3.14}$$

$$\bar{\rho} = \frac{\rho - R_{min}}{R_{max} - R_{min}} \tag{3.15}$$

where R = a parameter defined as R = C/h, where C is a constant and h is pressure head.

The radii $\bar{r}$ and $\bar{\rho}$ change in the range from zero to one, under the assumption that both r and ρ vary between R_{min} and R_{max}, which correspond to h_{min} and h_{max}, respectively. Then, the behavior of a pore is taken to be fully defined by $f(\bar{r},\bar{\rho})$ and is independent of the states of the surrounding pores. This is called an "independent domain model."

The volumetric water content of the medium is obtained at any time by integrating the pore group distribution function over the portion of the unit square in $\bar{r}$-$\bar{\rho}$ space that corresponds to the wetted pores. The extent of this region defines the wetting history of the medium. Mualem's diagrams for main wetting and drying processes as well as primary and higher order processes are shown on Figures 7 and 8. The shaded area represents saturated pores.

The process of wetting is defined by an increase in the radius of the air-water interface. In the main wetting process (Figure 7a), when the capillary head changes from h(R) to h(R+dR), all the pores with radii $\bar{\rho}$ between R and R+dR are wetted. In the main drying process (Figure 7b), when h reduces from h(R) to h(R-dR), the groups with pore radii $\bar{\rho}$ between R and R-dR and with opening radii $\bar{r}$ less than R are emptied.

Any subsequent reversals result in a more complex

-a- -b-

Figure 7. The filled pore diagrams in the $\bar{r}$, $\bar{p}$ plane for the main processes: (a) main wetting, (b) main drying (after Mualem, 1974)

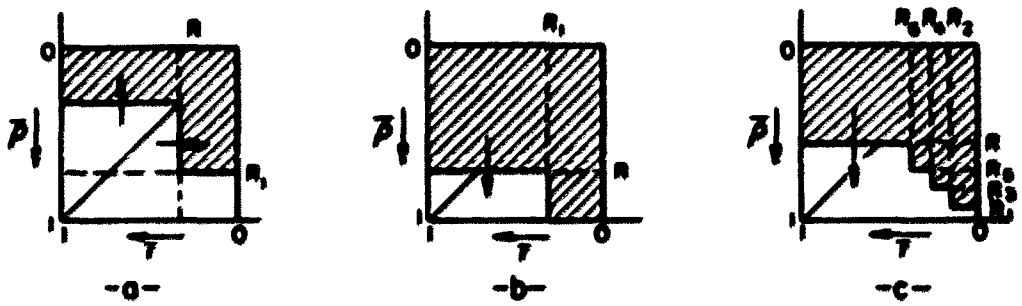

-a- -b- -c-

Figure 8. The filled pore diagrams in the $\bar{r}$, $\bar{p}$ plane for the scanning processes: (a) primary drying, (b) primary wetting, (c) wetting after six processes of imbibition and drainage (after Mualem, 1974)

situation. Figure 8 shows how the primary scanning curve and higher order scanning curve appear on the Mualem's diagram.

Mualem (1974) assumed that the pore group distribution function may be represented as a product of two independent functions as:

$$f(\bar{p}, \bar{r}) = \ell(\bar{p})\, m(\bar{r}) \qquad (3.16)$$

Eq. (3.16) constitutes the similarity hypothesis which says that the pores of any group are distributed according to the same distribution function.

The use of a conceptual model based on a capillary model of moisture retention to predict the behavior of hysteresis in the adsorption regime is open to question (Milly and Eagleson, 1980). However, Mualem (1977) found his model to be very good for pF up to 6, the highest value with which he worked.

In this study, Mualem's conceptual model was adopted with some modification for the higher order scanning curves.

The water content for any retention process can be determined by integrating Eq. (3.16) over the filled pore domain. As a matter of convenience, Θ is defined as:

$$\Theta(h) = \theta(h) - \theta_r \qquad (3.17)$$

where $\Theta(h)$ = effective water content,

$\theta(h)$ = actual water content, and

θ_r = residual water content, which is the minimum water content value at which $d\theta/dh$ approaches zero on a retention curve.

Mualem (1974) developed hysteretic water retention models for the primary and higher order scanning curves by integrating Eq. (3.16), and expressing the results in terms of two main curves. For the primary drying curve (Figure 8a):

$$\theta(h_{min}^{\ h_1}\ h) = \theta_w(h) + \frac{\theta_w(h_1) - \theta_w(h)}{\theta_u - \theta_w(h)} [\ \theta_d(h) - \theta_w(h)\ ] \tag{3.18}$$

For the primary wetting curve (Figure 8b):

$$\theta(^{h_{max}}_{\ h_1}\ h) = \theta_w(h) + \frac{\theta_u - \theta_w(h)}{\theta_u - \theta_w(h_1)} [\ \theta_d(h_1) - \theta_w(h_1)\ ] \tag{3.19}$$

where $\theta(h_{min}^{\ h_1}\ h)$ = effective water content at pressure head h after pressure head increased from h_{min} to h_1 (wetting) and then decreased to h (drying),

$\theta_w(h)$ = effective water content at pressure (suction) head h on the main wetting curve,

$\theta_d(h)$ = effective water content at pressure head h on the main drying curve,

$\theta_w(h_1)$ = effective water content at wetting reversal pressure head h_1 on the main wetting curve,

$\theta_d(h_1)$ = effective water content at wetting reversal pressure head h_1 on the main drying curve, and

θ_u = effective water content at saturation.

The relationship of Eqs. (3.18) and (3.19) are graphically illustrated on Figures 9a and 9b, where point 1 represents the wetting reversal point.

For the higher order scanning curves, which occur after a series of alternating processes of drainage and imbibition, water content can be determined by the same manner, applying integration from the Mualem's diagram using Eq. (3.16). However, the higher order scanning curves will introduce many operational problems as a results of the large number of variables. Therefore, simple models were developed from the equations for the primary curves by analogy.

For the higher order drying curves, $\theta_w(h_1)$ in Eq. (3.18) can simply be replaced by $\theta(h_1)$ by assuming that the higher order drying curves can be regarded as primary curves and can be extended vertically downward from the wetting reversal point to the main wetting curve as shown on Figure 9c. Then, for the higher order drying curves:

$$\theta(\ldots{}^{h_1}{}_h) = \theta_w(h) + \frac{\theta(h_1) - \theta_w(h)}{\theta_u - \theta_w(h)} [\, \theta_d(h) - \theta_w(h) \,] \quad (3.20)$$

where $\theta(\ldots{}^{h_1}{}_h)$ = effective water content at pressure head h after a series of drainage and

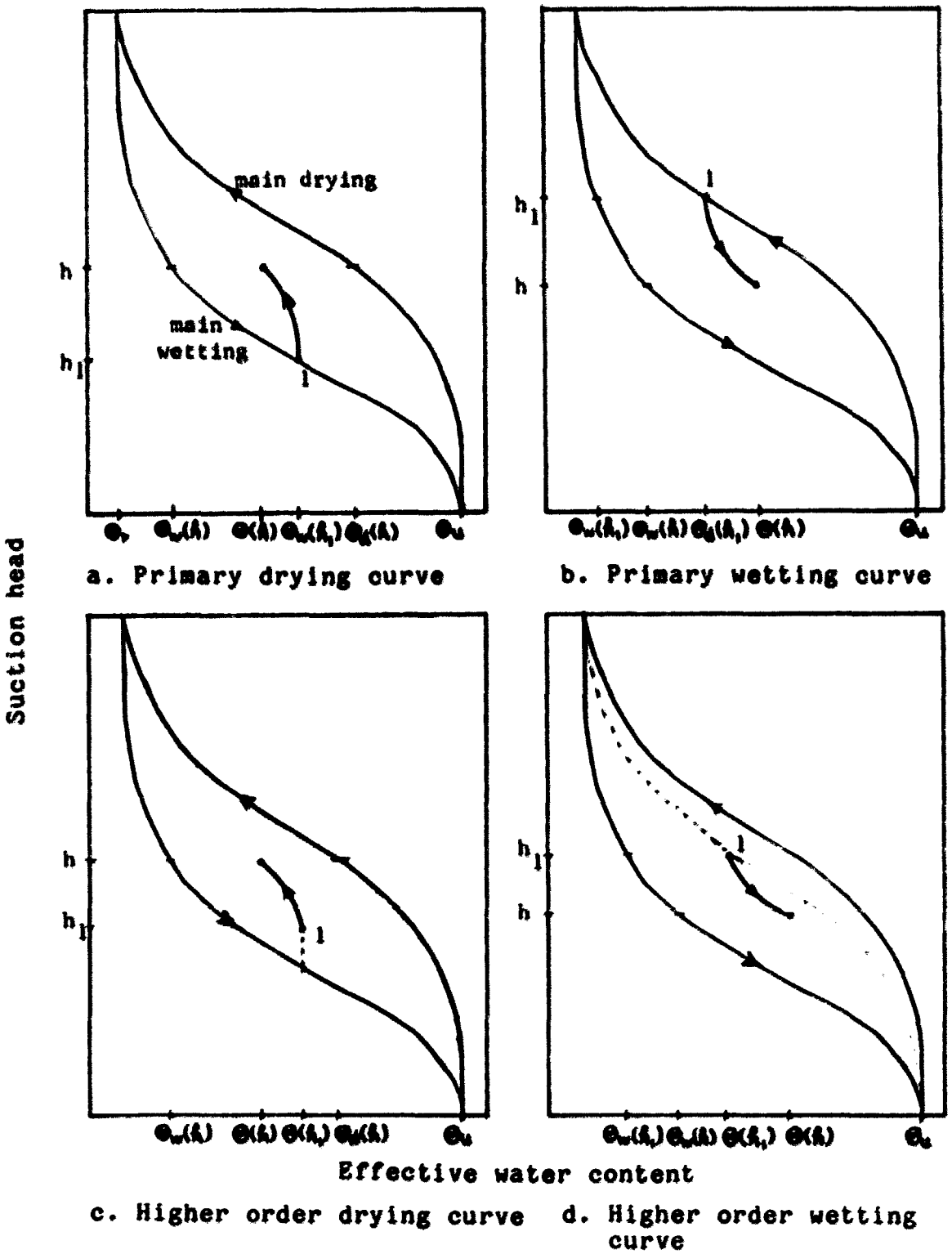

Figure 9. Primary and higher order scanning curves

imbibition and lastly pressure head decreased from h_1 to h, and

$\theta(h_1)$ = effective water content at the wetting reversal pressure head h_1.

For the higher order wetting curves, $\theta_d(h_1)$ in Eq. (3.19) can be replaced by $\theta(h_1)$ by assuming that an imaginary main drying curve (dashed line in Figure 9d) passes through the wetting reversal point 1 on Figure 9d. Then, for the higher order wetting curve:

$$\theta(\ldots_{h_1}{}^{h}) = \theta_w(h) + \frac{\theta_u - \theta_w(h)}{\theta_u - \theta_w(h_1)} \left[\theta(h_1) - \theta_w(h_1) \right] \quad (3.21)$$

where $\theta(\ldots_{h_1}{}^{h})$ = effective water content at pressure head h after a series of drainage and imbibition and lastly pressure head increased from h_1 to h.

Eqs. (3.18) to (3.21) are expressed in terms of two main curves. Preliminary study showed that these simplified models for the higher order scanning curves gave good results.

In a subsequent paper (Mualem, 1977), Mualem proposed an extended similarity hypothesis by assuming that the pore group distribution function may be represented by a one-variable function instead of a two-variable unknown function as:

$$f(\bar{\rho}, \bar{r}) = \ell(\bar{\rho})\, \ell(\bar{r}) \quad (3.22)$$

Using Eq. (3.22), Mualem showed that a universal hysteresis function can be derived. On the basis of one main curve, the other main curve and all scanning curves can be defined. The advantage of this model is that it greatly reduces the information necessary to define fully the water retention behavior of a soil. From this extended similarity hypothesis, the relationship between the two main curves can be derived as:

$$\theta_w(h) = \theta_u - [\, \theta_u(\, \theta_u - \theta_d(h)\,)\,]^{\frac{1}{2}} \tag{3.23}$$

and

$$\theta_d(h) = [\, 2 - \theta_w(h)\, \theta_u^{-1}\,]\, \theta_w(h) \tag{3.24}$$

By introducing either Eqs. (3.23) or (3.24) into Eqs. (3.18) to (3.21) the scanning curves can be expressed in terms of either one of the main curves. To express in terms of the main wetting curve, substitute Eq. (3.24) into Eqs. (3.18) and (3.19) for the primary curves:

$$\theta(h_{min}\ h_1\ h) = \theta_w(h) + \theta_w(h)\, \theta_u^{-1}\, [\, \theta_w(h_1) - \theta_w(h)\,] \tag{3.25}$$

$$\theta(h_{max}\ h_1\ h) = \theta_w(h) + \theta_w(h_1)\, [\, 1 - \theta_u^{-1}\, \theta_w(h)] \tag{3.26}$$

Now, Eqs. (3.23) to (3.26) can be expressed in terms of water content instead of effective water content by

substituting Eq. (3.17) into them:

$$\theta_w(h) = \theta_u - [\ (\theta_u - \theta_r)\ (\theta_u - \theta_d(h))\ ]^{\frac{1}{2}} \qquad (3.27)$$

$$\theta_d(h) = \theta_r + (\theta_w(h) - \theta_r)\ [\ \frac{2\theta_u - \theta_r - \theta_w(h)}{\theta_u - \theta_r}\ ] \qquad (3.28)$$

$$\theta(_{h_{min}}{}^{h_1}{}_{h}) = \theta_w(h) + [\ \frac{\theta_w(h) - \theta_r}{\theta_u - \theta_r}\ ]\ [\ \theta_w(h_1) - \theta_w(h)\ ] \qquad (3.29)$$

$$\theta(^{h_{max}}{}_{h_1}{}^{h}) = \theta_w(h) + [\ \frac{\theta_u - \theta_w(h)}{\theta_u - \theta_r}\ ]\ [\ \theta_w(h_1) - \theta_r\ ] \qquad (3.30)$$

Eqs. (3.27) and (3.28) are the relationships between the two main curves. Eqs. (3.29) and (3.30) are for the primary drying and wetting curves, respectively. The higher order wetting curves are obtained by substituting Eq. (3.17) into (3.21) as follows:

$$\theta(\ldots{}_{h_1}{}^{h}) = \theta_w(h) + [\ \frac{\theta_u - \theta_w(h)}{\theta_u - \theta_w(h_1)}\ ]\ [\ \theta(h_1) - \theta_w(h_1)\ ] \qquad (3.31)$$

For the higher order drying curves, Eq. (3.30) can be used by simply replacing $\theta_w(h_1)$ by $\theta(h_1)$.

In the computer programming, an approximate approach was used in determining wetting reversal points. The wetting history is spatially continuous and the wetting reversal occurs instantaneously between time steps. In the present model, however, a wetting reversal was assumed to

occur at any time step n at any node j when the water content at the node at the time step n is greater (less) than the water content at the time step n-1, where the node was previously drying (wetting). Then, the wetting reversal actually computed will precede the adoption of a new scanning curve by one time step.

This lag of wetting reversal can be removed by adopting a more rigorous procedure. But, considering the improvement of the accuracy of the model and the required efforts to implement the more rigorous procedure, it was decided not to adopt this rigorous procedure at this time.

Water content-pressure head relationship

The determination of the water content-pressure head relationship for a soil requires extensive field or laboratory measurements. For the field determination, several tensiometers at various depths and a neutron probe can be used for the pressure head and moisture content measurement, respectively. A neutron probe is very convenient since measurements can be read directly from the scaler and the corresponding water content found from a calibration curve. Other methods for determining water content were described in the previous chapter.

Laboratory determination of the water content-pressure head relationship has been widely used. A tension table or

pressure chamber is used for the determination of the soil water characteristic curve. The maximum tension attainable by a tension table is below 1 bar while the maximum tension attainable by a pressure chamber is below 20 bar, depending on the design of the chamber.

In determining soil water characteristic curves, the drying curve is measured by gradually extracting water from an initially saturated sample. This drying curve is applicable to the drying process such as drainage or evaporation. On the other hand, the wetting curve is needed whenever the wetting processes are concerned. For complete description of soil water retention curve, these two main curves and other scanning patterns at the wetting reversal are needed. Generally, the main drying curve is determined in the laboratory since the desorption method is easy to perform. The main wetting curve and the scanning curves can be calculated from the main drying curve by using Mualem's conceptual hysteresis model as discussed in the previous section.

Linear interpolation, cubic spline interpolation, or nonlinear regression models can be used to express mathematically the retention curve. The use of a regression equation is convenient because for a given value of the independent variable the value of the dependent variable is determined directly from the equation. In this study, the

same nonlinear parameters for the retention curve were used in the relative hydraulic conductivity model. Eq. (2.19) is used for the retention curve. Substituting effective saturation, S_e, which was defined in Eq. (2.18), into Eq. (2.19) gives:

$$\theta = \theta_r + (\theta_s - \theta_r) \left[\frac{1}{1 + (ah)^N} \right]^{1 - \frac{1}{N}} \qquad (3.32)$$

Retention data for the main drying curve, which were obtained from the laboratory measurement and Fritton et al. (1970) as shown in Appendix B, were used to determine the nonlinear regression parameters a, N and θ_r in Eq. (3.32). Those parameters were also used for the relative hydraulic conductivity model Eq. (2.20). Nonlinear parameters for the main wetting curve were determined from the retention data generated by Eq. (3.27) from the main drying data with the assumption that the residual water content is the same for the two curves. Fitted parameter values for the two main curves are included in Table 6. Figure 10 shows the fitted main retention curves using data from both laboratory measurements and Fritton et al. (1970) for a Webster silty clay loam.

Hydraulic conductivity and specific water capacity

The determination of hydraulic conductivity and specific water capacity for a given pressure head and water

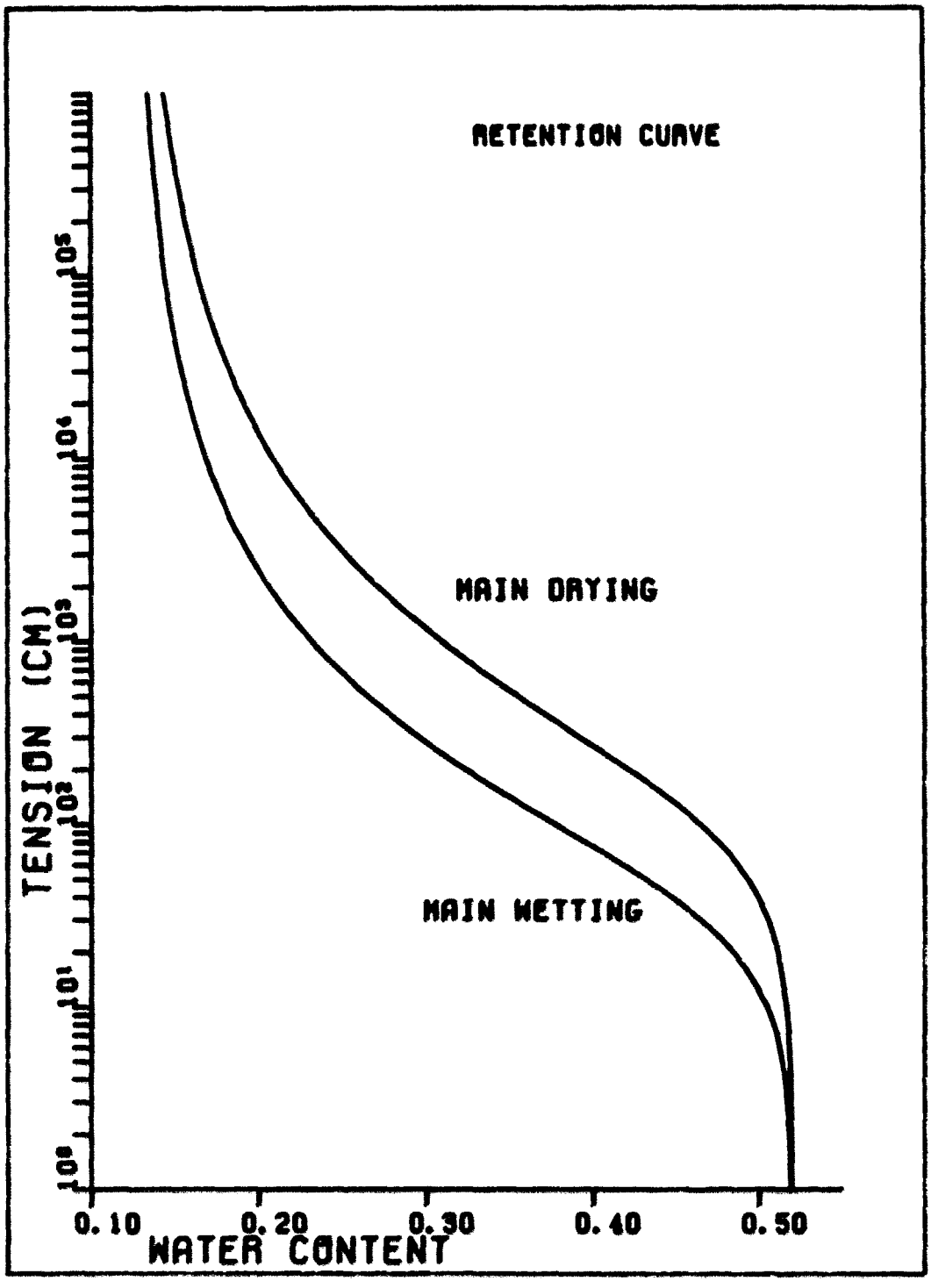

Figure 10. Main retention curves for Webster silty clay loam

content was done using the model developed by Van Genuchten (1980). Eq. (2.20) will be used to compute relative hydraulic conductivity for a given pressure head. However, the equation does not consider soil water hysteresis. Consequently, an additional consideration should be given for the hysteretic model. Two sets of nonlinear regression parameter values (one for drying and one for wetting) for the main curves were determined as explained in the previous section.

The generalized specific water capacity, C in Eq. (2.13), is either the slope of θ-h curve for the unsaturated zone or specific storage, S_s, for the saturated zone. The specific water capacity in the unsaturated zone was determined by differentiating Eq. (3.32). That is:

$$\frac{d\theta}{dh} = (N - 1)(\theta - \theta_r)\left[1 - \left(\frac{\theta - \theta_r}{\theta_s - \theta_r}\right)^{N/N-1}\right]/|h| \quad (3.33)$$

For a given value of h and θ, the specific water capacity and relative hydraulic conductivity for the scanning curves were determined by adjusting the parameters a and N by linear interpolation between the two main curves. Preliminary studies indicated a linear interpolation of the parameters a and N from the two main curves gave better prediction of the relative conductivity and specific water capacity than did linear interpolation of the relative conductivity and specific water capacity themselves from the

two main curves. Figure 11 shows the relative conductivity as a function of water content for the main wetting and drying curves for a Webster silty clay loam soil.

First order nearest neighbor model

Smith (1978), Smith and Freeze (1979a,b), and Smith and Schwartz (1980) used a nearest neighbor model in their stochastic analysis of saturated steady groundwater flow. The flow domain was divided into a finite set of discrete blocks. Saturated hydraulic conductivity values in neighboring blocks were autocorrelated by assuming that the spatial variations in conductivity could be represented by a first order nearest neighbor stochastic process model. Another assumption was that the distribution of saturated hydraulic conductivity values can be described by a stochastic process that was statistically homogeneous or stationary. Stochastic homogeneity requires that saturated hydraulic conductivity has the same expected value at every point in the domain and that the covariance between hydraulic conductivity at any two points depends only on the vector separating those points and not on their absolute position. The nearest neighbor model was designed to model spatial variations in a statistically homogeneous random field in which the stochastic dependence is local. It can be regarded as an autoregressive time series model extended

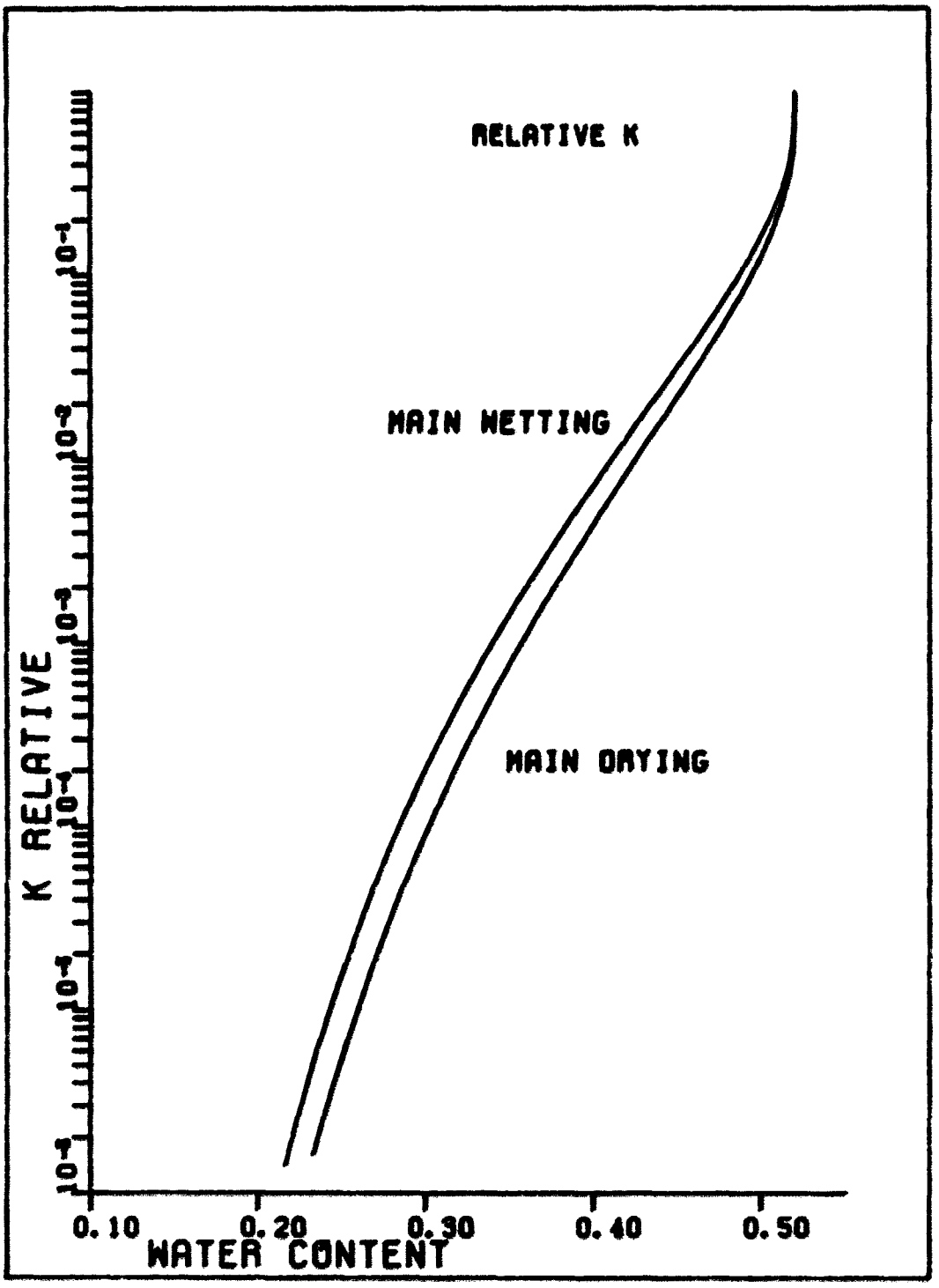

Figure 11. Relative hydraulic conductivity for Webster silty clay loam

into a spatial domain.

By dividing the flow domain into a set of square blocks for a two-dimensional domain or into blocks or layers for a one-dimensional domain, the correlation structure in the medium can be represented by an nth order nearest neighbor stochastic process model (Bartlett, 1975), where n is the number of blocks that are spatially correlated to a given block. Conductivity values in the block system are related through a simple linear equation expressing the dependence of the conductivity in one block upon those in surrounding blocks. In this study, only the saturated hydraulic conductivity was considered as a stochastic variable.

Saturated hydraulic conductivity, K_s, has been found to be log normally distributed (Willardson and Hurst, 1965; Nielsen et al., 1973; Baker and Bouma, 1976), that is, if $Y=\log K$, then Y is distributed as a normal probability density function. Various possible values of saturated hydraulic conductivity can be generated from the nearest neighbor model in such a manner to preserve the spatial correlations. For any block i in a one-dimensional domain, the nearest neighbor model used was (Smith, 1978; Smith and Freeze, 1979b):

$$Y_i = \frac{\alpha}{2} (Y_{i-1} + Y_{i+1}) + n\varepsilon_i \qquad (3.34)$$

where Y_i = random variable satisfying the nearest neighbor relation,

α = an autoregressive parameter,

ϵ_i = normally distributed random numbers with mean zero and standard deviation one, and

η = a factor multiplied to ϵ_i to yield a predetermined standard deviation σ_y.

The autoregressive parameter, α, expresses the degree of spatial dependence of Y_i upon its neighboring values and can be determined from field data. For one-dimensional flow, η is given by:

$$\eta = \sigma_y \left[\frac{\alpha^2}{2} + 1 - 2\alpha\rho(1) + \frac{\alpha^2\rho(2)}{2} \right]^{\frac{1}{2}} \qquad (3.35)$$

where σ_y = predetermined standard deviation of Y,

α = an autoregressive parameter, and

$\rho(1)$ and $\rho(2)$ = spatial autocorrelation coefficients for lag 1 and 2, respectively.

Autocorrelation functions can be obtained from each of the realizations generated during a Monte Carlo simulation. Smith and Freeze (1979a) show a change of autocorrelation function with respect to the values of autoregressive parameter as shown in Figure 12.

From Eq. (3.34), one equation was obtained for each block located in the domain. For boundary blocks, Eq. (3.34) was changed accordingly. This resulted in a set of n simultaneous linear equations that needed to be solved for log saturated hydraulic conductivity at each layer or block.

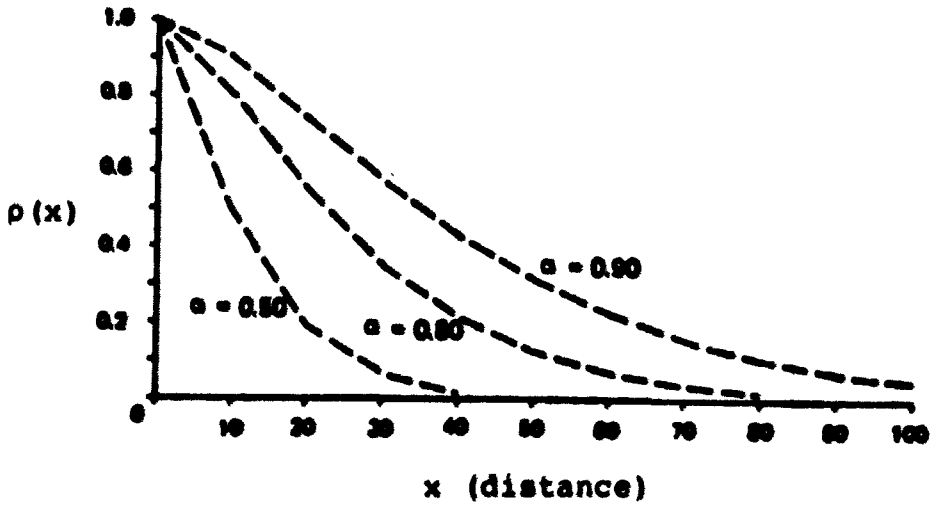

Figure 12. Effect of the autoregressive parameter (α) on the autocorrelation function, one-dimensional model (after Smith and Freeze, 1979a)

A saturated conductivity realization is generated by first selecting n independent values of ϵ_i. Then, compute η from known σ_y and ρ. Next, the system of equations is solved for the values of Y_i, yielding an internally correlated sequence of random variables satisfying the nearest neighbor relation. At this time, Y_i has mean zero and standard deviation σ_y. Therefore, the mean μ_y must be added to each Y_i to produce a realization that was normally distributed with mean μ_y. Finally, an exponential transformation was applied to obtain the saturated hydraulic conductivity for each block in a soil layer.

In this study, no hydraulic conductivity field data were available to determine the autoregressive parameter in Eq. (3.34). Therefore, a value of 0.35 was chosen from the

previous study by Smith (1978) considering the soil type in the study area. The autocorrelation coefficients for lag 1 and 2 were determined from Figure 12 by extrapolation.

The nearest neighbor model discussed is only for a statistically homogeneous flow domain. Therefore, if a flow domain is composed of a statistically nonhomogeneous layered geologic formation, each statistically homogeneous soil layer should be treated individually. In this case, there must be some correlation between the two blocks across the adjacent geologic soil layer interface because according to Bennion and Hope (1974) the field hydraulic conductivity was continuously distributed even though a soil showed statistical nonhomogeneity. However, no theory has been introduced in this respect. So, each statistically homogeneous soil layer was treated individually with no correlation between the two blocks across the soil layer interface in this study.

Monte Carlo simulation

The Monte Carlo method in stochastic groundwater studies involves repetition of a number of simulations using a mathematical model to have enough sets of outputs to perform a statistical analysis.

In each Monte Carlo run, a different set of the saturated hydraulic conductivities for all the nodal points

in the discretized flow system was determined using the first order nearest neighbor model. This model insures that the mean, standard deviation, and spatial correlation found in the field data were preserved in each Monte Carlo run. With these hydraulic conductivity values, a Monte Carlo run was made using the mathematical flow model for the length of the simulation period. The same procedure was repeated until the required number of Monte Carlo runs were made.

All the sets of outputs from each Monte Carlo run were then used to perform a statistical analysis to determine the means and standard deviations of the output variables.

Initial and boundary conditions

In order to solve the boundary value problem, two conditions were needed, namely initial and boundary conditions. The initial values of pressure head or water content at the beginning of the simulation period must be specified over the system domain. In addition, wetting history information must be given for a hysteretic model.

Two boundary conditions, top and bottom, were needed for the one-dimensional vertical flow problem. Top boundary condition was specified on the soil surface. Infiltration or evaporation was the major component of the top boundary flux across the soil surface. The following assumptions were made with respect to the top boundary flux:

1. The soil surface is near horizontal, and the moisture fluxes are normal to the surface.

2. Excess rainfall will be stored on the soil surface up to a maximum detention capacity and further excess will be discharged as surface runoff.

3. No lateral inflow on the soil surface into the system exists.

With these assumptions various boundary condition states can be defined as results of different rainfall and evaporation intensities. These states of the soil surface are:

1. At the beginning of a rainfall assuming the soil surface is not saturated, infiltration begins at the rainfall intensity with no surface retention or runoff. This state was the unsaturated infiltration state.

2. As rainfall continues beyond some critical time period, the soil surface reaches saturation, and the infiltration decreases. This was defined as the saturated infiltration state.

3. As rainfall continues, surface retention occurs followed by surface runoff beyond the retention capacity.

4. When rainfall ends, the retained water was depleted by evaporation and infiltration. Water infiltrates as long as there existed detention water on the soil surface. When the water on the soil surface was completely depleted, the

surface flux was only from evaporation. This was defined as the evaporation state.

All the states do not occur for all meteorological conditions, but depend upon the rainfall duration and intensity. The infiltration and evaporation will be discussed more in the following sections.

The bottom boundary flux condition was determined during the model calibration process. A fixed value of bottom boundary flux was used throughout the simulation period.

Precipitation

Published weather data generally give daily or hourly rainfall amounts. Incremental rainfall data can be obtained easily by installing a recording rain gauge on an experimental site. The precipitation data used in this model include the rainfall amount, and the beginning and ending time of the rainfall. These rainfall periods were then subdivided into several subperiods such that the rainfall intensity in a subperiod was nearly constant. That is, the subperiods were determined from changes of slope on a rain gauge mass curve chart.

The input data were the amount of rainfall, starting time and ending time of each subperiod. The subprogram PRECIP computes rainfall amount in each time step (0.2 hr).

If no rainfall exists for a day all the incremental rainfall amount was set to zero.

Interception

A simple interception subprogram was included in this model. During a rainfall event, water was intercepted by plants. Part of the intercepted water may flow down to the soil surface along the plant stem. However, the flow along the plant stem was not considered in this model.

The interception storage is a function of crop type and crop leaf area. In this study, the maximum potential interception storage was determined as a linear function of crop leaf area index (CLAI) for CLAI less than or equal to 3 following Anderson (1975):

INTCEP = 0.038*CLAI (3.36)

where INTCEP = potential interception in cm.

Infiltration

Holtan's infiltration equation (Holtan, 1961) modified by Huggins and Monke (1968) was used in this model. This method was successfully used in watershed modeling by DeBoer (1969) and Anderson (1975). A computer program by Anderson (1975) was incorporated in this model with minor changes. The main advantages of the modified Holtan's infiltration equation are the ability to determine infiltration during

periods of intermittent water supply, to predict infiltration recovery during dry periods, and the ease of computation. The modified Holtan's equation used was:

$$f = f_c + A\left(\frac{S - F}{T}\right)^P \qquad (3.37)$$

where f = average infiltration capacity during a time period, cm/hr.

f_c = wet soil infiltration capacity, cm/hr.

S = soil water storage potential above any impeding strata, cm.

F = accumulated infiltration, cm.

T = total pore volume above any impeding strata, cm.

A = a soil parameter representing the maximum potential increase of infiltration capacity above the wet soil value, cm/hr, and

P = a soil parameter representing the steepness of the slope of the infiltration capacity curve at the beginning of the infiltration process.

The initial infiltration capacity and the rate of decrease of infiltration capacity during a rainfall are a function of soil type, antecedent moisture content, plant cover and rainfall intensity. The parameters A and P in Eq. (3.37) were adjusted based on the antecedent moisture content in the top 15 cm soil layer just before the first rainfall event in a day. The function used for estimating

the parameter A was:

$$ASOIL = ASOILM * EXP(AM\ (AMC-FCS)) \quad (3.38)$$

where ASOIL = adjusted parameter A,

ASOILM = maximum value of ASOIL,

AM = fitted parameter to be determined,

AMC = antecedent moisture content in top 15 cm soil layer, %, and

FCS = field capacity of the top soil layer, %.

To consider the effect of crop growth on infiltration capacity, one half of the crop leaf area index for CLAI less than or equal to 3 was added to the adjusted ASOIL.

The function used for estimating the parameter P was:

$$PSOIL = PSOILM * (AMC/FCP)^{**PM} \quad (3.39)$$

where PSOIL = adjusted parameter P,

PSOILM = PSOIL value for AMC equal to field capacity of top 15 cm soil layer, %,

FCP = field capacity of top 15 cm soil layer, and

PM = exponential parameter to be determined.

The effect of rainfall intensity on infiltration was estimated by using the rainfall kinetic energy. Infiltration capacity reduces exponentially with increasing rainfall kinetic energy (Moldenhauer and Kemper, 1969). This reduction is primarily due to the compacting effect of rainfall kinetic energy, destruction of soil structure and consequent soil dispersion, and the blocking of pores by

fine soil particles. The equation used to estimate the reduction factor, which was called rainfall energy factor (REF), was:

$$REF = CE1 * SRKE^{-CE2} \tag{3.40}$$

where SRKE = summation of rainfall kinetic energy from the time of tillage, Joules/cm^2, and

CE1, CE2 = constants to be determined.

The rainfall energy factor varies between 0 and 1. Rainfall kinetic energy for each time period was calculated following Wischmeier and Smith (1978):

$$RKE = DDP\ (0.06133 + 0.02216\ \text{Log}\ DINT) \tag{3.41}$$

where RKE = rainfall kinetic energy during the calculation period, Joules/cm^2,

DDP = amount of direct rainfall after interception during the calculation period, in., and

DINT = intensity of rainfall during the calculation period, in/hr.

The computational procedure used to determine the infiltration capacity was adopted from Holtan et al. (1967). First, set up an inequality:

$$\frac{F_2 - F_1}{\Delta t} \leq \frac{1}{2} (f_1 + f_2) \tag{3.42}$$

Substitute Eq. (3.37) into Eq. (3.42) and rearranging to obtain:

$$f(F_2) = \frac{F_2 - F_1}{\Delta t} - \frac{A}{2}\left(\frac{S - F_1}{T}\right)^P - \frac{A}{2}\left(\frac{S - F_2}{T}\right)^P - f_c \leq 0 \tag{3.43}$$

Eq. (3.43) is solved by a numerical iteration method to determine the maximum possible F_2 at the end of a time period from a known starting value F_1. Either Newton's method or Bailey's method can be used for the iterative solution of Eq. (3.43). The Newton's method has quadratic convergence while Bailey's method has cubic convergence (McCalla, 1967). Bailey's method is:

$$F_2^{n+1} = F_2^n - \frac{f(F_2^n)}{f'(F_2^n) - \dfrac{f(F_2^n)\ f''(F_2^n)}{2f'(F_2^n)}} \tag{3.44}$$

where superscript n is an iteration step, and primes are first and second derivatives. Eq. (3.44) can be derived from the truncated Taylor series expansion. Details can be found in McCalla (1967). DeBoer (1969) showed that Bailey's method was the most efficient among several iterative methods he compared. Bailey's method was adopted in this study.

After surface saturation the excess water beyond infiltration capacity was allowed to stay on the soil surface as depression storage. When the maximum depression storage was reached, the excess water was forced to runoff and was removed from the system.

Potential evapotranspiration

The potential evapotranspiration rate was calculated from daily pan evaporation data. A regression equation for brome grass developed by Saxton et al. (1974b) was used in this study. The regression equation was:

$$PET = 0.025 + 0.83 * PAN \quad (3.45)$$

where PET = daily potential evapotranspiration, cm, and

PAN = daily pan evaporation, cm.

The hourly distribution of the potential evapotranspiration of each day cannot be determined exactly since no such data were available. The distribution of daily potential evapotranspiration was assumed following Anderson et al. (1978). Six four-hour periods are used to distribute the daily PET in such a way that:

Midnight to 4:00 a.m.	:	2.4 % of daily PET
4:00 a.m. to 8:00 a.m.	:	4.8 %
8:00 a.m. to 12:00 noon	:	29.0 %
12:00 noon to 4:00 p.m.	:	39.7 %
4:00 p.m. to 8:00 p.m.	:	19.5 %
8:00 p.m. to midnight	:	4.6 %

Evapotranspiration

Actual evapotranspiration should be calculated from the potential evapotranspiration. The method developed by Saxton et al. (1974b) was used with some simplification.

The PET was divided into three parts. First, the PET energy was used to evaporate interception storage. The remaining PET energy was divided between potential soil evaporation and potential transpiration according to a canopy shading percentage. Ritchie (1972) related the fractional net radiation at the soil surface and the crop leaf area index for several different row crops. The relationship was:

$$R_{ns} = R_{no} * EXP (-0.398*CLAI) \quad (3.46)$$

where R_{ns} = net radiation at the soil surface (mm/day),

R_{no} = net radiation above the crop canopy (mm/day),

CLAI = crop leaf area index.

Saxton et al. (1974b) gave calculated values of soil evaporation, plant transpiration and root density distribution for corn and brome grass.

Actual soil evaporation was assumed to occur only in the top 15 cm of soil. Actual soil evaporation was reduced from the potential value by the relationship of actual/potential evaporation ratio versus soil moisture content in the top 15 cm of soil. Figure 13, which is simplified from Saxton et al. (1974b), shows this relationship used in this study.

Potential transpiration should be distributed in the root depth after considering the plants' phenological state which depicts their ability to transpire. Plant root density distribution was used to assign a percentage of

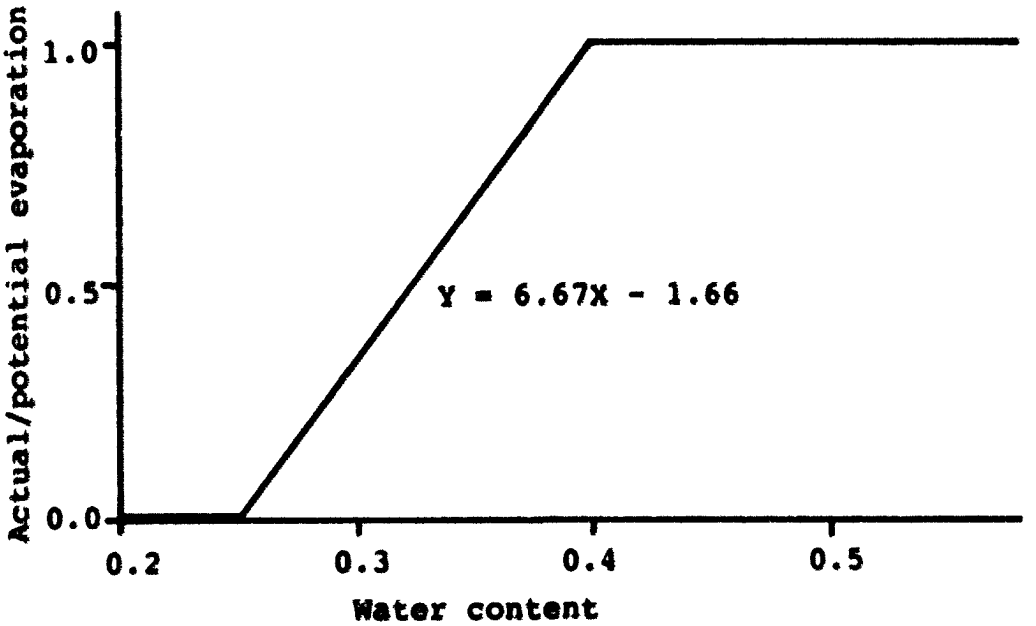

Figure 13. Relation used to calculate actual evaporation developed from data on loess soils near Treynor, Iowa (Saxton et al., 1974b)

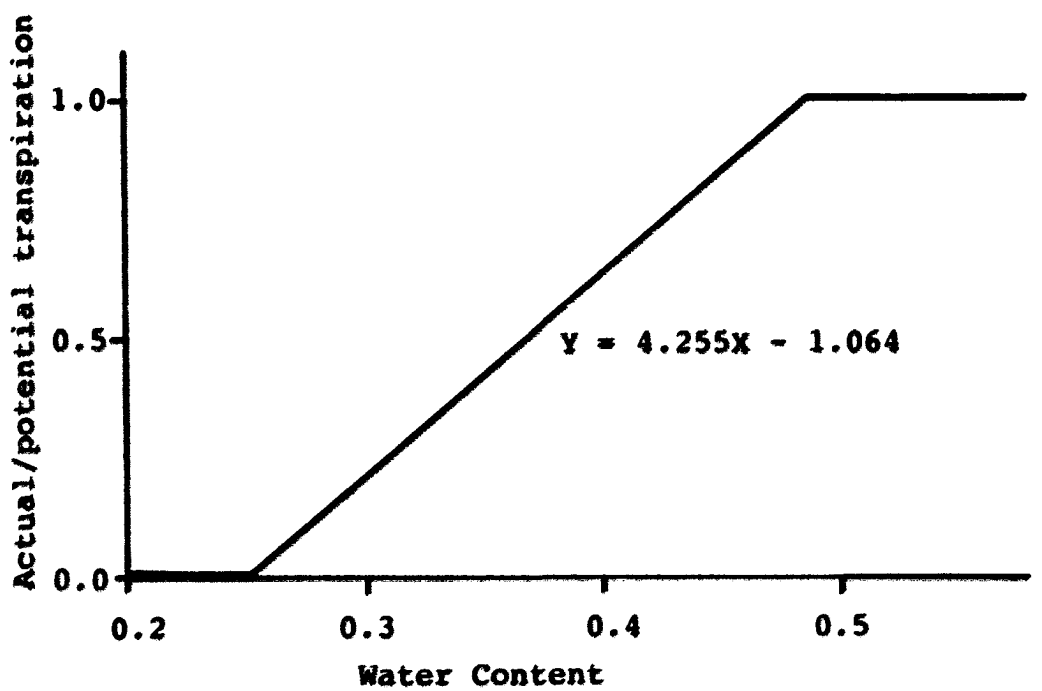

Figure 14. Relation used to calculate actual transpiration developed from data on loess soils near Treynor, Iowa (Saxton et al., 1974b)

potential transpiration to each nodal point in the discretized flow domain. Potential transpiration was reduced according to the moisture availability. The actual/potential transpiration ratio depends upon the soil moisture content and the total PET demand by the atmosphere. A linear relationship simplified from Saxton et al. (1974b) for PET value of 0.65 cm/day for grass was developed as shown in Figure 14. The unused energy in a layer was transferred to the next lower soil layer.

Plant system

The plant system was considered in this model. Infiltration and evapotranspiration components of the hydrologic cycle are closely interrelated through the plant system, since the amount of soil moisture stored in the root zone affects both the infiltration rate and evapotranspiration rate.

Crop canopy development, root system development, and fraction of existing crop canopy which is actually transpiring are three major factors which are important in water balance model. Different values of these factors at different stages of growth should be given to the model. However, because of the short period of simulation length in this model, a constant value for the crop canopy development and the root system development with a total root depth of

65 cm were used for simplification. Additional subroutines could be added at a later date.

Molz and Remson (1970) developed an equation for the extraction pattern of plant roots by reasonably distributing the total transpiration requirement as 40%, 30%, 20%, and 10%, respectively to each successively deeper part of the root zone. That was given by:

$$W(z) = -\frac{1.6T}{v^2} z + \frac{1.8T}{v} \qquad 0 \leq z \leq v \qquad (3.47)$$

where W(z) = root extraction rate from a differential volume,

z = soil depth from which root extraction occurs,

v = total root zone depth, and

T = total transpiration.

Then, the total extraction rate from a volume of soil of unit cross section bounded by horizontal planes $z = z_1$ and $z = z_2$ where $z_1 < z_2$ was obtained by integration:

$$\int_{z_1}^{z_2} W(z)\, dz = -\frac{1.6T}{v^2} \frac{z^2}{2}\Bigg|_{z_1}^{z_2} + \frac{1.8Tz}{v}\Bigg|_{z_1}^{z_2} \qquad (3.48)$$

Eq. (3.48) was used to distribute potential transpiration in this model. Subprogram PLANT was called only once since a constant root distribution and crop leaf area index were used for the short simulation period in this model.

Computer Program

The numerical model described in this chapter has been coded in the FORTRAN language for computer execution. The WATFIV compiler was used on the AS/6 computer system at Iowa State University. The computer program listing appears in Appendix A.

CHAPTER IV. CALIBRATION AND TEST OF THE MODEL

Introduction

The performance of a numerical model should be evaluated to examine its validity because any numerical scheme may introduce instability, truncation and round off errors. A model is valid only if the approximate solution is satisfactorily accurate or close to the exact solution if one exists. The accuracy of a model can be more specifically defined in terms of its convergence and stability.

Convergence is satisfied when the approximation approaches the exact solution as step sizes of the spatial and temporal discretization approach zero. A model is said to be stable if the amplification of the error is restricted or has a finite limit as computation marches forwards in time.

The validity of a model can be tested by comparing the numerical solution with either an analytical solution, if it is available, or observed data.

In this chapter, the experimental plots, field and laboratory measurement, calibration, and test of the model are discussed.

Description of the Experimental Plots

Field measurements were made on a farm located two miles east and three miles north of Harcourt, Webster County, Iowa. The reason for selecting the experimental site near Harcourt was that there is a U.S. Geological Survey observation well which has long term records of water table elevation. This record gives the range of water table fluctuation and can be used as a reference.

The experimental area is nearly flat, with a slope of 0 to 2 percent, and the soil in the area is classified as Webster silty clay loam (Soil Conservation Service, 1975). The experimental site was planted in grass meadow with surrounding land planted in corn. The nearby farm land was tile drained at about 1 meter below the soil surface.

Soil profile description of the study area was obtained from field observation during the installation of the instruments and from the Webster County soil survey (Soil Conservation Service, 1975). In addition, the driller's log for the U.S. Geological Survey observation well, located 37 meters southeast of the experimental plots, was available and referenced in determining the soil profile description. Table 4 shows the description of the soil profile of the area.

The field experiment was composed of three plots, one water table well, and one recording rain gauge. Each plot

Table 4. Soil profile description of study area

Depth (cm)	Horizon	Texture	Description
0- 20	A_p	Silty clay loam	Black
20- 50	A	Silty clay loam	Dark brown
50-100	B	Clay loam	Olive-gray Gracial till
100-160	C	Loam	Light olive-gray Gracial till

contained a 1.5 m deep aluminum neutron access tube and 8 tensiometers around the tube at depths of 10 cm to 150 cm with 20 cm intervals. Two plots were used for measurements of pressure head and water content for the natural weather condition and the third plot was used for measurement of infiltration rate by surface ponding. The water table well was a 1.8 m deep perforated plastic pipe with 3.8 cm diameter. A standard 8" recording rain gauge was installed near the plots. Figure 15 shows the layout of the experimental site.

Field and Laboratory Measurements

Field measurements included precipitation, soil water content, pressure head, and water table elevation. Three runs were made in the ponding plot to measure infiltration rates at different antecedent moisture contents. Field

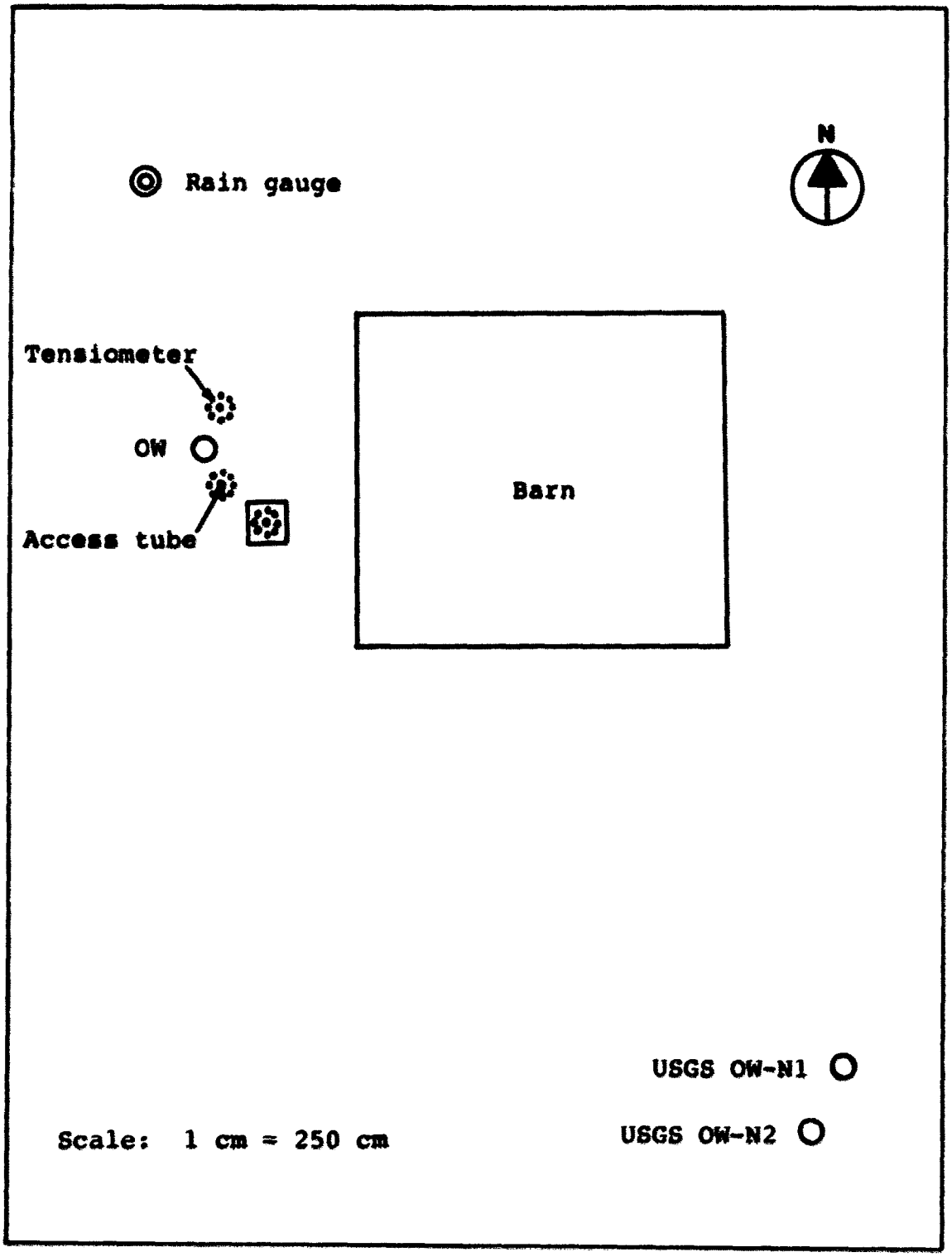

Figure 15. Layout of the experimental plot

measurements were made for 7 weeks with two readings per week. Rainfall data were collected from the recording rain gauge. A portable pressure transducer was used to measure the moisture tension (pressure head) in the tensiometers. A neutron depth meter with scaler, manufactured by TROXLER, was used to measure soil water content. However, because of the availability of the neutron meter, and problem with its operation, it could not be used after the initial observations. Tensiometer readings gave consistent numbers except for some readings from the 10 cm and 30 cm depths when the soil surface was very dry and cracks allowed air entering into the soil near the porous cups. The water table elevation was measured from the observation well installed.

The flow system domain included the top 160 cm of soil. It was selected considering the range of water table fluctuation during the simulation period and the depth of the tensiometers installed. The system domain was divided into two layers considering the soil profile description in the site. The top layer was 100 cm in thickness and the bottom layer was 60 cm in thickness.

The laboratory measurements included porosity, saturated hydraulic conductivity, water content of the soil samples, and soil water retention. A falling head permeameter described by Bouwer (1978) was used for

conductivity measurements. Soil water retention for the drying curve was determined using both a pressure funnel and a pressure plate. The former measured tensions from 0 to 400 cm of water and the latter up to 15 bar. Laboratory setups in the soil physics lab at Iowa State University were used for the retention measurements. Undisturbed soil samples with 7.6 cm diameter and 7.6 cm depth were taken from the field site using a undisturbed soil sampler.

Three soil samples were used to determine porosity after the retention measurements were made. Dry bulk density of the soil samples were determined by drying and weighing three samples. The porosity was determined from the relationship:

$$n = \frac{V_v}{V_t} = 1 - \frac{\rho_b}{\rho_s} \qquad (4.1)$$

where V_v = volume of the void,

V_t = volume of the total soil sample,

ρ_b = dry bulk density, and

ρ_s = density of soil particle, assumed to be 2.65.

Table 5 shows the average soil parameter values obtained from the laboratory measurements. Although there were only few data points, the standard deviations were determined for the porosity, dry bulk density, and saturated hydraulic conductivity in the top layer to be 0.05 cm^3/cm^3, 0.13 gr/cm^3, and 0.19 cm/hr, respectively. The top layer has larger porosity and smaller hydraulic conductivity than the

Table 5. Soil water parameter values used in the model

Parameter	Bottom layer	Top layer
Depth from surface	100-160 cm	0-100 cm
Porosity	0.48 cm^3/cm^3	0.52 cm^3/cm^3
Dry bulk density	1.378 gr/cm^3	1.272 gr/cm^3
Saturated hydraulic conductivity	0.67 cm/hr	0.58 cm/hr

bottom layer does.

Data Availability

Water table elevation, soil water pressure head, and precipitation were obtained directly from the field measurements. Porosity, water content, saturated hydraulic conductivity and soil water retention for the drying curve were obtained from the laboratory measurements. No evaporation data were available at the vicinity of the experimental site, so, daily pan evaporation data from the ISU Agronomy farm west of Ames, Iowa, which was located about 50 Km southeast from the site, were used.

Soil water retention data for the Webster silty clay loam were available from Fritton et al. (1970) which were considered together with laboratory data in determining retention equation parameters.

Calibration of the Model

Calibration is a process to adjust some of the parameter values to fit the results of the mathematical model with the measured values. Parameters which cannot be determined or are hard to estimate can be approximated through the calibration process.

Estimation of model parameters can be done either by trial and error or by computerized search. A trial and error method was applied in this study. Each parameter was assigned an initial value and varied over a reasonable range. The difference between the observed and computed water table elevations and pressure head distribution for each set of parameter values were compared. This procedure was continued until the difference was within the satisfactory range, and the parameter values for the minimum difference were selected.

Data collected at the field site during the period July 21 to August 1, 1984, were used in the calibration process. During this period, there were rainfall events and fluctuating water table elevation. Calibrated values for CE1 and CE2 in the rainfall energy factor equation (3.40) by Shahghasemi (1980) were used. Table 6 shows the calibrated parameter values. The stochastic property of the soil water property was not introduced in the calibration stage.

The fluctuation in the simulated water table elevation

Table 6. Parameter definitions and calibrated values as used in the model

Parameter	Parameter definition	Calibrated value
S_s[a]	Specific storage of the unconfined aquifer	0.00010 cm
FLUX1[a]	Boundary flux across the bottom boundary	0.0010 cm/hr
COND	Wet soil infiltration capacity, f_c in Eq. (3.37)	0.58 cm/hr
DEPRES	Maximum depression storage	1.0 cm
ASOILM	Maximum value of ASOIL in Eq. (3.38)	36.0 cm/hr
AM	Exponential coefficient used in ASOIL equation, Eq. (3.38)	-0.120
PSOILM	Value of PSOIL at the field capacity of the top 15 cm soil layer in Eq. (3.39)	1.480
PM	Exponential coefficient used in PSOIL equation, Eq. (3.39)	0.20
FCS	Field capacity of top 15 cm soil layer in Eq. (3.38)	28.96%
FCP	Field capacity of top 15 cm soil layer in Eq. (3.39)	28.96%
CE1	Coefficient in the rainfall energy factor equation, Eq. (3.40)	0.125
CE2	Exponential coefficient in the rainfall energy factor equation, Eq. (3.40)	1.25
ALPA	Autoregressive coefficient in the nearest neighbor model	0.35

[a]Varied during calibration run.

Table 6 (Continued)

Parameter	Parameter definition	Calibrated value
RHO1	Lag 1 autocorrelation coefficient in the nearest neighbor model	0.35
RHO2	Lag 2 autocorrelation coefficient in the nearest neighbor model	0.11
ALPAD	Fitted value of 'a' for the main drying curve in Van Genuchten's retention model	0.00826
ALPAW	Fitted value of 'a' for the main wetting curve in Van Genuchten's retention model	0.02515
END	Fitted value of 'N' for the main drying curve in Van Genuchten's retention model	1.3572
ENW	Fitted value of 'N' for the main wetting curve in Van Genuchten's retention model	1.4102
THETAR	Fitted value of residual water content in Van Genuchten's retention model	0.1279

during the simulation period was compared with the observed water table elevation. Figure 16 shows a plot of observed and computed water table elevations. The water table rose during the period July 26 to 28 as a result of rainfalls on July 26 and 27. The decline in water table before July 26 and after July 28 were very close to each other and to that observed. Figure 17 shows the observed and computed pressure head distributions at selected times. They are very close to each other for the soil depth greater than 50 cm. These comparisons show the numerical model developed does approximate the field condition.

Test of the Model

Since an analytical solution of the flow in the saturated-unsaturated zone was not available, it was not possible to test the entire model against the analytical solution. However, before testing the entire model with calibrated parameters, it is better to test each segment of the model against an analytical solution if one exists. Therefore, each subprogram was tested and modifications were made until satisfactory results were obtained. Having established the validity of the various subprograms independently, the entire model can be tested.

The test of the subprogram FLOW will be shown here for an unsaturated flow problem. The infiltration problem using

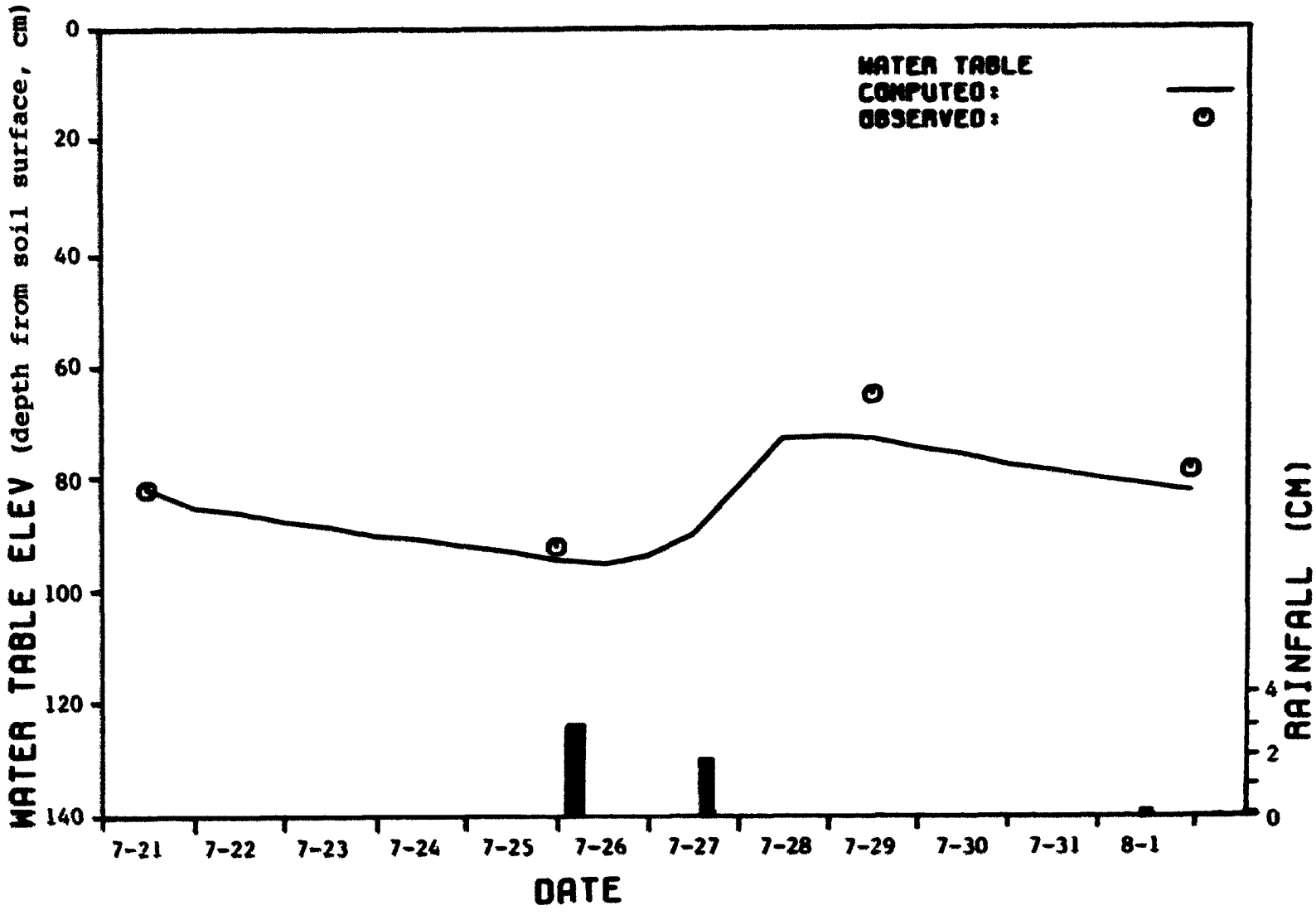

Figure 16. Comparison of water table elevations

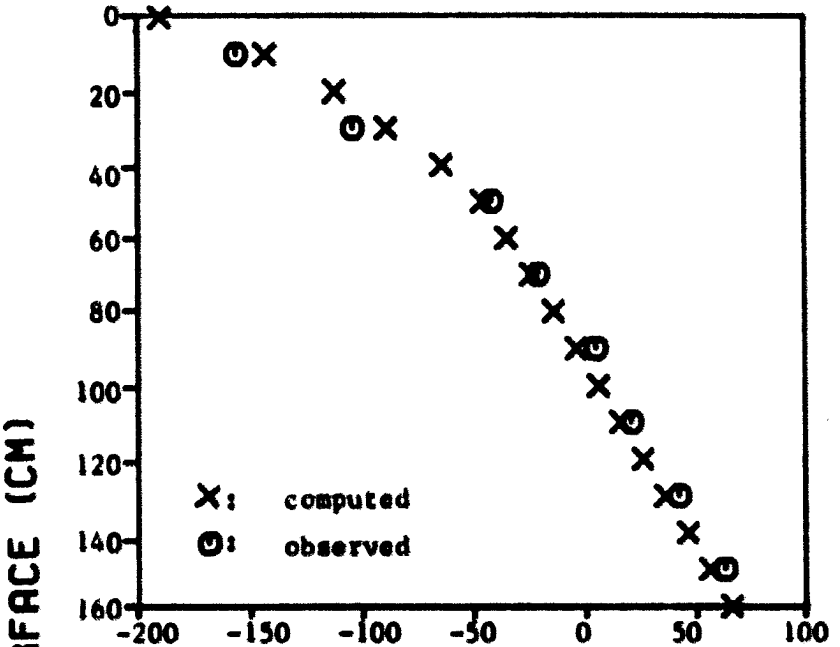

a. at 5:00 p.m. July 25, 1984

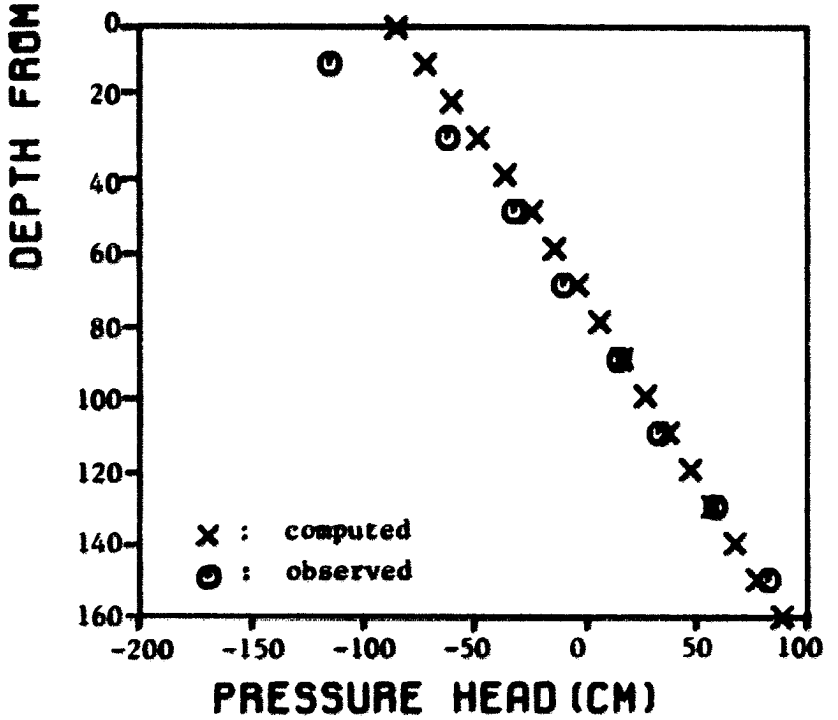

b. at 3:30 p.m. July 29, 1984

Figure 17. Comparison of pressure head distribution

a Yolo light clay was solved by Philip (1957) using a quasianalytical procedure. His classic example has since been a standard against which many subsequent solutions have been compared (e.g., Haverkamp et al., 1977; Milly and Eagleson, 1980). Only unsaturated flow was considered in his study. The governing equation with z-coordinate positive downward is:

$$\frac{\partial \theta}{\partial h}\frac{\partial h}{\partial t} = \frac{\partial}{\partial z}\left[K(h)\frac{\partial h}{\partial z} - 1 \right] \qquad (4.2)$$

and with the following initial and boundary conditions:

$h = -600$ cm $\quad t = 0 \quad 0 \leq z \leq 50$ cm

$h = 0$ cm $\quad t > 0 \quad z = 0$

Since a semi-infinite medium was considered, the lower boundary condition was not needed.

Haverkamp et al. (1977) have fitted a retention and hydraulic conductivity equation from the data describing the Yolo light clay. Those equations were:

$$\theta = 0.124 + \frac{274.2}{739 + (\ln|h|)^4} \qquad h < -1 \text{ cm} \qquad (4.3)$$

$$K(h) = K_s \times \frac{124.6}{124.6 + |h|^{1.77}} \qquad h < -1 \text{ cm} \qquad (4.4)$$

For pressure heads h greater than or equal to -1 cm, saturated water content of 0.495, and saturated hydraulic conductivity of 1.23×10^{-5} cm/sec were used.

The subroutine FLOW was used with Eqs. (4.3) and (4.4)

to solve the infiltration problem. The computations were made for a time period of 2×10^5 seconds using a time step varying from 25 seconds (for short time) to 250 seconds (for time $> 5 \times 10^4$) and with a depth interval of 1 cm. The solution obtained using Eqs. (4.3) and (4.4) is plotted in Figure 18 along with Philip's solution. The agreement with Philip's quasianalytical solution was favorable.

After testing all the segments of the program, the entire model was investigated to see if the model gave reasonable results. The pressure head distributions at various depths at selected times were checked. The pressure head distributions in the soil profile before, during, and after a rainfall event were investigated to see how the pressure head distribution changes and the wetting front advances during a rainfall. The pressure head distribution appeared reasonable and showed no abrupt change across the saturated-unsaturated interface. This confirms the continuity theory in the incorporated saturated-unsaturated flow. Figure 19 shows the change of pressure head distribution during and after the rainfall event of July 26 (208 Julian day) when rainfall of 3.0 cm started at 3:00 a.m. and ended at 6:40 a.m. The changes of pressure head distribution look reasonable.

The moisture balance in the flow domain was checked at the selected time steps. The change of moisture amount in

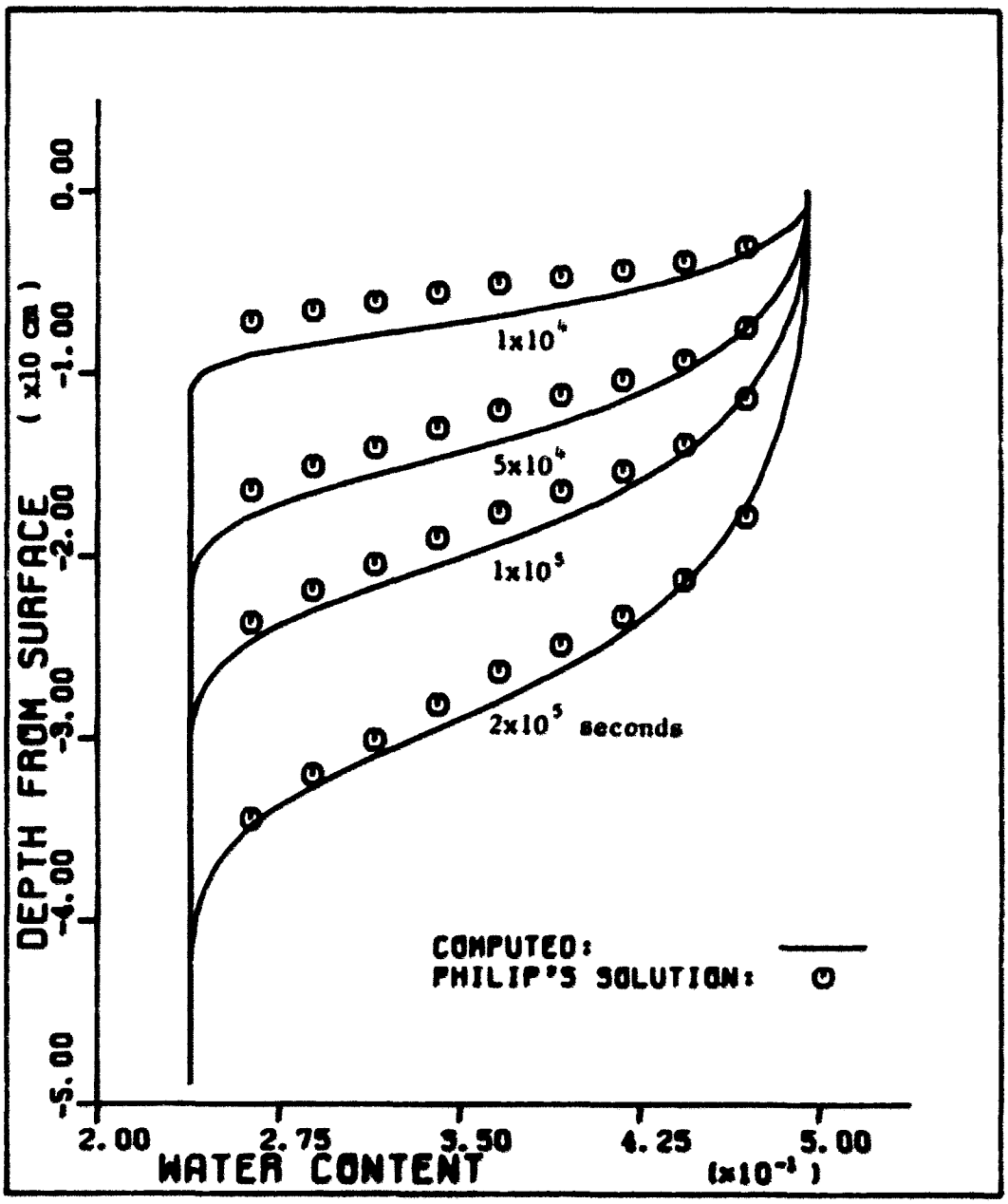

Figure 18. Infiltration into Yolo light clay

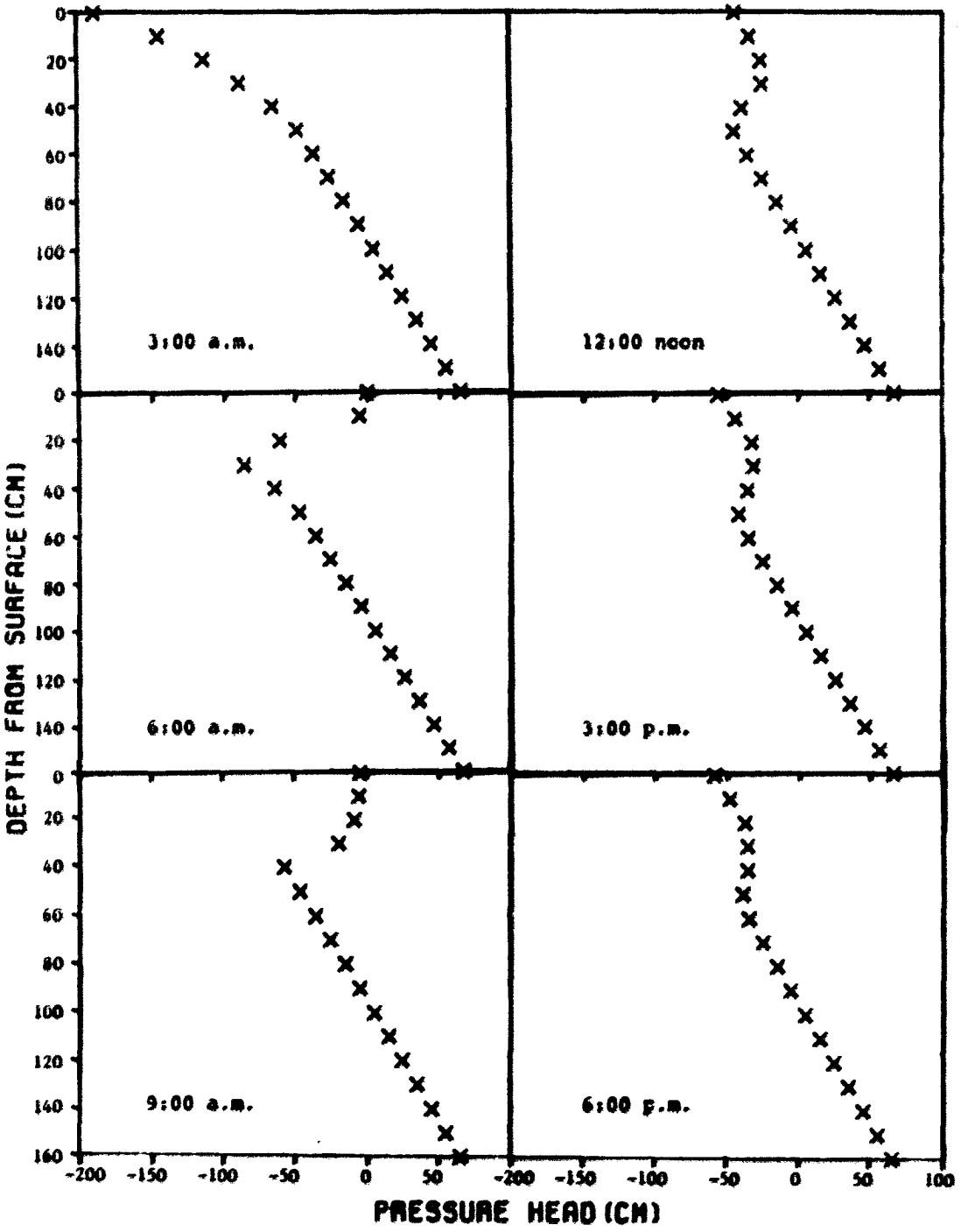

Figure 19. Pressure head distribution during and after a rainfall event - July 26, 1984. Rainfall (3.0 cm) occurred from 3:00 a.m. to 6:40 a.m.

the flow domain was compared with the boundary inflow and outflow. The difference between the two was less than 4% throughout the simulation period.

Evaluation of the Stochastic Model

With the satisfactory results of the model test, the stochastic property of the hydraulic conductivity was introduced into the model by assigning a nonzero value to standard deviation of log saturated hydraulic conductivity. A series of two Monte Carlo runs, each run having 100 different sets of hydraulic conductivities, were made for a 12 day simulation period. The spatial and temporal step sizes of 10 cm and 0.2 hour were used. The outputs were used to compute the means and standard deviations of the water table elevation and pressure heads at various depths.

Table 7. Input parameter values used in the Monte Carlo simulation

Parameter	Layer 1	Layer 2
Depth from surface	100 - 160 cm	0 - 100 cm
Mean of log K_s	-0.173925 cm/hr	-0.236572 cm/hr
S.D. of log K_s		
RUN A: 20% of mean	0.034785	0.047314
RUN B: 40% of mean	0.069570	0.094629

Input standard deviation values of log saturated hydraulic conductivity were taken as 20% and 40% of the mean of the log saturated hydraulic conductivity as given in Table 7. Preliminary studies showed that input standard deviations greater than 60% of the mean of the log hydraulic conductivity used in this model did not give satisfactory solutions.

Statistical analysis was done to compute the mean and standard deviation of the outputs of the Monte Carlo runs, and those were compared with each other to see the relationship between the input and output standard deviations. Tables 8 and 9 show the results of the statistical analysis of the water table elevation and the pressure heads, respectively. The standard deviations of the output variables were greater when the standard deviation of the inputs was larger.

The standard deviation of the water table elevation was stable after 3 or 4 days from the beginning of the simulation, then it abruptly increased at around midnight July 27, and then decreased to the previous stable value as time elapsed. This abrupt increase of standard deviation might have been caused by the rainfall on July 26 (3.0 cm) and on July 27 (1.8 cm) which made the water table rise. The standard deviation of the pressure (suction) head in the unsaturated zone became greater as the mean of the pressure

Table 8. Statistical analysis of water table elevation

Date	Time	Mean (cm)[a]		S.D. (cm)	
		Run A	Run B	Run A	Run B
7-21-84	12:00	82.0000	82.0000	0.0000	0.0000
7-21-84	24:00	85.6017	85.3632	0.6056	0.8461
7-22-84	12:00	86.5597	86.2826	0.6327	1.3833
7-22-84	24:00	88.5642	88.1242	1.0104	1.9568
7-23-84	12:00	89.6630	88.9623	1.2743	2.2719
7-23-84	24:00	91.2979	90.1762	1.5606	2.7136
7-24-84	12:00	92.2616	90.7553	1.8585	3.0562
7-24-84	24:00	93.8175	91.7923	2.2626	3.6362
7-25-84	12:00	94.6333	92.2851	2.5016	4.1008
7-25-84	24:00	95.7000	92.9697	2.7407	4.6765
7-26-84	12:00	96.1702	93.2091	2.7909	5.0952
7-26-84	24:00	94.7816	91.7151	2.4761	4.7193
7-27-84	12:00	91.7714	89.4670	2.4985	4.5338
7-27-84	24:00	85.2008	83.5161	5.2094	8.5393
7-28-94	12:00	77.8793	78.1935	4.7811	7.8212
7-28-84	24:00	77.1658	77.3950	3.9512	6.9535
7-29-84	12:00	77.3217	77.3550	3.5009	6.4523
7-29-84	24:00	78.1275	77.8255	2.9320	5.8584
7-30-84	12:00	78.6392	78.0417	2.6734	5.4667
7-30-84	24:00	79.6739	78.7423	2.4195	4.9618
7-31-84	12:00	80.2911	79.0137	2.3954	5.0396
7-31-84	24:00	81.3188	79.7802	2.4801	4.8989
8-01-84	12:00	81.9601	80.2158	2.6260	4.9299
8-01-84	24:00	82.7141	80.7190	2.8332	5.0439

[a]Water table depth from soil surface.

Table 9. Statistical analysis of soil water pressure head

Node	Mean (cm)		S.D. (cm)	
	Run A	Run B	Run A	Run B
Date: 7-22-84	Time: 24:00			
1	71.5880	72.0227	0.9495	1.9264
2	61.5731	62.0074	0.9327	1.9219
3	51.5552	51.9903	0.9098	1.9127
4	41.5362	41.9724	0.8933	1.9048
5	31.5153	31.9516	0.8951	1.9074
6	21.4921	21.9299	0.9024	1.9123
7	11.4680	11.9076	0.9048	1.9150
8	1.4404	1.8808	0.9101	1.9191
9	-8.6048	-8.1617	0.9214	1.9305
10	-18.7944	-18.3472	0.9774	1.9663
11	-29.1953	-28.7509	1.1024	1.9086
12	-40.3144	-39.9722	1.2688	1.8390
13	-54.5208	-53.4976	0.9946	2.1398
14	-70.3609	-68.7994	3.5525	4.0921
15	-87.7446	-87.1725	6.4598	8.0676
16	-114.5357	-111.8210	9.9173	11.0905
17	-154.3362	-146.5090	16.8406	21.7725
Date: 7-24-84	Time: 24:00			
1	66.3122	68.3284	2.2331	3.6165
2	56.2961	58.3137	2.2246	3.6110
3	46.2801	48.2986	2.2162	3.6085
4	36.2618	38.2808	2.2135	3.6062
5	26.2420	28.2633	2.2176	3.6098
6	16.2220	18.2444	2.2200	3.6137
7	6.1989	8.2250	2.2220	3.6174
8	-3.8310	-1.8001	2.2275	3.6246
9	-13.9354	-11.8830	2.2726	3.6693
10	-24.1603	-22.1109	2.3195	3.7044
11	-34.6069	-32.6765	2.4084	3.7112
12	-46.2820	-44.9146	2.1055	3.3807
13	-62.4133	-61.0016	1.3039	3.3176
14	-84.7563	-82.7989	2.8559	5.2779
15	-107.2246	-105.7564	4.6840	7.5565
16	-134.3064	-131.8086	8.1408	11.4676
17	-178.2010	-173.6082	15.7442	22.6004

Table 9 (Continued)

Node	Mean (cm)		S.D. (cm)	
	Run A	Run B	Run A	Run B
Date: 7-26-84	**Time: 24:00**			
1	65.2352	68.3129	2.4545	4.7081
2	55.2225	58.2991	2.4474	4.7037
3	45.2131	48.2901	2.4401	4.7011
4	35.2075	38.2823	2.4372	4.6978
5	25.2053	28.2785	2.4397	4.6979
6	15.2064	18.2774	2.4393	4.6977
7	5.2113	8.2787	2.4390	4.6969
8	-4.7773	-1.7155	2.4400	4.6949
9	-14.6684	-11.6594	2.4021	4.6648
10	-24.2630	-21.3428	2.3473	4.6042
11	-32.7414	-30.1611	2.0646	4.6097
12	-37.4440	-35.8164	2.6749	4.8575
13	-38.2011	-38.2271	2.6165	4.1561
14	-41.1214	-41.7295	3.7579	4.2406
15	-46.5610	-47.6036	6.1284	6.0208
16	-55.1996	-56.0598	6.5376	6.8326
17	-63.7928	-64.8980	6.7765	6.9809
Date: 7-28-84	**Time: 24:00**			
1	82.9631	82.7202	3.9879	6.9805
2	72.9487	72.7062	3.9789	6.9768
3	62.9341	62.6924	3.9724	6.9738
4	52.9190	52.6787	3.9675	6.9711
5	42.9044	42.6645	3.9595	6.9668
6	32.8904	32.6521	3.9572	6.9643
7	22.8752	22.6399	3.9545	6.9622
8	12.8599	12.6264	3.9491	6.9587
9	2.8419	2.6121	3.9427	6.9551
10	-7.1685	-7.3501	3.9013	6.8584
11	-17.1494	-17.2110	3.7652	6.6866
12	-27.1894	-26.9136	3.4586	6.2990
13	-37.4273	-36.6246	3.1051	5.8889
14	-47.7759	-46.6425	2.8507	5.7236
15	-58.1889	-56.8367	2.6121	5.6012
16	-68.5670	-67.1358	2.3742	5.4579
17	-78.8426	-77.3583	2.3842	5.3999

Table 9 (Continued)

Node	Mean (cm)		S.D. (cm)	
	Run A	Run B	Run A	Run B
Date: 7-30-84 Time: 24:00				
1	80.4787	81.3983	2.4293	4.9747
2	70.4638	71.3840	2.4163	4.9731
3	60.4476	61.3684	2.4100	4.9696
4	50.4305	51.3525	2.4025	4.9664
5	40.4127	41.3360	2.3949	4.9616
6	30.3944	31.3195	2.3967	4.9624
7	20.3745	21.3027	2.3976	4.9626
8	10.3527	11.2836	2.3969	4.9621
9	0.3271	1.2619	2.3978	4.9625
10	-9.7241	-8.8023	2.4362	5.0245
11	-20.0960	-19.1770	2.5101	5.1108
12	-31.1175	-30.3228	2.7521	5.3088
13	-42.9041	-42.2052	3.0286	5.7017
14	-55.3441	-54.6247	3.1135	6.0645
15	-68.5485	-67.6755	3.3244	6.4491
16	-82.4181	-81.3861	4.7589	7.5334
17	-96.5869	-95.0557	8.7567	10.6854
Date: 8-01-84 Time: 24:00				
1	77.4253	79.4132	2.8275	5.0466
2	67.4103	69.3993	2.8219	5.0440
3	57.3940	59.3844	2.8131	5.0392
4	47.3781	49.3680	2.8085	5.0367
5	37.3612	39.3519	2.8056	5.0353
6	27.3431	29.3351	2.8087	5.0365
7	17.3250	19.3181	2.8100	5.0380
8	7.3042	9.3000	2.8113	5.0400
9	-2.7238	-0.7242	2.8159	5.0458
10	-12.7971	-10.7929	2.8565	5.0893
11	-23.1323	-21.1280	2.7690	5.1049
12	-34.1316	-32.2748	2.7121	5.1342
13	-46.3821	-44.6735	2.8553	5.4382
14	-60.5424	-58.7196	3.3422	6.1866
15	-77.3579	-75.1632	4.5303	7.3286
16	-95.0708	-92.9359	5.5015	8.3007
17	-116.2975	-113.8907	8.9770	12.2619

head became smaller (more negative). During dry weather (7-22-84 to 7-24-84 in Table 9), the standard deviation of the pressure head decreased rapidly with depth from the soil surface. This corresponds to a rapid change in pressure head with depth from the lowest pressure head (most negative) at the soil surface. Below a depth of 40 cm, the standard deviation did not change as much even though the mean pressure head did change considerably.

Figures 20 and 21 show plots of observed water table elevations and 90% confidence intervals of mean water table elevations for Runs A and B, respectively. The equation used to compute the 90% confidence intervals was:

$$\text{Confidence interval} = \text{Mean} \pm 1.645 \times \text{SD} \qquad (4.5)$$

where SD = standard deviation of water table elevation. Observed water table elevation except for the value on July 29 fit well to averages and within confidence intervals. One possible cause of the observed value on July 29 deviating from the average value and being outside of the 90% confidence interval was that the water may have flowed directly from the soil surface to the water table along the observation well pipe because the well pipe was not perfectly sealed or grouted. Another possible cause was that rain water flowed downward toward water table through the cracks near the soil surface which appeared during the dry weather.

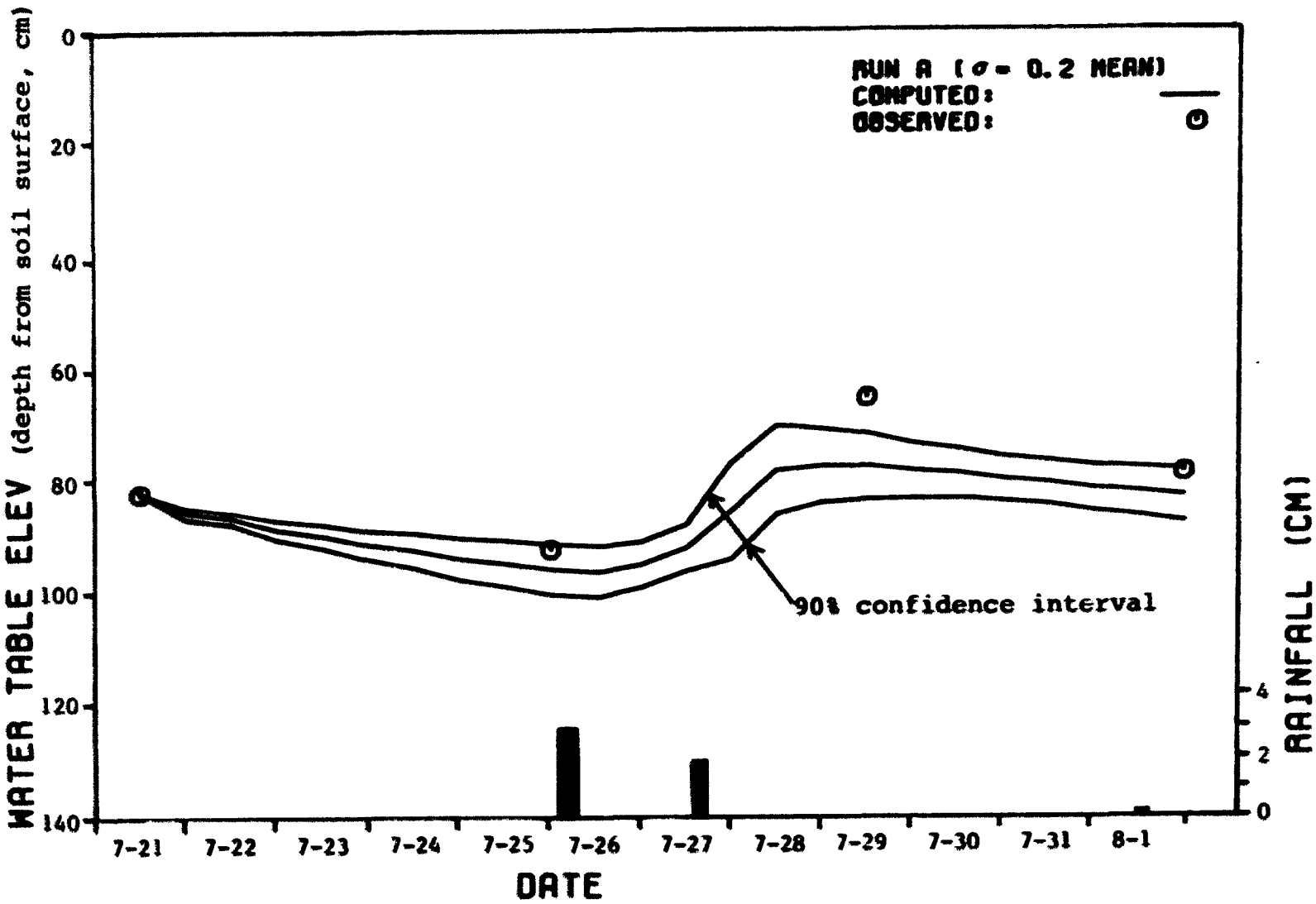

Figure 20. 90% confidence interval of the water table elevation for Run A

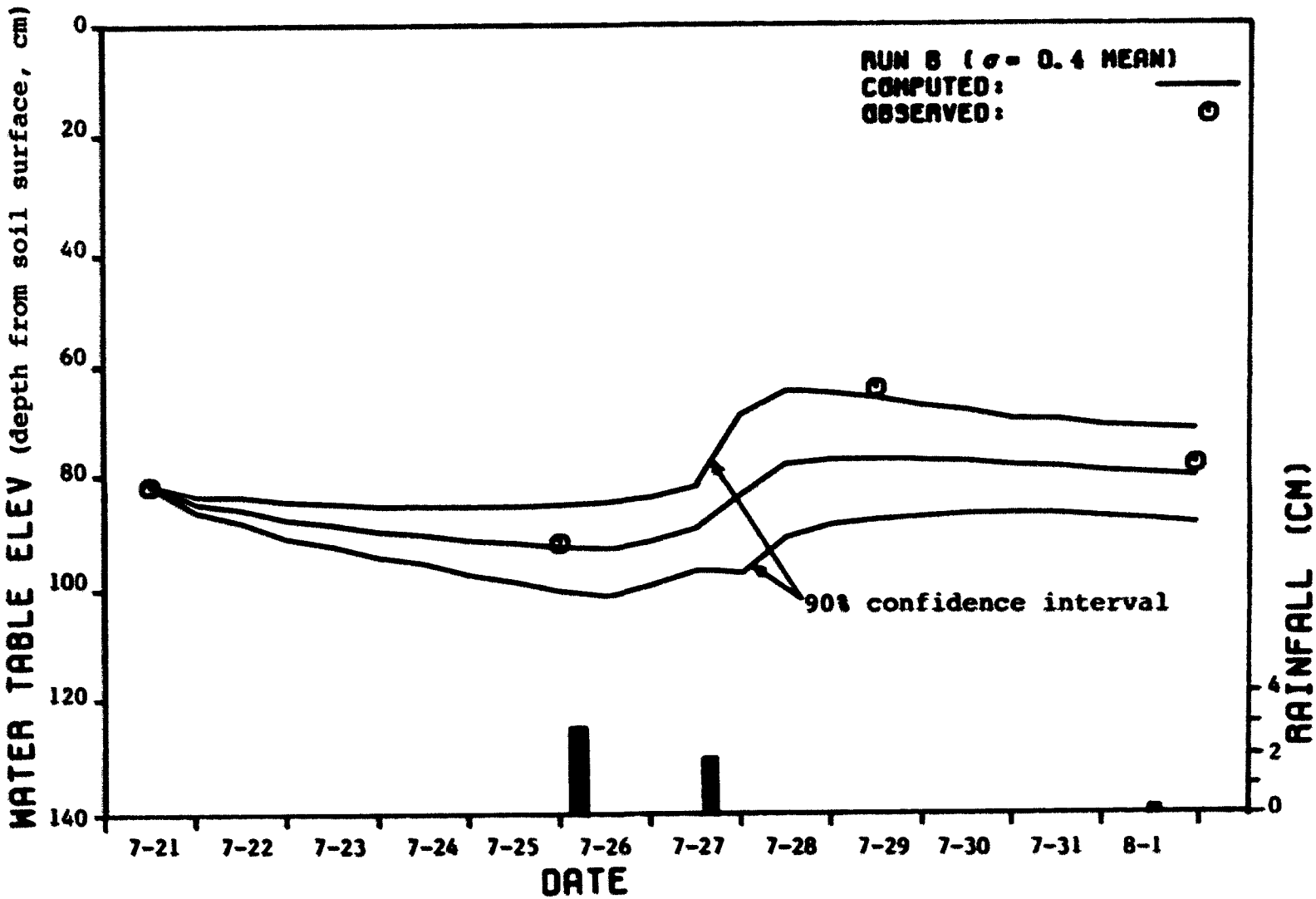

Figure 21. 90% confidence interval of the water table elevation for Run B

CHAPTER V. CONCLUSIONS AND RECOMMENDATIONS FOR FUTURE STUDY

It appears that the model of the incorporated saturated-unsaturated flow developed herein gives satisfactory results. Conclusions based on the present study are listed as follows:

1. The continuity theory of saturated-unsaturated flow was used in the model. The results matched the observed field data well.

2. The Monte Carlo method was applied satisfactorily for the present stochastic model study.

3. The standard deviation of the stochastic hydraulic conductivity has an important role in determining the variations of the outputs, water table elevation, water content, and pressure head. As the former increases, the latter increases also.

4. The standard deviation of the pressure head increased as the mean of the pressure head became smaller (more negative) in the unsaturated zone.

The following recommendations are made for future study:

1. Collection of extensive field data representing pressure head observations is needed in order to account for field spatial variability and to develop reliable input parameters, such as mean and variance of hydraulic

conductivity, infiltration parameters, and evaporation rate.

2. Develop a model to correlate the stochastic soil water parameters between the two nodes across the adjacent geologic soil layer interface in applying the nearest neighbor model.

3. Find a relationship between the standard deviation of the log saturated hydraulic conductivity and the mean of the log saturated hydraulic conductivity that satisfies convergence criteria of the stochastic model.

4. Implement an automatic time step adjusting scheme in the numerical method. The automatic time step adjusting strategy would use small time steps when the transient flow behavior is dominant. Whenever, the transient flow is less dominant, larger time steps would be used. This obviously would minimize the computer time required.

5. Modify the computer program for microcomputer application since microcomputer is much more inexpensive to run the simulation model.

6. Develop algorithms for plant root growth and crop leaf area index for longer simulation periods.

7. Futher apply the developed model to other field problems to evaluate the model.

REFERENCES

Afshar, A., and Marino, M. A. 1978. "Model for simulating soil-water content considering evapotranspiration." Journal of Hydrology 37:309-322.

Anderson, C. E. 1975. "A Water balance model for agricultural watersheds on deep loess soils." Ph.D. Thesis. Kansas State University, Manhattan, Kansas.

Anderson, C. E., Johnson, H. P., and Powers, W. L. 1978. "A water-balance model for deep loess soils." Trans. ASAE 21(2):314-320.

Andersson, J., and Shapiro, A. M. 1983. "Stochastic analysis of one-dimensional steady state unsaturated flow: A comparison of Monte Carlo and pertubation methods." Water Resources Research 19(1):121-133.

Babu, D. K. 1980. "Saturated-unsaturated flow in radial directions generated by an injection well." Soil Science Society of America Journal 44:915-921.

Baker, F. G., and Bouma, J. 1976. "Variability of hydraulic conductivity in two subsurface horizons of two silt loam soils." Soil Science Society of America Proceedings 40:219-222.

Bakr, A. A., Gelhar, L. W., Gutjahr, A. L., and MacMillan, J. R. 1978. "Stochastic analysis of spatial variability in subsurface flows: 1. Comparison of one- and three-dimensional flows." Water Resources Research 14(2):263-271.

Bartlett, M. S. 1975. The Statistical Analysis of Spatial Pattern. Chapman and Hall, London.

Bear, J. 1972. Dynamics of Fluids in Porous Media. American Elsevier, Inc., New York, N. Y.

Bear, J. 1979. Hydraulics of Groundwater. McGraw-Hill Inc., New York, N. Y.

Bennion, D. W., and Hope, A. C. A. 1974. "Mathematical modeling of reservoir rock properties." Journal of Canadian Petroleum Technology 13(2):46-55.

Bouwer, H. 1978. Groundwater Hydrology. McGraw-Hill Inc., New York, N. Y.

Bresler, E., and Dagan, G. 1983. "Unsaturated flow in spatially variable fields: 2. Application of water flow models to various fields." Water Resources Research 19(2):421-428.

Bresler, E., and Green, R. E. 1982. "Soil parameters and sampling scheme for characterizing soil hydraulic properties of a watershed." Technical Report No. 148. Water Resources Research Center, University of Hawaii at Manoa, Honolulu, Hawaii.

Brooks, R. H., and Corey, A. T. 1964. "Hydraulic properties of porous media." Colorado State University Hydrology Paper No. 3.

Buckman, H. O., and Brady, N. C. 1969. The Nature and Properties of Soils. Macmillan Co., New York.

Campbell, G. S. 1974. "A simple method for determining unsaturated conductivity from moisture retention data." Soil Science 117(6):311-314.

Chu, S. T. 1978. "Infiltration during an unsteady rain." Water Resources Research 14(3):461-466.

Cooley, R. L. 1983. "Some new procedures for numerical solution of variably saturated flow problems." Water Resources Research 19(5):1271-1285.

Dagan, G. 1979. "Models of groundwater flow in statistically homogeneous porous formations." Water Resources Research 15(1):47-63.

Dagan, G., and Bresler, E. 1983. "Unsaturated flow in spatially variable fields: 1. Derivation of models of infiltration and redistribution." Water Resources Research 19(2):413-420.

Dane, J. H., and Mathis, F. H. 1981. "An adaptive finite difference scheme for the one-dimensional water flow equation." Soil Science Society of America Journal 45:1048-1054.

DeBoer, D. W. 1969. "Flood hydrology of watersheds with depressional storage." Ph.D. Thesis. Iowa State University, Ames, Iowa.

Douglas, J., and Jones, B. F. 1963. "On predictor-corrector methods for nonlinear parabolic differential equations." Journal of the Society for Industrial and Applied Mathematics 11(1):195-204.

Emery, A. F., and Carson, W. W. 1971. "An evaluation of the use of the finite element method in the computation of temperature." Journal of Heat Transfer 93(2):136-145.

Freeze, R. A. 1969. "The mechanism of natural groundwater recharge and discharge: 1. One-dimensional, vertical, unsteady, unsaturated flow above a recharging or discharging groundwater flow system." Water Resources Research 5(1):153-171.

Freeze, R. A. 1975. "A stochastic-conceptual analysis of one-dimensional groundwater flow in nonuniform homogeneous media." Water Resources Research 11(5):725-741.

Fritton, D. D., Kirkham, D., and Shaw, R. H. 1970. "Soil water evaporation, isothermal diffusion, and heat and water transfer." Soil Science Society of America Proceedings 34(2):183-189.

Fujioka, Y., and Kitamura, T. 1964. "Approximate solution of a vertical drainage problem." Journal of Geophysical Research 69(24):5249-5255.

Gelhar, L. W. 1976. "Effects of hydraulic conductivity variations on groundwater flows." pp. 409-429 in Proceedings 2nd International IAHR Symposium in Stochastic Hydraulics. Lund Institute of Technology, Lund, Sweden.

Gilding, B. H. 1983. "The soil-moisture zone in a physically-based hydrologic model." Advances in Water Resources 6:36-43.

Green, W. H., and Ampt, G. A. 1911. "Studies on soil physics: I. Flow of air and water through soils." Journal of Agricultural Science 4:1-24.

Hammersley, J. M., and Handscomb, D. C. 1964. Monte Carlo Methods. Methuen & Co., Ltd., London.

Haverkamp, R., Vauclin, M., Touma, J., Wierenga, P. J., and Vachaud, G. 1977. "A comparison of numerical simulation models for one-dimensional infiltration." Soil Science Society of America Journal 41:285-294.

Higuchi, M. 1984. "Numerical simulation of soil-water flow during drying in a nonhomogeneous soil." Journal of Hydrology 71:303-334.

Hillel, D. 1980a. Fundamentals of Soil Physics. Academic Press, New York, N. Y.

Hillel, D. 1980b. Applications of Soil Physics. Academic Press, New York, N. Y.

Holtan, H. N. 1961. "A concept for infiltration estimates in watershed engineering." U.S. Department of Agriculture, Agricultural Research Service, ARS 41-51.

Holtan, H. N., England, C. B., and Shanholtz, V. O. 1967. "Concepts in hydrologic soil grouping." Trans. ASAE 10(3):407-410.

Hornberger, G. M., and Remson, I. 1970. "A moving boundary model of a one-dimensional saturated-unsaturated, transient porous flow system." Water Resources Research 6(3):898-905.

Hornung, U., and Messing, W. 1980. "A predictor- corrector alternating-direction implicit method for two-dimensional unsteady saturated-unsaturated flow in porous media." Journal of Hydrology 47:317-323.

Huber, W. C., Heaney, J. P., Nix, S. J., Dickinson, R. E., and Polmann, D. J. 1982. Storm Water Management Model: User's Manual, Version III. Department of Environmental Engineering Science, University of Florida.

Huggins, L. F., and Monke, E. J. 1968. "A mathematical model for simulating the hydrologic response of a watershed." Water Resources Research 4(3):529-539.

Kirkham, D., and Powers, W. L. 1972. Advanced Soil Physics. Wiley Interscience, New York, N. Y.

Landau, H. G. 1950. "Heat conduction in a melting solid." Quarterly of Applied Mathematics 8(2):81-94.

Lapidus, L., and Pinder, G. F. 1982. Numerical Solution of Partial Differential Equations in Science and Engineering. John Wiley & Sons, New York.

Libardi, P. L., Reichardt, K., Nielsen, D. R., and Biggar, J. W. 1980. "Simple field methods for estimating soil hydraulic conductivity." Soil Science Society of America Journal 44:3-7.

Lotkin, M. 1960. "The calculation of heat flow in melting solids." Quarterly of Applied Mathematics 18(1):79-85.

McCalla, T. R. 1967. Introduction to Numerical Methods and FORTRAN Programming. John Wiley and Sons Inc., New York.

McMillan, W. D. 1966. "Theoretical analysis of groundwater basin operation." Technical Report 6-25. Hydraulic Lab., University of California, Berkeley.

McQueen, I. S., and Miller, R. F. 1974. "Approximating soil moisture characteristics from limited data: Empirical evidence and tentative model." Water Resources Research 10(3):521-527.

Mein, R. G., and Larson, C. L. 1973. "Modeling infiltration during a steady rain." Water Resources Research 9(2):384-394.

Miller, E. E., and Miller, R. D. 1955. "Theory of capillary flow: I. Practical implications." Soil Society of America Proceedings 19(3):267-271.

Miller, E. E., and Miller, R. D. 1956. "Physical flow for capillary flow phenomena." Journal of Applied Physics 27(4):324-332.

Milly, P. C. D. 1982. "Moisture and heat transport in hysteretic, inhomogeneous porous media: A matric-based formulation and a numerical model." Water Resources Research 18(3):489-498.

Milly, P. C. D., and Eagleson, P. S. 1980. "The coupled transport of water and heat in a vertical soil column under atmospheric excitation." Report No. 258. Department of Civil Engineering, Massachusetts Institute of Technology, Cambridge, Massachusetts.

Moldenhauer, W. C., and Kemper, W. D. 1969. "Interdependence of waterdrop energy and clod size on infiltration and clod stability." Soil Science Society of America Proceedings 33:297-301.

Molz, F. G., and Remson, I. 1970. "Extraction term models of soil moisture use by transpiring plants." Water Resources Research 6(5):1346-1356.

Mualem, Y. 1973. "Modified approach to capillary hysteresis based on a similarity hypothesis." Water Resources Research 9(5):1324-1331.

Mualem, Y. 1974. "A conceptual model of hysteresis." Water Resources Research 10(3):514-520.

Mualem, Y. 1976. "A new model for predicting the hydraulic conductivity of unsaturated porous media." Water Resources Research 12(3):513-522.

Mualem, Y. 1977. "Extension of similarity hypothesis used for modeling the soil water characteristics." Water Resources Research 13(4):773-780.

Mualem, Y., and Dagan, G. 1975. "A dependent domain model of capillary hysteresis." Water Resources Research 11(3):452-460.

Neuman, S. P. 1973. "Saturated-unsaturated seepage by finite elements." Journal of the Hydraulics Division, ASCE 99(12):2233-2250.

Neuman, S. P., Feddes, R. A., and Bresler, E. 1974. "Finite element simulation of flow in saturated-unsaturated soils considering water uptake by plants." Israel Institute of Technology, Hydrodynamics & Hydraulic Eng. Laboratory, Haifa, Israel.

Nielsen, D. R., Biggar, J. W., and Erh, K. T. 1973. "Spatial variability of field-measured soil-water properties." Hilgardia 42(7):215-259

Philip, J. R. 1957. "The theory of infiltration: 1. The infiltration equation and its solution." Soil Science 83(5):345-357.

Philip, J. R., and De Vries, D. A. 1957. "Moisture movement in porous materials under temperature gradients." Transactions of American Geophysical Union 38:222-228.

Rawls, W. J., and Brakensiek, D. L. 1983. "A procedure to predict Green and Ampt infiltration parameters." Advances in Infiltration. ASAE Publication 11-83.

Remson, I., Hornberger, G. M., and Molz, F. J. 1971. Numerical Methods in Subsurface Hydrology with an Introduction to the Finite Element Method. Wiley Interscience, New York.

Richtmyer, R. D., and Morton, K. W. 1967. Difference Methods for Initial Value Problems. 2nd ed. Wiley Interscience, New York, N. Y.

Ritchie, J. T. 1972. "Model for predicting evaporation from a row crop with incomplete cover." Water Resources Research 8(5):1204-1213.

Russo, D., and Bresler, E. 1982. "A univariate versus a multivariate parameter distribution in a stochastic-conceptual analysis of unsaturated flow." Water Resources Research 18(3):483-488.

Saxton, K. E., Johnson, H. P., and Shaw, R. H. 1974a. "Watershed evapotranspiration estimated by the combination method." Trans. ASAE 17(4):668-672.

Saxton, K. E., Johnson, H. P., and Shaw, R. H. 1974b. "Modeling evapotranspiration and soil moisture." Trans. ASAE 17(4):673-677.

Shahghasemi, E. 1980. "Simulation modeling of erosion processes on small agricultural watersheds." Ph.D. Thesis. Iowa State University, Ames, Iowa.

Skaggs, R. W. 1978. "A water management model for shallow water table soils." Report No. 134. Water Resources Research Institute, North Carolina State University, Raleigh, N. C.

Smith, J. L. 1978. "A stochastic analysis of steady-state groundwater flow in a bounded domain." Ph.D. Thesis. University of British Columbia, Canada.

Smith, L., and Freeze, R. A. 1979a. "Stochastic analysis of steady state groundwater flow in a bounded domain: 1. One-dimensional simulations." Water Resources Research 15(3):521-528.

Smith, L., and Freeze, R. A. 1979b. "Stochastic analysis of steady state groundwater flow in a bounded domain: 2. Two-dimensional simulations." Water Resources Research 15(6):1543-1559.

Smith, L., and Schwartz, F. W. 1980. "Mass transport: 1. A stochastic analysis of macroscopic dispersion." Water Resources Research 16(2):303-313.

Smith, R. E. and Hebbert, R. H. B. 1979. "A Monte Carlo analysis of the hydrologic effects of spatial variability of infiltration." Water Resources Research 15(2):419-429.

Sobol, I. M. 1974. The Monte Carlo Method. The University of Chicago Press, Chicago.

Soil Conservation Service. 1975. Soil Survey: Webster County, Iowa. U.S. Department of Agriculture, Washington, D.C.

Sophocleous, M. 1978. "Analysis of heat and water transport in unsaturated-saturated porous media." Ph.D. Thesis. University of Alberta, Edmonton, Canada.

Sophocleous, M. 1979. "Analysis of water and heat flow in unsaturated-saturated porous media." Water Resources Research 15(5):1195-1206.

Tang, D. H., and Pinder, G. F. 1977. "Simulation of groundwater flow and mass transport under uncertainty." Advances in Water Resources 1(1):25-30.

Van Genuchten, M. T. 1980. "A closed equation for predicting the hydraulic conductivity of unsaturated soils." Soil Science Society of America Journal 44:892-898.

Van Genuchten, M. T. 1982. "A comparison of numerical solutions of the one-dimensional unsaturated-saturated flow and mass transport equations." Advances in Water Resources 5:47-55.

Warrick, A. W., Mullen, G. J., and Nielsen, D. R. 1977. "Prediction of soil water flux based upon field-measured soil water properties." Soil Science Society of America Journal 41:14-19.

White, F. M. 1979. Fluid mechanics. McGraw-Hill Book Co., New York, N. Y.

Willardson, L. S., and Hurst, R. L. 1965. Sample size estimates in permeability studies." Journal of Irrigation and Drainage division, ASCE 91(IR1):1-9.

Wischmeier, W. H., and Smith, D. D. 1978. "Predicting rainfall-erosion losses - a guide to conservation planning." U.S. Department of Agriculture, Agriculture Handbook No. 537.

ACKNOWLEDGMENTS

The author wishes to express his sincere appreciation to his major professor, Dr. T. Al Austin, for his guidance and supervision throughout the course of this study. Appreciation is also expressed to his graduate committee members: Drs. E. R. Baumann, R. A. Rohnes, and R. L. Rossmiller, all of the Civil Engineering Department, Dr. C. E. Anderson of the Agricultural Engineering Department, and Dr. R. Horton of the Agronomy Department for their guidance.

The author's graduate program was financially supported by Iowa State Water Resources Research Institute and Engineering Research Institute of Iowa State University. Computer money was supported by the Civil Engineering Department. All of these supports are deeply appreciated.

The author would like to express his thanks to Mr. R. Helms and Mr. R. Littwiller who provided the author with the land for the field experiments. Also, thanks are extended to his fellow students for their help during the field and laboratory measurements.

Finally, the author would like to express his great thanks to his wife Jin-Sook for her sacrifices, patience, and encouragement during the course of this study and to his daughters Hee-Jin and Kyu-Jin for their understanding and sacrifices.

APPENDIX A: LIST OF FORTRAN PROGRAM

```
1.      //DOCTOR  JOB  13264,SOC
2.      /*JOBPARM LINES=30000
3.      //S1  EXEC  WATFIV,REGION=300K,TIME=(20,0)
4.      //SYSIN  DD  *
5.      $JOB            DOCTOR,PAGES=500,TIME=1200
6.      C
7.      C*************************************************************************
8.      C
9.      C                                  SWMSUZ
10.     C
11.     C     STOCHASTIC MODELING OF WATER MOVEMENT IN THE SATURATED-UNSATURATED
12.     C     ZONE.       DECEMBER, 1984.     BY SANG-OK CHUNG
13.     C
14.     C     THIS PROGRAM SIMULATES ONE-DIMENSIONAL WATER MOVEMENT IN THE
15.     C     SATURATED-UNSATURATED ZONE USING MONTE-CARLO METHOD WITH FIRST
16.     C     ORDER NEAREST NEIGHBOR STOCHASTIC MODEL.
17.     C     STOCHASTIC PROPERTIES OF THE SATURATED HYDRAULIC CONDUCTIVITY ARE
18.     C     INPUTS AND DIFFERENT SETS OF PRESSURE HEAD, WATER CONTENT
19.     C     AND WATER TABLE LEVEL ARE OUTPUTS.  THESE OUTPUTS CAN BE
20.     C     USED TO DETERMINE MEAN AND STANDARD DEVIATION OF THEMSELVES.
21.     C     FINITE DIFFERENCE METHOD USING DOUGLAS-JONES PREDICTOR-CORRECTOR
22.     C     NUMERICAL SCHEME IS USED.
23.     C     CM AND HOUR UNITS ARE USED.  VERTICAL COORDINATE IS POSITIVE
24.     C     UPWARD, AND NODAL POINTS ARE NUMBERED ACCORDINGLY.
25.     C
26.     C*************************************************************************
27.     C
28.     C     VARIABLE DESCRIPTIONS (GLOBAL)
29.     C
30.     C*************************************************************************
31.     C
32.     C     ABST      AMOUNT OF INTECEPTION STORAGE AT A GIVEN TIME.
33.     C     ASVAP     ACTUAL SOIL SURFACE EVAPORATION RATE (CM/HR)
34.     C     ALPA      AUTOREGRESIVE PARAMETER IN THE NEAREST NEIGHBOR MODEL
36.     C     ALPAD     FITTED PARAMETER 'A' FOR THE MAIN DRYING IN VAN
36.     C               GENUCHTEN'S RETENTION MODEL
37.     C     ALPAW     FITTED PARAMETER 'A' FOR THE MAIN WETTING IN
38.     C               VAN GENUCHTEN'S RETENTION MODEL
39.     C     AM        EXPONENTIAL COEFFICIENT IN INFILTRATION EQUATION.
40.     C     ANC       ANTECEDENT MOISTURE CONTENT IN THE TOP SOIL LAYER.
41.     C     ASOIL     SOIL PARAMETER IN THE INFILTRATION EQUATION.
42.     C     ASOILM    MAXIMUM VALUE OF ASOIL.
43.     C     CE1       COEFFICIENT USED IN RAINFALL ENERGY FACTOR EQUATION.
44.     C     CE2       COEFFICIENT USED IN RAINFALL ENERGY FACTOR EQUATION.
45.     C     CLAI      CROP LEAF AREA INDEX.
46.     C     COND      SATURATED HYDRAULIC CONDUCTIVITY IN THE TOP LAYER
47.     C     DELF      INFILTRATION AMOUNT DURING A TIME PERIOD
48.     C     DELP(I,J) AMOUNT OF EXCESS RAINFALL DURING A TIME STEP
49.     C     DELPO(I,J)AMOUNT OF TOTAL RAINFALL DURING A TIME STEP.
50.     C     DELT      SIZE OF TIME STEP IN HOUR
51.     C     DELZ      SIZE OF THE BLOCK IN VERTICAL DIRECTION IN CM
52.     C     DEPMAX    MAXIMUM VALUE OF DEPRESSION STORAGE (CM)
53.     C     DEPRES    DEPRESSION STORAGE (CM)
54.     C     DSEED     SEED FOR THE RANDOM NUMBER GENERATION
55.     C     ENDRY     FITTED PARAMETER 'N' FOR THE MAIN DRYING IN
56.     C               VAN GENUCHTEN'S RETENTION MODEL
57.     C     ENWET     FITTED PARAMETER 'N' FOR THE MAIN WETTING IN
58.     C               VAN GENUCHTEN'S RETENTION MODEL
59.     C     F         GENERALIZED SPECIFIC WATER CAPACITY (DTHETA/DH)
60.     C     FCP       FIELD CAPACITY IN TOP SOIL LAYER IN INFILTRATION EQ.
```

```
C     FCS       MAXIMUM VALUE OF ANTECEDENT MOISTURE CONTENT IN TOP LAYER.
C     FLUX1     BOUNDARY FLUX AT BOTTOM BOUNDARY (CM/HR)
C     FLUXN     BOUNDARY FLUX AT THE TOP BOUNDARY (CM/HR)
C     IBEGIN(NL)NODAL POINT INDICATOR FOR THE BEGINNING OF EACH SOIL LAYER
C     IEND(NL)  NODAL POINT INDICATOR FOR THE END OF EACH SOIL LAYER
C     IDAY      JULIAN DAY
C     IDAYB     BEGINNING DAY OF SIMULATION
C     IDAYE     ENDING DAY OF SIMULATION
C     IHIS(L)   WETTING DIRECTION INDICATOR: 1 FOR WETTING; 2 FOR DRYING
C     IHOURB    BEGINNING TIME OF SIMULATION ON THE FIRST DAY
C     IHOURE    ENDING TIME OF SIMULATION ON THE LAST DAY
C     IRAIN(I)  RAINFALL EVENT INDICATOR: 1: RAIN.  2: NO RAIN
C     ISUBNO(I) NUMBER OF BLOCKS IN EACH SOIL LAYER
C     ISCAN(I)  RETENTION CURVE INDICATOR:  1: MAIN CURVE
C                                           2: PRIMARY SCANNING CURVE
C                                           3: HIGHER ORDER SCANNING CURVE
C     ITSTEP    NUMBER OF TIME STEPS IN A DAY
C     K(N)      HYDRAULIC CONDUCTIVITY
C     LENGS     LENGTH OF SIMULATION PERIOD IN DAYS
C     MC        NUMBER OF MONTE-CARLO SIMULATION RUNS
C     MCOUNT    COUNTER OF MONTE-CARLO SIMULATION RUNS
C     N         NUMBER OF NODAL POINT IN THE FINITE DIFFERENCE FLOW DOMAIN
C     N1        INDEX SHOWING SEQUENTIAL NUMBER OF RAINY DAYS
C     NL        NUMBER OF SOIL LAYERS
C     NR        LENGTH OF NORMAL RANDOM NUMBERS TO BE GENERATED
C     NR2       NUMBER OF SOIL BLOCKS WITHIN THE PLANT ROOT ZONE.
C     PAN(J)    DAILY PAN EVAPORATION AMOUNT (CM).
C     PERCT     PERCENT DIFFERENCE IN WATER BALANCE CALCULATION
C     PET(I,J)  POTENTIAL EVAPOTRANSPIRATION FOR A TIME PERIOD (CM).
C               'I' IS DAY INDEX AND 'J' IS TIME STEP INDEX.
C     PN        EXPONENTIAL COEF. IN PSOIL EQUATION.
C     POR(NL)   POROSITY OF SOIL LAYER
C     PSI(N)    PRESSURE HEAD AT THE END OF CURRENT TIME STEP (CM OF WATER)
C     PSIB(N)   PRESSURE HEAD AT THE BEGINNING OF CURRENT TIME STEP
C     PSIMIN    MINIMUM PRESSURE HEAD CONSTRAINT ON THE SOIL SURFACE
C     PSOIL     SOIL PARAMETER IN THE INFILTRATION EQUATION.
C     PSOILM    PSOIL VALUE AT THE FIELD CAPACITY OF TOP SOIL LAYER.
C     R         GENERATED NORMAL RANDOM NUMBERS OF LENGTH NR
C     RELK(N)   RELATIVE HYDRAULIC CONDUCTIVITY
C     RATE      AVERAGE INFILTRATION RATE DURING A TIME PERIOD
C     RE(N)     ACTUAL ROOT EXTRACTION FOR TRANSPIRATION (1/HR)
C     RHO1      LAG 1 AUTOCORRELATION COEFFICIENT IN NEAREST NEIGHBOR MODEL
C     RHO2      LAG 2 AUTOCORRELATION COEFFICIENT IN NEAREST NEIGHBOR MODEL
C     RROT(I)   PLANT ROOT DENSITY DISTRIBUTION IN EACH SOIL BLOCK.
C     SABST     SUM OF INTERCEPTION SINCE THE BEGINNING OF A RAINFALL.
C     SDELF     ACCUMULATED INFILTRATION SINCE A CERTAIN TIME.
C     SKSAT(N)  STOCHASTIC SATURATED HYDRAULIC CONDUCTIVITY AT EACH NODE
C               BY NEAREST NEIGHBOR MODEL.
C     SMASM     TOTAL REMAINING UNUSED WATER STORAGE CAPACITY IN TOP
C               SOIL LAYER.
C     SRKE      SEASONAL ACCUMULATED RAINFALL KINETIC ENERGY.
C     SS        SPECIFIC STORAGE
C     STORE1    INITIAL AMOUNT OF WATER STORED IN THE SYSTEM DOMAIN (CM)
C     SUBL(NL)  THICKNESS OF EACH SOIL LAYER (CM)
C     TABLE     WATER TABLE DEPTH FROM THE GROUND SURFACE
C     TARE      TOTAL ACTUAL ROOT EXTRACTION RATE (CM/HR)
C     TFLUX1    TOTAL AMOUNT OF WATER FLOW ACROSS BOTTOM BOUNDARY
C               SINCE THE BEGINNING OF THE SIMULATION
C     TFLUXN    TOTAL AMOUNT OF WATER FLOW ACROSS TOP BOUNDARY
C               SINCE THE BEGINNING OF THE SIMULATION
```

```
121.      C     THETAM(N) WATER CONTENT EVALUATED AT PRESENT PRESSURE HEAD ON THE
122.      C               MAIN WETTING CURVE.
123.      C     THETMB(N) WATER CONTENT EVALUATED AT PREVIOUS PRESSURE HEAD ON
124.      C               THE MAIN WETTING CURVE
125.      C     THETAI(N) WATER CONTENT EVALUATED AT THE WETTING REVERSAL POINT
126.      C     THETMI(N) WATER CONTENT EVALUATED AT THE WETTING REVERSAL VALUE
127.      C               OF PSI ON THE MAIN WETTING CURVE
128.      C     THETAR(I) RESIDUAL VOLUMETRIC WATER CONTENT
129.      C     THETAS(I) SATURATED VOLUMETRIC WATER CONTENT
130.      C     TIME      TIME OF A DAY
131.      C     TOTSTR    TOTAL SOIL MOISTURE CAPACITY IN THE TOP SOIL LAYER (CM).
132.      C     TPET      DAILY POTENTIAL EVAPOTRANSPIRATION (CM/DAY)
133.      C     YMEAN(NL) AVERAGE OF COMMON LOG OF SATURATED HYDRAULIC CONDUCTIVITY
134.      C     YSD(NL)   STANDARD DEVIATION OF LOG OF SATURATED CONDUCTIVITY
135.      C     W(I,J)    COEFFICIENT OF TRIDIAGONAL MATRIX
136.      C
137.      C*****************************************************************************
138.      C
139.      C     LIST OF SUBPROGRAMS
140.      C
141.      C*****************************************************************************
142.      C
143.      C     BALANS    COMPUTE THE DIFFERENCE IN WATER STORAGE BETWEEN THAT
144.      C               FROM INITIAL STORAGE AND BOUNDARY FLUXES AND THAT FROM
145.      C               PRESENT WATER CONTENTS IN THE SOIL PROFILE.
146.      C     CONDUC    COMPUTE HYDRAULIC CONDUCTIVITY AND SPECIFIC WATER
147.      C               CAPACITY
148.      C     ET        COMPUTE ACTUAL SOIL EVAPORATION AND PLANT TRANSPIRATION
149.      C               FROM THE PET.
150.      C     FLOW      SOLVE FLOW EQUATION USING IMPLICIT FINITE DIFFERENCE METHOD
151.      C     GGNML     IMSL LIBRARY SUBROUTINE WHICH GENERATES NORMALLY
152.      C               DISTRIBUTED RANDOM NUMBERS WITH MEAN ZERO AND S.D. 1.0
153.      C     HYSTER    UPDATE THE WETTING HISTORY
154.      C     INFILT    COMPUTE INFILTRATION RATE
155.      C     INTCEP    COMPUTE INITIAL INTERCEPTION OF RAINFALL
156.      C     NEIBOR    COMPUTE STOCHASTIC SATURATED HYDRAULIC CONDUCTIVITY VALUES
157.      C               USING FIRST ORDER NEAREST NEIGHBOR STOCHASTIC MODEL
158.      C     PANEVP    COMPUTE HOURLY DISTRIBUTED POTENTIAL EVAPOTRANSPIRATION
159.      C               RATES FROM THE DAILY PAN EVAPORATION INPUT DATA
160.      C     PLANT     COMPUTES PLANT ROOT DENSITY DISTRIBUTION AND CROP
161.      C               LEAF AREA INDEX.
162.      C     PRECIP    COMPUTE THE AVERAGE RAINFALL INTENSITY AND AMOUNT
163.      C               DURING EACH TIME STEP IN RAINY DAYS
164.      C     RETENT    COMPUTE WATER CONTENT(THETA) BY MUALEM'S MODEL
165.      C     TRIDIA    SOLVE TRIDIAGONAL MATRIX PROBLEMS
166.      C     WTABLE    COMPUTE WATER TABLE DEPTH AT A TIME
167.      C
168.      C*****************************************************************************
169.      C
170.            IMPLICIT REAL*8 (A-H,O-Z)
171.            REAL*8 K
172.            REAL*4 R(30)
173.            COMMON/NUMB/ISUBNO(5),N,NL
174.            COMMON/DEL/DELT,DELZ
175.            COMMON/NEIBO/YMEAN(5),YSD(5),RHO1,RHO2,ALPA,DSEED
176.            COMMON/PREC1/TSTART(5,6),TEND(5,6),AMOUNT(5),LENGTH(5)
177.            COMMON/INFIL/COND,DEPRES,DEPMAX,DELF,RATE,TOTSTR,SRKE,SMASH,
178.           ;             ASOIL,PSOIL,SDELF,TOLER,CE1,CE2
179.            COMMON/WATER/IMIS(25),ISCAN(25),PSI(25),PSIB(25),THETA(25),
180.           ;     THETA1(25),THETAM(25),THETMB(25),THETMI(25),THETAB(25),PBR(5)
```

```
      COMMON/BALAN/STORE1,TFLUX1,TFLUXN,STORE1,STORE2,PERCT
      COMMON/CONDU/K(20),SKSAT(25),THETAR(5),THETAS(5)
      COMMON/VAN/ALPAD,ALPAW,ENORY,FNWET
      COMMON/FLUX/FLUX1,FLUXN,DTDZ,DTDZS,DZDZ,PSINR,CONNR,FLUXNP
      DIMENSION PET(15,120),IRAIN(20),PAN(20),F(25),SS(5),SUBL(5),
     1  TITLE(20),INISO(25),ISCANO(25),PSIO(25),THETAO(25),THTAPO(25),
     1  DELP(15,120),DELPO(15,120),RE(20),ROOT(10)
C
C     READ AND WRITE TITLE, STEP SIZE, DOMAIN LENGTH, ETC
C
      READ(5,104) TITLE
      READ(5,100) N,NL,MC
      READ(5,101) (SUBL(I), I=1,NL)
      READ(5,102) (POR(I),SS(I),  I=1,NL)
      READ(5,102) (VMEAN(I), VSD(I), I=1,NL)
      READ(5,101) DELZ, DELT
      READ(5,102) (THETAR(I), THETAS(I), I=1,NL)
      READ(5,100) IDAYB,IHOURB, IDAYE, IHOURE
      WRITE(6,505) TITLE
      WRITE(6,500) MC,N,NL, DELZ, DELT,IDAYB,IHOURB,IDAYE, IHOURE
      DO 10 I=1,NL
      ISUBNO(I) = SUBL(I)/DELZ
      WRITE(6,501) I,SUBL(I), VMEAN(I), VSD(I), POR(I) ,SS(I)
   10 CONTINUE
C
C     INCLUDE THE FIRST SOIL LAYER INTERFACE NODAL POINT IN THE FIRST
C     SUBLAYER
C
      ISUBNO(1) = ISUBNO(1) + 1
C
  100 FORMAT(5I5)
  101 FORMAT(5F10.3)
  102 FORMAT(5F10.7)
  104 FORMAT(20A4)
  500 FORMAT(//1HO,'NUMBER OF MONTE CARLO RUNS:',I9,//
     1,1HO,'LIST OF PHYSICAL PARAMETERS:',//
     1,1HO,'NUMBER OF VERTICAL NODE POINTS:',I5,/
     1,1HO,'NUMBER OF SOIL LAYERS:          ',I5,/
     1,1HO,'SIZE OF SPACE GRID (CM):        ',F5.1,/
     1,1HO,'SIZE OF TIME STEP  (HR):        ',F5.1,/
     1,1HO,'BEGINNING OF SIMULATION:   ',I3,' JULIAN DAY',I5,' HOURS',/
     1,1HO,'ENDING OF SIMULATION:      ',I3,' JULIAN DAY',I5,' HOURS',///)
  501 FORMAT(1HO,'THICKNESS OF SUBLAYER #',I2,' (CM): ',19X,F6.1,/
     1,' ','MEAN OF LOG SATURATED HYDRAULIC CONDUCTIVITY:      ',F7.2,/
     1,1HO,'STANDARD DEV. OF LOG SAT. HYDRAULIC CONDUCTIVITY :',F7.2,/
     1,1HO,'POROSITY:',41X,F7.2,/1HO,'SPECIFIC STORAGE:',33X,F7.6,///)
  505  FORMAT(1H1,20A4)
C
C     READ AND WRITE INITIAL CONDITION
C     INITIAL CONDITION OF WATER CONTENTS, THETAO AND THTABO, SHOULD
C     HAVE VALUES BETWEEN THE TWO MAIN RETENTION CURVES.
C
      READ(5,108) (INISO(I), I=1,N)
      READ(5,109) (ISCANO(I), I=1,N)
      READ(5,111) (PSIO(I), I=1,N)
      READ(5,112) (THETAO(I), I=1,N)
      READ(5,112) (THTABO(I), I=1,N)
      WRITE(6,503) (PSIO(I), I=1,N)
C
C     READ DAILY EVAPORATION DATA AND PRECIPITATION INDEX
```

```
241.      C
242.            LENGS= IDAYE-IDAYB+1
243.           READ(5,109) (IRAIN(I), I=1,LENGS)
244.           READ(5,103) (PAN(I), I=1,LENGS)
245.       103 FORMAT(16F5.2)
246.       109 FORMAT(2012)
247.       111 FORMAT(10F8.3/7F8.3)
248.       112 FORMAT(10F8.4/7F8.4)
249.       503 FORMAT('1','INITIAL CONDITION:',1X,10F10.4/20X,10F10.4)
250.      C
251.      C     COMPUTE POTENTIAL EVAPOTRANSPIRATION RATE DURING EACH TIME STEP
252.      C     FOR ALL THE SIMULATION PERIOD FROM PAN INPUT DATA
253.      C
254.           CALL PANEVP(PAN,LENGS,PET,DELT,IHOURB,IHOURE)
255.      C
256.      C     COMPUTE PLANT ROOT DENSITY DISTRIBUTION AND CROP LEAF AREA INDEX.
257.      C
258.           CALL PLANT(DELZ,NRZ,CLAI,ROOT)
259.      C
260.      C     COMPUTE RAINFALL AMOUNT DURING EACH TIME STEP FOR ALL THE
261.      C     SIMULATION PERIOD
262.      C
263.           CALL PRECIP(DELPO,DELT,IRAIN,LENGS,IHOURB,IHOURE)
264.      C
265.      C*****************************************************************************
266.      C
267.      C     INPUT PARAMETERS
268.      C
269.      C*****************************************************************************
270.      C
271.           DTDZ = DELT/DELZ
272.           DTDZS = DELT/DELZ/DELZ
273.           DZDZ = DELZ*DELZ
274.      C
275.      C     FOR SUBROUTINE NEIBOR
276.      C
277.           ALPA = 0.36D0
278.           RHO1 = 0.35D0
279.           RHO2 = 0.11D0
280.      C
281.      C     FOR SUBROUTINES MYSTER, RETENT AND CONDUC
282.      C
283.           ALPAD=0.00026476
284.           ALPAW=0.02514586
285.           ENDRY=1.36717125
286.           ENWET=1.41024034
287.      C
288.      C     FOR SUBROUTINES INFILT AND FLOW
289.      C
290.           AM=-0.12D0
291.           PM= 0.20D0
292.           ASOILM=36.0D0
293.           PSOILM=1.48D0
294.           TOTSTR=25.0D0
295.           TOLER=0.001D0
296.           FCS=28.96
297.           FCP=28.96
298.           CE1=0.125D0
299.           CE2=1.25D0
300.           DEPMAX=1.0D0
```

```
      PSIMIN=-15000.
      FLUXI =+0.0010
      FLUXNR=0.
C
C     FOR SUBROUTINE BALANS
C
      NN1=N-1
      STORE1 = (THETA0(1) + THETA0(N)) *0.500 *DEL2
        DO 20 J=2,NN1
          STORE1 = STORE1 + THETA0(J) *DEL2
 20     CONTINUE
C
C     GENERATE FIRST STRINGS OF RANDOM NUMBERS AND DISCARD THEM
C
      DSEED = 123457.00
      NR=30
      DO 30 J=1,6
      CALL GGNML(DSEED,NR,R)
 30   CONTINUE
C
C*************************************************************************
C
C     MAIN DO LOOP COUNTING MONTE CARLO RUNS
C
      MCOUNT =1
      WHILE(MCOUNT.LE.MC) DO
C
C*************************************************************************
C
C     COMPUTE STOCHASTIC SATURATED HYDRAULIC CONDUCTIVITY FOR
C     EACH BLOCK IN EACH SOIL LAYER USING NEAREST NEIGHBOR MODEL
C
      CALL NEIBOR(SKSAT,DEPRES,PSIMIN)
      WRITE(6,606) (SKSAT(I), I=1,N)
 606  FORMAT(' ','STOKASTIC KSAT(I)= ',10F10.5/20X,10F10.5/)
C
C     SET INITIAL VALUES
C
      TFLUX1 =0.00
      TFLUXN =0.00
      DEPRES=0.00
      TABLE=82.000
      ABST=0.
      COND =0.58
      SDELF=0.00
      SRKE=0.00
      DO 37 I =1,N
        IHIS(I) =IHIS0(I)
        ISCAN(I)=ISCAN0(I)
        PSI (I) =PSI0(I)
        THETA(I) =THETA0(I)
        THETAM(I)=THETA0(I)
        THETAB(I) =THTAB0(I)
 37   CONTINUE
        PSINB=PSI(N)
C
C*************************************************************************
C
C     COMPUTE INITIAL VALUES OF HYDRAULIC CONDUCTIVITY AND
C     SPECIFIC WATER CAPACITY
```

```
C
      CALL CONDUC(PSI,THETA,SS,F)
        CONNB=K(N)
C
C**********************************************************************
C
C     DO LOOP FOR THE LENGTH OF THE DAYS OF THE SIMULATION PERIOD
C
C**********************************************************************
C
        N1=0
       KOUNT =1
       WHILE (KOUNT.LE.LENGS) DO
        IF(IRAIN(KOUNT).GT. 0) N1=N1+1
C
C     DETERMINE NUMBER OF TIME STEPS AND BEGINNING TIME IN A DAY
C
       IF(KOUNT.NE.1 .AND. KOUNT.NE.LENGS) THEN
            ITSTEP= (24/DELT+0.01)
            TIME=0.00
       ELSE
        IF(KOUNT.EQ.1) THEN
            ITSTEP= ((24-IHOURB)/DELT+0.01)
            TIME=OFLOAT(IHOURB)
        ELSE
            ITSTEP= (IHOURE/DELT+0.01)
            TIME=0.00
        END IF
       END IF
       SABST=0.
C**********************************************************************
C
C     COMPUTATION FOR EACH TIME STEP IN A DAY
C
C**********************************************************************
C
       DO 40 J=1,ITSTEP
        TIME=TIME+DELT
C       WRITE(6,6) 'DAY= ',IDAYB+KOUNT-1,'TIME= ',TIME
        RATE=0.00
       IF(IRAIN(KOUNT).EQ.0.) THEN
        DELP(KOUNT,J)=DELPO(KOUNT,J)
        GO TO 30
       END IF
C
C     COMPUTE INTERCEPTION IF NECESSARY BY CALLING INTCEP.
C
       IF(DELPO(KOUNT,J).GT.0. .AND. SABST.LT.0.1) THEN
        CALL INTCEP(DELPO(KOUNT,J),DELP(KOUNT,J),ABST,SABST)
       ELSE
        DELP(KOUNT,J)=DELPO(KOUNT,J)
       END IF
C
C     UPDATE INFILTRATION PARAMETERS FROM THE AMC AT TOP 10 CM SOIL
C     AND CROP LEAF AREA INDEX JUST BEFORE THE FIRST RAINFALL IN A DAY.
C
       IF(TIME.LE.TSTART(N1,1).AND.(TIME+DELT).GT.TSTART(N1,1)) THEN
        AMC=(THETA(N)+ 2.*THETA(N-1))/3.* 100.
        ASOIL=ASOILM*DEXP(AM*(AMC-FCS))
        IF(ASOIL.GT.ASOILM) ASOIL=ASOILM
```

```
421.            IF(CLAI.GT.3.0) CLAI=3.0
422.            ASOIL=ASOIL +0.5*CLAI
423.            PSOIL=PSOILN*(AMC/FCP)**PM
424.      C     COMPUTE AVAILABLE PORE SPACE IN TOP 60 CM OF SOIL (CM).
425.            SMASM= TOTSTR-(THETA(N)/2.+THETA(N-1)+THETA(N-2)+THETA(N-3)
426.           $          +THETA(N-4)+THETA(N-5)+THETA(N-6)/2.)*DELZ
427.            IF(SMASM.LT.0.) SMASM=0.
428.           END IF
429.      C
430.       30   IF(DELP(KOUNT,J).GT.0.0001 .OR. DEPRES.GT.0.0001) THEN
431.             CALL INFILT(DELP(KOUNT,J),DELT)
432.      C      WRITE(6,*)'      INFILT RATE=',RATE
433.           END IF
434.      C
435.      C     COMPUTE ACTUAL SOIL EVAPOLATION AND PLANT TRANSPIRATION FROM
436.      C     THE PET.
437.      C
438.            CALL ET(THETA,PET(KOUNT,J),RE,TARE,AEVAP,DEPRES,ABST,CLA),*001,
439.           $         NRZ,N)
440.            FLUXN=AEVAP-RATE
441.      C
442.            CALL FLOW(SS,F,DEPRES,DEPMAX,PSIMIN,RE)
443.      C
444.      C     UPDATE TOTAL BOUNDARY FLUXES
445.      C
446.            TFLUXI = TFLUXI + FLUXI*DELT
447.            TFLUXN = TFLUXN + (FLUXN+TARE)*DELT
448.      C     WRITE(6,*)'FLUXN=',FLUXN,' TFLUXN=',TFLUXN
449.      C
450.      C     COMPUTE WATER TABLE ELEVATION AND WATER BALANCE AT SELECTED
451.      C     TIME STEPS
452.      C
453.            IF(J.EQ.30. OR.J.EQ.60 .OR. J.EQ.90. OR. J.EQ.120) THEN
454.             CALL WTABLE(N,DELZ,PSI,TABLE)
455.             CALL BALANS(N, DELZ, THETA)
456.             WRITE(6,610) IDAY0+KOUNT-1, TIME, TABLE
457.             WRITE(6,620) STORE1, STORE2, PERCT
458.             WRITE(6,630) (THETA(I), I=1,N)
459.             WRITE(6,640) (PSI(I), I=1,N)
460.            END IF
461.       40   CONTINUE
462.      C
463.       610  FORMAT(/' ','JULIAN DAY =',I4,10X, 'TIME =', F6.2, 10X,
464.           $      'WATER TABLE =', F9.4, 'CM')
465.       620   FORMAT(' ','STORAGE FROM BOUNDARY FLUXES=',F7.2,'    STORAGE FROM
466.           $ WATER CONTENT=', F7.2,'       DIFFERENCE IN % =', F8.2)
467.       630  FORMAT(/' ','THETA(L)=',17F7.4)
468.       640  FORMAT(/' ','PSI(L)= ',10F11.4/9X,7F11.4)
469.      C
470.      C     END OF COMPUTATION FOR A DAY
471.            KOUNT = KOUNT + 1
472.            END WHILE
473.      C
474.      C     END OF A MONTE CARLO RUN
475.            MCOUNT = MCOUNT + 1
476.            END WHILE
477.            STOP
478.            END
479.      C
480.      C*************************************************************************
```

```
C*****************************************************************************
C
      SUBROUTINE NEIBOR(SKSAT,DEPRES,PSIMIN)
C
C     THIS SUBROUTINE COMPUTES THE STOCHASTIC SATURATED HYDRAULIC
C     CONDUCTIVITY DISTRIBUTION USING THE FIRST ORDER NEAREST NEIGHBOR
C     STOCHASTIC MODEL.  OUTPUTS ARE VALUES OF SATURATED HYDRAULIC
C     CONDUCTIVITIES FOR THE BLOCKS IN EACH SOIL LAYER, SKSAT
C
C*****************************************************************************
C
C     VARIABLE DEFINITION (LOCAL)
C
C     B          RIGHT HAND SIDE VALUES OF TRIDIAGONAL MATRIX
C     C          SOLUTION OF NEAREST NEIGHBOR MODEL
C     ETA        MULTIPLIER IN THE NEAREST-NEIGHBOR MODEL
C     R          GENERATED NORMAL PSEUDORANDOM NUMBERS
C     Y          COMMON LOGARITHMIC SATURATED HYDRAULIC CONDUCTIVITY
C     W(I,J)     COEFFICIENTS OF TRIDIAGONAL MATRIX
C     NNN        INDEX USED IN SUBROUTINE TRIDIA
C
C*****************************************************************************
C
      IMPLICIT REAL*8 (A-H,O-Z)
      REAL*4 R(30)
      COMMON/NUMB/ISUBNO(8),N,NL
      COMMON/NEIBO/YMEAN(5),YSD(5),RHO1,RHO2,ALPA,DSEED
      DIMENSION B(25),C(25),Y(25),W(25,3),SKSAT(25)
C
      NNN=1
      IBEGIN=1
      IEND=ISUBNO(1)
      DO 50 K=1,NL
C
C     SET UP TRIDIAGONAL MATRIX COEFFICIENTS
C
      NM1 =ISUBNO(K)-1
      W(1,2)=1.D0
      W(1,3)=-ALPA
      W(ISUBNO(K),1)= -ALPA
      W(ISUBNO(K),2)=1.D0
      DO 20 J=2,NM1
        W(J,1)=-ALPA/2.D0
        W(J,2)=1.D0
        W(J,3)= W(J,1)
 20   CONTINUE
C
C     GENERATE NORMALLY DISTRIBUTED RANDOM NUMBERS AND SET UP RHS
C
      NR=ISUBNO(K)
      CALL GGNML(DSEED,NR,R)
      ETA=YSD(K)*DSQRT(ALPA*ALPA/2.D0+ 1.D0 -2.D0*ALPA*RHO1
     ;    + ALPA*ALPA*RHO2/2.D0)
      DO 30 J=1,NR
        B(J)=ETA*R(J)
 30   CONTINUE
C
C     SOLVE TRIDIAGONAL MATRIX BY CALLING TRIDIA
C
      CALL TRIDIA(NR,W,B,BBN,NNN,DEPRES,PSIMIN)
```

```
541.              DO 35 J=1,NR
542.                JJ=IBEGIN+J-1
543.                C(JJ)=B(J)
544.       35     CONTINUE
545.      C
546.      C     CALCULATE THE STOCHASTIC SATURATED HYDRAULIC CONDUCTIVITIES
547.      C
548.            DO 40 KK=IBEGIN,IEND
549.                  Y(KK)= YMEAN(K) + C(KK)
550.                  SKSAT(KK) = DEXP(2.302600*Y(KK))
551.       40   CONTINUE
552.            IF (K.EQ.NL) GO TO 50
553.            IBEGIN=IEND+1
554.            IEND= IEND+ISUBNO(K+1)
555.       50   CONTINUE
556.            RETURN
557.            END
558.      C
559.      C*****************************************************************************
560.      C
561.            SUBROUTINE PLANT(DELZ,NRZ,CLAI,ROOT)
562.      C
563.      C     THIS SUBROUTINE DETERMINES THE ROOT DENSITY DISTRIBUTION USING
564.      C     EQUATION BY HOLZ AND BENSON (1970). AND CROP LEAF AREA INDEX.
565.      C     CONSTANT CLAI AND TOTAL ROOT DEPTH OF 3.0 AND 60 CM WERE USED.
566.      C     OUTPUTS ARE NRZ AND ROOT(I).
567.      C
568.      C*****************************************************************************
569.      C
570.            IMPLICIT REAL*8 (A-H,O-Z)
571.            DIMENSION ROOT(10),RDOT1(10)
572.      C     USE FUNCTION DEFINITION FOR ACCUMULATED ROOT DENSITY.
573.            DO(Z,DEPTH)=1.00Z/DEPTH -0.00Z*Z/DEPTH/DEPTH
574.            CLAI =3.0
575.            NRZ=7
576.            DEPTH=(NRZ-0.5)*DELZ
577.            DO 10 I=1,NRZ
578.              Z=(I-0.5)*DELZ
579.              ROOT1(I)=DO(Z,DEPTH)
580.              IF(I.GE.2) ROOT(I)=ROOT1(I)-ROOT1(I-1)
581.              IF(I.EQ.1) ROOT(I)=ROOT1(I)
582.       10   CONTINUE
583.            RETURN
584.            END
585.      C
586.      C*****************************************************************************
587.      C
588.            SUBROUTINE PANEVP(PAN,LENGS,PET,DELT,IHOURB,IHOURE)
589.      C
590.      C     THIS SUBROUTINE CALCULATE THE POTENTIAL EVAPOTRANSPIRATION FROM
591.      C     PAN EVAPORATION DATA USING SAXTON'S MODEL (1974). AND DISTRIBUTE
592.      C     THE DAILY PET OVER SIX FOUR-HOUR PERIODS.
593.      C     OUTPUT IS PET AMOUNT IN EACH TIME STEP (CM).
594.      C
595.      C*****************************************************************************
596.      C
597.            IMPLICIT REAL*8 (A-H,O-Z)
598.            DIMENSION PET(15,120),PAN(20)
599.      C
600.            DO 10 I=1,LENGS
```

```
601.              IF(I.NE.1 .AND. I.NE.LENGS) THEN
602.                ITSTEP = (24/DELT + 0.01)
603.              ELSE
604.                IF(I.EQ.1) ITSTEP = ((24-IHOURB)/DELT + 0.01)
605.                IF(I.EQ.LENGS) ITSTEP = (IHOURF/DELT + 0.01)
606.              END IF
607.            TPET=0.025D0+ 0.83*PAN(I)
608.            DPET=TPET*DELT/4.0
609.            DO 20 J=1,ITSTEP
610.              K =J
611.              IF(I.EQ.1) K = (IHOURB/DELT + 0.01) + J
612.              IF(K.LE.20)                  PET(I,J) =DPET*2.4D-2
613.              IF(K.GT.20 .AND. K.LE.40) PET(I,J) =DPET*4.8D-2
614.              IF(K.GT.40 .AND. K.LE.60) PET(I,J) =DPET*2.9D-1
615.              IF(K.GT.60 .AND. K.LE.80) PET(I,J) =DPET*3.9D-1
616.              IF(K.GT.80 .AND.K.LE.100) PET(I,J) =DPET*1.9D-1
617.              IF(K.GT.100)                 PET(I,J) =DPET*4.6D-2
618.       20   CONTINUE
619.       10   CONTINUE
620.            RETURN
621.            END
622.       C
623.       C*****************************************************************************
624.       C
625.            SUBROUTINE PRECIP(DELPO,DELT,IRAIN,LENGS,IHOURB,IHOURE)
626.       C
627.       C     THIS SUBROUTINE READS DAILY RAINFALL DATA AND COMPUTES RAINFALL
628.       C     AMOUNT DURING EACH TIME STEP FOR THE SIMULATION PERIOD.
629.       C     INPUT IS FROM READING THE CARD AS DESCRIBED BELOW.
630.       C     OUTPUT IS DELPO(I,J).
631.       C
632.       C*****************************************************************************
633.       C
634.       C     VARIABLE DESCRIPTIONS (LOCAL)
635.       C
636.       C     TSTART     BEGINNING TIME OF EACH SUBPERIOD OF A RAINFALL DURING WHICH
637.       C                THE RAINFALL INTENSITY CAN BE ASSUMED CONSTANT
638.       C     TEND       ENDING TIME OF EACH SUBPERIOD OF A RAINFALL DURING WHICH
639.       C                THE RAINFALL INTENSITY CAN BE ASSUMED CONSTANT
640.       C     AMOUNT     RAINFALL AMOUNT DURING EACH SUBPENIOD OF THE RAINFALL EVENT
641.       C     LENGTH     NUMBER OF TIME STEPS IN (TEND-TSTART)
642.       C     M          NUMBER OF THE SUBPERIODS OF THE RAINFALL DURING A DAY
643.       C
644.       C*****************************************************************************
645.       C
646.            IMPLICIT REAL*8 (A-H,O-Z)
647.            COMMON/PREC1/TSTART(5,6),TEND(5,6),AMOUNT(6),LENGTH(6)
648.            DIMENSION DELPO(15,120), IRAIN(20)
649.       C
650.            M1 = 0
651.            DO 60 I=1,LENGS
652.              IF(I.NE.1. AND. I.NE.LENGS) THEN
653.                ITSTEP= (24/DELT + 0.01)
654.                TIME = 0.00
655.              ELSE
656.                IF(I .EQ.1) THEN
657.                  ITSTEP = ((24-IHOURB)/DELT + 0.01)
658.                  TIME = DFLOAT(IHOURB)
659.                ELSE
660.                  ITSTEP = (IHOURE/DELT + 0.01)
```

```
                TIME = 0.00
              END IF
            END IF
          IF(IRAIN(I).EQ.0) THEN
            DO 10 J=1,ITSTEP
 10       DELPO(I,J)=0.00
          ELSE
            N1 = N1 + 1
          READ(5,800) M,(TSTART(N1,I),TEND(N1,I),AMOUNT(I), I=1,M)
          DO 20 K=1,M
            IF(TEND(N1,K)-TSTART(N1,K) .LE.DELT) THEN
              LENGTH(K)=1
            ELSE
              LENGTH(K)= ((TEND(N1,K)-TSTART(N1,K))/DELT +0.4999)
            END IF
 20       CONTINUE
C     COMPUTE DELPO DURING EACH TIME STEP
          DO 50 J=1,ITSTEP
            TIME= TIME + DELT
            DELPO(I,J) = 0.00
          IF(TIME.LT.TSTART(N1,1)+DELT/2.OR.TIME.GE.TEND(N1,M)+DELT/2)GOTO50
           DO 100 K=1,M
            IF(TIME.GE.TSTART(N1,K)+DELT/2.AND.TIME.LT.TEND(N1,K)+DELT/2)
     1       DELPO(I,J)=AMOUNT(K)/LENGTH(K)
              IF(DELPO(I,J).NE.0) GO TO 50
 100       CONTINUE
  50       CONTINUE
          END IF
  60      CONTINUE
 800      FORMAT(I1,3(2F7.2, F7.3))
          RETURN
          END
C
C*************************************************************************
C
          SUBROUTINE INTCEP(DELPO,DELP,ABST,SABST)
C
C*************************************************************************
C
C     THIS SUBROUTINE COMPUTE THE AMOUNT OF INITIAL ABSTRACTION AT THE
C     BEGINNING OF A RAINFALL EVENT.  MAXIMUM VALUE OF SABST IS 0.10 CM.
C     OUTPUTS ARE ABST, SABST AND DELP(I,J).
C
C*************************************************************************
C
          IMPLICIT REAL*8 (A-H,O-Z)
              IF(SABST+DELPO.LE.0.10) THEN
                ABST =ABST+ DELPO
                SABST=SABST+DELPO
                DELP=0.
              ELSE
                DELP =DELPO-(0.10-SABST)
                ABST=ABST+(0.10-SABST)
                SABST=0.10
              END IF
          RETURN
          END
C
C*************************************************************************
C
```

```
      SUBROUTINE INFILT(DELP,DELT)
C
C     THIS SUBROUTINE COMPUTE AVERAGE INFILTRATION RATE FOR A TIME PERIOD.
C     MODIFIED HOLTAN'S EQUATION WITH BAILEY'S ITERATION METHOD IS USED.
C     OUTPUTS ARE RATE, DEPRES, SMASM,SDELP, AND SRKE.
C
C*****************************************************************************
C
C     VARIABLE DESCRIPTIONS (LOCAL)
C
C     F1          ACCUMULATED INFILTRATION AT THE BEGINNING OF A TIME STEP
C     F2          ACCUMULATED INFILTRATION AT THE END OF A TIME STEP.
C     FF2         VALUE OF FUNCTION F(F2) IN THE HOLTAN'S EQUATION.
C     FF2SD       VALUE OF FIRST DERIVATIVE OF F(F2) IN THE HOLTAN'S EQ
C     FF2SD       VALUE OF SECOND DERIVATIVE OF F(F2) IN THE HOLTAN'S EQ
C     RKE         RAINFALL KINETIC ENERGY DURING A TIME STEP.
C     RRATE       DIRECT RAINFALL INTENSITY (IN/HR).
C     REF         RAINFALL ENERGY REDUCTION FACTOR AFFECTING INFILTRATION
C
C*****************************************************************************
C
      IMPLICIT REAL*8(A-H,O-Z)
      COMMON/INFIL/COND,DEPRES,DEPMAX,DELF,RATE,TOTSTR,SRKE,SMASM,
     1             ASOIL,PSOIL,SDELP,TOLER,CE1,CE2
C
C     COMPUTE RAINFALL KINETIC ENERGY (RKE) AND IT'S REDUCTION FACTOR
C     ON INFILTRATION AND ADJUST ASOIL
C
      RRATE=DELP/DELT/2.54
      IF(RRATE.LE.0.) GO TO 10
        RKE=DELP*(0.06173+0.0221*DLOG10(RRATE))
        IF(RKE.LT.0. .OR. DEPRES.GT.1.) RKE=0.
        SRKE=SRKE+RKE
   10 IF(SRKE.GT.0.) THEN
        REF=CE1*SRKE**(-CE2)
        IF(REF.GT.1.0) REF=1.0
      ELSE
        REF=1.0
      END IF
      ASOIL=ASOIL*REF
      F1=TOTSTR-SMASM
C
C     COMPUTE F2
C
      IF(F1.GE.TOTSTR) THEN
        F2=F1+COND*DELT
      ELSE
        F2=F1
        IF(DELP.GT.0.) GO TO 20
        IF(DEPRES.LE.0.) GO TO 40
C
C     USE BAILEY'S ITERATION METHOD TO DETERMINE F2.
C
   20   FF1=F1/DELT+COND+ASOIL/2.*((TOTSTR-F1)/TOTSTR)**PSOIL
        AP2T=ASOIL/2.*PSOIL/TOTSTR
        APT=ASOIL*PSOIL*(PSOIL-1.)/(2.*TOTSTR*TOTSTR)
        DO 30 J=1,7
          SR=(TOTSTR-F2)/TOTSTR
          FF2=F2/DELT-ASOIL/2.*SR**PSOIL -FF1
          IF(DABS(FF2).LE.TOLER) GO TO 40
```

```
            FF2PD=1./DELT+AP2T*SR**(PSOIL-1.)
            FF2SD=-APT*SR**(PSOIL-2.)
            F2=F2 -FF2/(FF2PD-FF2*FF2SD/FF2PD/2.00)
              IF(F2.GE.TOTSTR) THEN
                F2=F1+COND*DELT
                GO TO 40
              END IF
   30     CONTINUE
            WRITE(6,*) 'ITERATION LIMIT EXCEEDED'
          END IF
C
C     DETERMINE ACTUAL INFILTRATION RATE DURING A TIME STEP CONSIDERING
C     SOIL WATER AVAILABILITY.
C
   40     DELF=F2-F1
          IF(DELF.GT.DELP+DEPRES) DELF=DELP+DEPRES
          DEPRES=DEPRES+DELP-DELF
          IF(DEPRES.GT.DEPMAX) DEPRES=DEPMAX
          RATE=DELF/DELT
          SMASM=SMASM-DELF
          IF(SMASM.LT.0.) SMASM=0.
          SDELF=SDELF+DELF
          RETURN
          END
C
C*************************************************************************
C
          SUBROUTINE ET(THETA,PET,RE,TARE,AEVAP,DEPRES,ABST,CLAI,ROOT,NRZ,N)
C
C*************************************************************************
C
C     THIS SUBROUTINE COMPUTES ACTUAL INTERCEPTION EVAPORATION, SOIL
C     EVAPORATION, AND PLANT TRANSPIRATION FROM THE PET FOLLOWING THE
C     SAXTON ET AL.(1974).
C     OUTPUTS ARE RE(I), AEVAP, TARE, AND UPDATED DEPRES AND ABST.
C
C*************************************************************************
C
C     VARIABLE DESCRIPTIONS (LOCAL)
C
C     ARE(N)      ACTUAL ROOT EXTRACTION FOR EACH LAYER (CM)
C     PRE(N)      POTENTIAL ROOT EXTRACTION FOR EACH SOIL LAYER (CM)
C     PETI        REMAINING PET AFTER EVAPORATING INTERCEPTION STORAGE(CM)
C     PEVAP       POTENTIAL SOIL EVAPORATION DURING A TIME STEP (CM).
C     PTRANS      POTENTIAL PLANT TRANSPIRATION DURING A TIME STER (CM).
C     AWCON       AVERAGE WATER CONTENT IN TOP 10 CM SOIL LAYER.
C     UNEVAP      UNUSED ENERGY IN SOIL EVAPORATION (CM).
C     RATIO       ACTUAL/POTENTIAL RATIO
C
C*************************************************************************
C
          IMPLICIT REAL*8 (A-H,O-Z)
          COMMON/DEL/DELT,DELZ
          DIMENSION THETA(25),RE(25),PRE(25),UNPRE(25),ARE(25),ROOT(10)
          TARE=0.
C
C     FIRST SUBTRACT EVAPORATION FROM INITIAL ABSTRACTION.  IF NO ENERGY
C     IS AVAILABLE AFTER THIS STAGE GO TO RETURN
C
          IF(PET .GT.ABST) GO TO 10
```

```
841.            ABST =ABST-PET
842.            AEVAP=0.
843.            DO 20 J=1,N
844.         20   RE(J)=0.
845.            GO TO 100
846.         10 PET1 =PET -ABST
847.            ABST =0.
848.       C
849.       C    NEXT DIVIDE ANY REMAINING ENERGY BETWEEN THE SOIL EVAPORATION AND
850.       C    PLANT TRANSPIRATION BY USING RITCHIE'S EQUATION (1972).
851.       C
852.            PEVAP = PET1*DEXP(-0.398*CLAI)
853.            PTRANS=PET1-PEVAP
854.       C
855.       C    NEXT SUBTRACT ENERGY TO EVAPORATE SURFACE DEPRESSION IF ANY
856.       C
857.            IF(PEVAP .GT.DEPRES) GO TO 30
858.              DEPRES =DEPRES -PEVAP
859.              AEVAP =0.
860.              GO TO 40
861.         30 PEVAP = PEVAP- DEPRES
862.            DEPRES =0.
863.       C
864.       C    CALCULATE ACTUAL SOIL EVAPORATION CONSIDERING SOIL MOISTURE CONTENT
865.       C
866.            AWCON=(THETA(N)+2.*THETA(N-1))/3.
867.            IF(AWCON.GT.0.25. AND. AWCON.LT. 0.4) THEN
868.              RATIO=0.67*AWCON -1.66
869.              AEVAP=PEVAP*RATIO
870.            ELSE
871.              IF(AWCON.LE. 0.25) AEVAP=0.
872.              IF(AWCON.GE. 0.40) AEVAP=PEVAP
873.            END IF
874.              UNEVAP =PEVAP-AEVAP
875.              AEVAP=AEVAP/DELT
876.       C
877.       C    TRANSFER UNUSED ENERGY IF ANY TO THE PLANT TRANSPIRATION
878.       C
879.            PTRANS =PTRANS+UNEVAP
880.         40 CONTINUE
881.       C
882.       C    FOR EACH SOIL LAYER DISTRIBUTE THE POTENTIAL TRANSPIRATION
883.       C    ACCORDING TO ROOT DENSITY AND THEN COMPUTE THE ACTUAL TRANSPIRATION
884.       C    CONSIDERING SOIL WATER AVAILABILITY.  TRANSFER UNUSED ENERGY TO
885.       C    THE NEXT LAYER.
886.       C
887.            DO 60 J=1,N
888.              K=N+1-J
889.              IF(J.GT.NRZ) THEN
890.                RE(K)=0.
891.              ELSE
892.                PRE(K)=PTRANS*ROOT(J)
893.              END IF
894.         60 CONTINUE
895.            DO 70 J=1,NRZ
896.              K=N+1-J
897.              IF(THETA(K).GT.0.25 .AND. THETA(K).LT.0.4) THEN
898.                RATIO= 4.266*THETA(K) -1.064
899.                ARE(K) =PRE(K)*RATIO
900.                RE(K)=ARE(K)/DELZ/DELT
```

```
              ELSE
                IF(THETA(K).GE.0.40) ARE(K)=PRE(K)
                IF(THETA(K).LE.0.25) ARE(K)=0.
                RE(K)=ARE(K)/DELZ/DELT
              END IF
C
C     TRANSFER UNUSED ENERGY TO THE NEXT SOIL LAYER
C
              IF(J.EQ.NRZ) GO TO 70
              UNPRE(K)= PRE(K) -ARE(K)
              PRE(K-1) =PRE(K-1) +UNPRE(K)
   70       CONTINUE
C     ADJUST FOR TOP NODE WHICH TAKES CARE OF ONLY DELZ/2
                RE(N)=RE(N)*2.
C
C     COMPUTE TOTAL TRANSPIRATION FOR THE TOTAL BOUNDARY FLUX COMPUTATION
C
              DO 80 J=1,NRZ
                K=N+1-J
   80         TARE=TARE+ARE(K)
              TARE=TARE/DELT
  100       RETURN
            END
C
C*************************************************************************
C
            SUBROUTINE HYSTER(THETAR,THETAS)
C
C     THIS SUBROUTINE UPDATES THE WETTING HISTORY AND COMPUTES WATER
C     CONTENT EVALUATED AT THE WETTING REVERSAL POINT (THETAI), AND
C     WATER CONTENT EVALUATED AT THE WETTING REVERSAL VALUE OF PSI
C     ON THE MAIN WETTING CURVE (THETAM).
C     OUTPUTS ARE THETAI, THETAM, ISCAN  AND IMIS.
C
C*************************************************************************
C
            IMPLICIT REAL*8(A-H,O-Z)
            COMMON/NUMB/ISUBNO(6),N,NL
            COMMON/WATER/IMIS(25),ISCAN(25),PSI(25),PSIB(25),THETA(25),
           :    THETAI(25),THETAM(25),THETMB(25),THETMI(25),THETAB(25),POR(6)
            COMMON/VAN/ALPAD,ALPAW,ENDRY,ENWET
            DIMENSION THETAR(6), THETAS(6)
C
            IBEGIN=1
            IEND=ISUBNO(1)
            DO 60 J=1,NL
            THERAN=THETAS(J)-THETAR(J)
C
            DO 50 L=IBEGIN,IEND
            IF(IMIS(L).EQ.2) GO TO 20
            IF(THETAB(L).LE.THETA(L)) GO TO 50
            IMIS(L) = 2
C
            IF(THETAB(L) .GE. THETAS(J)-0.001) THEN
              ISCAN(L)=1
            ELSE
              ISCAN(L)=ISCAN(L) +1
              ISCAN(L)=MIN0(ISCAN(L),3)
              THETAI(L)=THETAB(L)
            END IF
```

```
      GO TO 50
   20 IF(THETAB(L).GE.THETA(L)) GO TO 50
      IHIS(L)=1
C
      IF (THETAB(L) .LE.THETAR(J)+0.001) THEN
        ISCAN(L)=1
      ELSE
        ISCAN(L)=ISCAN(L)+1
        ISCAN(L)=MINO(ISCAN(L),3)
        THETA1(L)=THETAB(L)
        THETM1(L)=THETMB(L)
      END IF
   30 CONTINUE
      IF(J.EQ.NL) GO TO 60
      IBEGIN=IEND+1
      IEND=IEND+ISUBNO(J+1)
   40 CONTINUE
C         WRITE(6,100) (IHIS(I),I=1,N)
C         WRITE(6,100) (ISCAN(I),I=1,N)
C100      FORMAT(' ',10I5)
      RETURN
      END
C
C*************************************************************************
C
      SUBROUTINE RETENT(THETAR,THETAS)
C
C     THIS SUBROUTINE COMPUTE VOLUMETRIC WATER CONTENT FOR A GIVEN
C     PRESSURE HEAD USING THETA-PSI RELATIONSHIP.
C     EQUATIONS (3.29) TO (3.31) IN THE TEXT ARE USED.
C     OUTPUT ARE THETA(L) AND UPDATED THETAB(L) AND THETMB(L).
C
C*************************************************************************
C
      IMPLICIT REAL*8 (A-H,O-Z)
      COMMON/NUMB/ISUBNO(8),N,NL
      COMMON/WATER/IHIS(25),ISCAN(25),PSI(25),PSIB(25),THETA(25),
     ;     THETA1(25),THETAM(25),THETMO(25),THETM1(25),THETAB(25),POR(5)
      COMMON/VAN/ALPAD,ALPAW,ENORV,ENWET
      DIMENSION THETAR(5),THETAS(5)
C
      IBEGIN=1
      IEND=ISUBNO(1)
      DO 40 J=1,NL
      THERAN=THETAS(J)-THETAR(J)
      DO 30 L=IBEGIN,IEND
C
C     UPDATE THETAB AND THETMB
        THETAB(L)=THETA(L)
        THETMB(L)=THETAM(L)
        IF(PSI(L).GE.-0.5) GO TO 10
        XP=-PSI(L)
      THETAM(L)=THETAR(J)+THERAN/(1.+(ALPAW*XP)**ENWET)**
     ;          ((ENWET-1.)/ENWET)
      THETAD=THETAR(J)+THERAN /(1.+(ALPAD*XP)**ENORV)**
     ;          ((ENORV-1.)/ENORV)
      IF(IHIS(L).EQ.1) THEN
        IF(ISCAN(L).EQ.1) THEN
          THETA(L)=THETAM(L)
        ELSE
```

```
1021.                IF(ISCAN(L).EQ.2) THEN
1022.                  THETA(L)=THETAM(L)+(THETAS(J)-THETAM(L))*
1023.          &                (THETM)(L)-THETAR(J))/THERAN
1024.                ELSE
1025.                  THETA(L)=THETAM(L) +(THETAS(J)-THETAM(L))*
1026.          &                (THETA)(L)-THETM)(L))/(THETAS(J)-THETM)(L))
1027.                END IF
1028.              END IF
1029.            ELSE
1030.              IF(ISCAN(L).EQ.1) THEN
1031.                THETA(L)=THETAD
1032.              ELSE
1033.                THETA(L)=THETAM(L) +(THETAM(L)-THETAR(J))*
1034.          &               (THETA)(L)-THETAM(L))/THERAN
1035.              END IF
1036.            END IF
1037.            IF(THETA(L).GT.THETAD) THETA(L) = THETAD
1038.            IF(THETA(L).LT.THETAM(L)) THETA(L) = THETAM(L)
1039.            GO TO 30
1040.       10   THETA(L)=PCR(J)
1041.       30   CONTINUE
1042.            IF (J.EQ.NL) GO TO 40
1043.            IBEGIN=IEND+1
1044.            IEND=IEND+ISUBNO(J+1)
1045.       40   CONTINUE
1046.      C           WRITE(6,100) (THETA(L), L=1,N)
1047.      C100        FORMAT(' ',9THETA(L)=',17F6.4)
1048.            RETURN
1049.            END
1050.      C
1051.      C*************************************************************************
1052.      C
1053.            SUBROUTINE CONDUC(PSI,THETA,SS,F)
1054.      C
1055.      C     THIS SUBROUTINE COMPUTES BOTH HYDRAULIC CONDUCTIVITY AND SPECIFIC
1056.      C     WATER CAPACITY USING THE RELATIVE CONDUCTIVITY MODEL AND
1057.      C     RETENTION MODEL BY VAN GENUCHTEN
1058.      C     OUTPUTS ARE K(L) AND F(L)
1059.      C
1060.      C*************************************************************************
1061.      C
1062.      C     VARIABLE DESCRIPTION (LOCAL)
1063.      C
1064.      C     ALPA        PARAMETER IN VAN GENUCHTEN'S CONDUCTIVITY MODEL
1065.      C     EN          EXPONENTIAL PARAMETER IN CONDUCTIVITY MODEL
1066.      C     SDRY        RELATIVE SATURATION AT A GIVEN PSI ON MAIN DRYING CURVE
1067.      C     SWET        RELATIVE SATURATION AT A GIVEN PSI ON THE MAIN WETTING
1068.      C                 CURVE
1069.      C     THETAD      WATER CONTENT AT A GIVEN PSI ON THE MAIN DRYING CURVE
1070.      C     THETAM      WATER CONTENT AT A GIVEN PSI ON THE MAIN WETTING CURVE
1071.      C
1072.      C*************************************************************************
1073.      C
1074.            IMPLICIT REAL*8(A-H,O-Z)
1075.            REAL*8 K
1076.            COMMON/NUMO/ISUBNO(5),N,NL
1077.            COMMON/CONDU/K(25),SKSAT(25),THETAR(5),THETAS(5)
1078.            COMMON/VAN/ALPAD,ALPAW,ENDRY,ENWET
1079.            DIMENSION THETA(25),F(25),RELK(25),PSI(25),SS(5)
1080.      C
```

```
      COMMON/CONDU/K(26),SKSAT(26),THETAR(5),THETAS(5)
      COMMON/VAN/ALPAD,ALPAW,ENDRY,ENWET
      DIMENSION THETA(26),F(26),RELK(26),PSI(26),SS(5)
C
      IBEGIN=1
      IEND=ISUBNO(1)
      DO 10 J=1,NL
        THERAN=THETAS(J)-THETAR(J)
      DO 20 L=IBEGIN,IEND
      IF(PSI(L).GE.-0.5) GO TO 50
      XP=-PSI(L)
      SDRY=(1.+(ALPAD*XP)**ENDRY)**((ENDRY-1.)/ENDRY)
      SWET=(1.+(ALPAW*XP)**ENWET)**((ENWET-1.)/ENWET)
      THETAD=THETAR(J) +THERAN/SDRY
      THETAW=THETAR(J) + THERAN/SWET
      ALPA=(ALPAD*(THETA(L)-THETAW) *ALPAW*(THETAD-THETA(L)))/
     1       (THETAD-THETAW)
      EN=(ENDRY*(THETA(L)-THETAW) + ENWET*(THETAD-THETA(L)))/
     1     (THETAD-THETAW)
      EN=1. -1./EN
      SE= (THETA(L)-THETAR(J))/THERAN
      DENOM=1.+(ALPA*XP)**EN
      F(L)= ENGEM*THERAN*SE**(1.-SE**(1./EM))/XP
      RELK(L)=(1.-(ALPA*XP)**(EN-1.)*DENOM**(-EM))**2
     1         /DENOM**(EN/2.)
      K(L)=SKSAT(L)*RELK(L)
      GO TO 20
   50 F(L)=SS(J)
      K(L)=SKSAT(L)
   20 CONTINUE
      IF (J.EQ.NL) GO TO 10
        IBEGIN=IEND+1
        IEND=IEND+ISUBNO(J+1)
   10 CONTINUE
C          WRITE(6,100) (K(L),L=1,N)
C          WRITE(6,200) (F(L),L=1,N)
C100        FORMAT(' ',*CONDUCTIVITY ', 17F6.4)
C200        FORMAT(' ',*CAPACITY ', 17F7.6)
      RETURN
      END
C
C*************************************************************************
C
      SUBROUTINE FLOW(SS,F,DEPRES,DEPMAX,PSIBIN,RC)
C
C     THIS SUBROUTINE COMPUTES THE SOIL WATER PRESSURE HEAD IN THE
C     SATURATED-UNSATURATED ZONE BY SOLVING THE FINITE DIFFERENCE
C     EQUATION.  IN THIS SUBROUTINE DOUGLAS-JONES PREDICTOR-CORRECTOR
C     SCHEME IS USED.
C     OUTPUTS ARE PSI, PSIB, THATA THETAB AND ADJUSTED FLUXN.
C
C*************************************************************************
C
C     VARIABLE DESCRIPTIONS (LOCAL)
C
C     D(I)        RIGHT HAND SIDE VALUES OF TRIDIAGONAL MATRIX EQUATION
C     W(I,J)      COEFFICIENTS OF THE TRIDIAGONAL MATRIX
C     SBN         SOLUTION FOR PSI(N) ON SOIL SURFACE BEFORE CONSIDERING
C                 BOUNDARY CONSTRAINTS
C     PSINP1      PRESSURE HEAD AT IMAGINARY POINT N+1.
```

```
      IMPLICIT REAL*8 (A-H,O-Z)
      REAL*8 K
      COMMON/DEL/DELT,DELZ
      COMMON/NUMB/ISUBNO(5),N,NL
      COMMON/FLUX/FLUX1,FLUXN,DTDZ,DTDZS,DZDZ,PSINB,CONNB,FLUXNP
      COMMON/WATER/INIS(20),ISCAN(20),PSI(25),PSIB(25),THETA(25),
     1     THETA1(25),THETAM(25),THETMB(25),THETM1(25),THETAB(25),POR(5)
      COMMON/CONDU/K(25),SKSAT(20),THETAR(5),THETAS(5)
      DIMENSION SS(5),F(25),D(25),W(25,3),RE(25)
      NNN=2
      NM1=N-1
      FLUXN1=FLUXN
      FLUXN2=FLUXN
C
C     PREDICTOR STAGE
C     SET UP TRIDIAGONAL MATRIX
C
      W(1,2)= F(1) +K(1)*DTDZS
      W(1,3)= -K(1)*DTDZS
      D(1)= (K(1)-K(2))*FLUX1*DTDZ/K(1)/2. +F(1)*PSI(1)
     1      +K(1)*DTDZ *(FLUX1/K(1) +1.0) -RE(1)*DELT/2.
      IF(DEPRES .LE.0.00001) THEN
        W(N,1) = -K(N)*DTDZS
        W(N,2) = F(N) +K(N)*DTDZS
        D(N) = (K(N-1)-K(N)) *FLUXN*DTDZ/K(N)/2. +F(N)*PSI(N)
     1         -K(N)*DTDZ *(FLUXN/K(N)+1.0 ) -RE(N)*DELT/2.
      ELSE
        W(N,1) =0.
        W(N,2) =1.
        D(N) =DEPRES
      END IF
      DO 10 J=2,NM1
      W(J,1)=-K(J)*DTDZS
      W(J,2)=2.*(F(J) + K(J)*DTDZS)
      W(J,3)=W(J,1)
      D(J)=(K(J+1)-K(J-1))*(PSI(J+1)-PSI(J-1)+2.*DELZ)*DTDZS/4.00
     1     +2.*F(J)*PSI(J) -RE(J)*DELT
   10 CONTINUE
C
C     SOLVE THE TRIDIAGONAL MATRIX
      CALL TRIDIA(N,W,D,BN,NNN,DEPRES,PSIMIN)
C
C     UPDATE PRESSURE HEAD VALUES
C
        DO 30 I=1,N
                PSIB(I)=PSI(I)
                PSI(I) = D(I)
   30   CONTINUE
C
C     IF PSI(N) EXCEEDED CONSTRAINTS GIVEN, THEN
C     CALCULATE ACTUAL SURFACE FLUX
C
      IF(BN.NE.D(N)) THEN
        PSINP1=2.*PSI(N)-PSI(N-1) +DZDZ/K(N)*(2.*F(N)/DELT*(PSI(N)-
     :     PSIB(N))-(K(N)-K(N-1))*(PSIB(N)-PSIB(N-1)*DELZ)/DZDZ+RE(N))
        FLUXN1 = -K(N)* ((PSINP1-PSI(N-1))/DELZ/2. +1.)
        IF(DABS(FLUXN1) .GT. DABS(FLUXN)) FLUXN1=FLUXN
      END IF
C
C     COMPUTE K AND F FOR THE TIME STEP N + 1/2
```

```
C     FROM THE PRESSURE HEAD SOLUTION AT THE TIME STEP N + 1/2
C
C        WRITE(6,200) (PSI(L), L=1,N)
         CALL HYSTER(THETAR,THETAS)
         CALL RETENT(THETAR,THETAS)
         CALL CONDUC(PS),THETA,SS,F)
C
C     END OF THE PREDICTOR STAGE
C
C*****************************************************************************
C
C     BEGIN THE CORRECTOR STAGE
C     COMPUTE THE PRESSURE HEAD AT TIME STEP N+1 USING K AND F OF N+1/2
C
          W(1,2)= F(1) *K(1)*DTDZS
          W(1,3)= -K(1)*DTDZS
          D(1)= (K(1)-K(2))*FLUX1*DTDZ/K(1) *K(1)*DTDZS*(PSIB(2)
     1       -PSIB(1) *FLUX1*DELZ/K(1) *DELZ) *F(1)*PSIB(1)
     1       *K(1)*DTDZ*(FLUX1/K(1) *1.0) -RE(1)*DELT
          IF(DEPRES .LE.0.0000) THEN
            W(N,1) = -K(N)*DTDZS
            W(N,2) = F(N) *K(N)*DTDZS
            D(N) = (K(N-1)-K(N))*FLUXN*DTDZ/K(N) *K(N)*DTDZS*(PSIB(N-1)
     1          -PSIB(N)-FLUXN*DELZ/COND -DELZ) *F(N)*PSIB(N)
     1          -K(N)*DTDZ*(FLUXN/K(N) *1.0) -RE(N)*DELT
          ELSE
            W(N,1) =0.
            W(N,2) =1.
            D(N) =DEPRES
          END IF
          DO 40 J=2,NM1
          W(J,1)= -K(J)*DTDZS
          W(J,2)= 2.0 (F(J) * K(J)*DTDZS)
          W(J,3)=W(J,1)
          D(J)=(K(J+1)-K(J-1)) *(PSI(J+1)-PSI(J-1)+2.*DELZ)*DTDZS/2.00
     1       *K(J)*DTDZS *(PSIB(J-1)-2.*PSIB(J)+PSIB(J+1))
     1       * 2.*F(J)* PSIB(J) -2.*RE(J)*DELT
  40      CONTINUE
C
C     SOLVE THE TRIDIAGONAL MATRIX
          CALL TRIDIA(N,W,D,BBN,NNM,DEPRES,PSIMIN)
C
C     UPDATE PRESSURE HEAD VALUES
          DO 50 I=1,N
            PSIB(I)=PSI(I)
            PSI(I)=D(I)
  50    CONTINUE
C        WRITE(6,200) (PSI(L), L=1,N)
C
C     IF PSI(N) EXCEEDED CONSTRAINTS GIVEN, THEN
C     CALCULATE ACTUAL SURFACE FLUX
C
          IF(BBN.NE.D(N)) THEN
            PSINP2= 2.*PSI(N)-PSI(N-1) +DZDZ/K(N) *(F(N)/DELT*(PSI(N)-
     1        PSINB)-(K(N)-K(N-1))*(PSIB(N)-PSIB(N-1)+DELZ)/DZDZ+RE(N))
            FLUXN2 = -K(N)* ((PSINP2 - PSI(N-1))/DELZ/2. +1.)
            IF(DABS(FLUXN2) .GT. DABS(FLUXN)) FLUXN2=FLUXN
          END IF
C
C     AVERAGE TOP BOUNDARY FLUX IN THIS TIME STEP.
```

```
      C
       FLUXN= (FLUXN1+FLUXN2)/2.
      C
      C     UPDATE PARAMETER VALUES FOR THE BOUNDARY NODE.
      C
       FLUXN0=FLUXN
       CONN0=K(N)
       PSINR=PSI(N)
      C
      C     COMPUTE K AND F FOR THE TIME STEP N+1
      C     FROM THE PRESSURE HEAD SOLUTION AT N+1
      C
       CALL HYSTER(THETAR,THETAS)
       CALL RETENT(THETAR,THETAS)
       CALL CONDUC(PSI,THETA,SS,F)
      C
      C200    FORMAT(' ','PSI(L)=',10F10.4/8X,7F10.4)
      C
      C     END OF THE CORRECTOR STAGE
       RETURN
       END
      C
      C**********************************************************************
      C
       SUBROUTINE TRIDIA(N,W,B,BBN,NNN,DEPRES,PSININ)
      C
      C     THIS SUBROUTINE SOLVES TRIDIAGONAL MATRIX WITHOUT PIVOTING.
      C     DIAGONALLY DOMINANT MATRICES ARE SAFE.
      C
      C**********************************************************************
      C
      C     VARIABLE DESCRIPTIONS (LOCAL)
      C
      C     BBN         SOLUTION FOR B(N) BEFORE CONSIDERING BOUNDARY CONSTRAINTS
      C     NNN         INDICATOR OF CALLING SUBROUTINE:  1: NEIBOR, 2: FLOW
      C
      C**********************************************************************
      C
       IMPLICIT REAL*8 (A-H,O-Z)
       DIMENSION W(25,3),B(25)
      C
      C     FF IS MULTIPLIER FOR THE FORWARD ELIMINATION STEP
       DO 10 J=2,N
         FF=W(J,1)/W(J-1,2)
         W(J,2)=W(J,2) - FF*W(J-1,3)
         W(J,1)=FF
  10   CONTINUE
      C
      C     FORWARD ELIMINATION STEP
      C     B:  ON INPUT, VECTOR OF RIGHT HAND SIDES
      C         ON EXIT, SOLUTION VECTOR
       DO 20 J=2,N
         B(J) = B(J) - W(J,1)*B(J-1)
  20   CONTINUE
      C
      C     BACK SUBSTITUTION LOOP
      C
       B(N) = B(N)/W(N,2)
       BBN = B(N)
       IF(NNN.EQ.1) GO TO 100
```

```
1321.      C
1322.      C     TEST PRESSURE HEAD CONSTRAINT AT THE SOIL SURFACE
1323.      C     AND ADJUST IF NECESSARY
1324.      C
1325.            IF(B(N).GT.DEPRES) B(N)= DEPRES
1326.            IF(B(N).LT.PSIMIN) B(N)=PSIMIN
1327.       100  DO 30 J=2,N
1328.              JB= N-J+1
1329.              B(JB) = (B(JB) - W(JB,3)*B(JB+1)) / W(JB,2)
1330.       30   CONTINUE
1331.            RETURN
1332.            END
1333.      C
1334.      C*************************************************************************
1335.      C
1336.            SUBROUTINE WTABLE(N, DELZ, PSI,TABLE)
1337.      C
1338.      C     THIS SUBROUTINE COMPUTES THE WATER TABLE DEPTH FROM THE GROUND
1339.      C     SURFACE USING PRESSURE HEAD VALUES BY LINEAR INTERPOLATION
1340.      C
1341.      C*************************************************************************
1342.      C
1343.            IMPLICIT REAL*8 (A-H,O-Z)
1344.            DIMENSION PSI(20)
1345.      C
1346.      C     FIND LOCATION OF CHANGE OF PRESSURE HEAD SIGN
1347.      C
1348.            NM1=N-1
1349.            DO 10 K=1,NM1
1350.               IF(PSI(K+1).GT.0. .AND. PSI(K).GT.0.) GO TO 10
1351.               IF(PSI(K+1).LE.0. .AND. PSI(K).GE.0.) GO TO 20
1352.       10   CONTINUE
1353.      C     ALL THE PRESSURE HEADS AT THE NODAL POINTS ARE GREATER THAN 0.
1354.      C     WATER TABLE IS ON THE TOP OF THE SOIL SURFACE
1355.            TABLE=0.00
1356.            GO TO 30
1357.       20   BOTTOM =(K * PSI(K+1)/(PSI(K)-PSI(K+1))) * DELZ
1358.            TABLE=DELZ*(N-1)-BOTTOM
1359.       30   RETURN
1360.            END
1361.      C
1362.      C*************************************************************************
1363.      C
1364.            SUBROUTINE BALANS(N, DELZ, THETA)
1365.      C
1366.      C     THIS SUBROUTINE COMPUTES THE DIFFERENCE OF CURRENT WATER STORAGE
1367.      C     IN THE DOMAIN BETWEEN, 1) FROM THE INITIAL WATER CONTENT AND
1368.      C     BOUNDARY FLUXES, AND 2) FROM THE CURRENT COMPUTED WATER CONTENTS
1369.      C     IN THE SOIL PROFILE USING SIMPSON'S INTEGRATION.
1370.      C
1371.      C*************************************************************************
1372.      C
1373.      C     VARIABLE DESCRIPTION (LOCAL)
1374.      C
1375.      C     STORE1     CURRENT WATER STORAGE FROM INITIAL WATER CONTENT AND
1376.      C                BOUNDARY FLUXES
1377.      C     STORE2     CURRENT WATER STORAGE FROM THE CALCULATED WATER CONTENTS
1378.      C                IN THE SOIL PROFILE
1379.      C     PERCT      PERCENT DIFFERENCE BETWEEN STORE1 AND STORE2
1380.      C
```

```
C*************************************************************************
C
      IMPLICIT REAL*8(A-H,O-Z)
      COMMON/BALAN/STORE1,TFLUX1,TFLUXN,STORE1,STORE2,PERCT
      DIMENSION THETA(20)
      STORE1 = STORE1 +TFLUX1 -TFLUXN
      STORE2 = 0.
      NM1=N-1
      DO 10 J=1,NM1,2
        STORE2 = STORE2 + THETA(J)+4.*THETA(J+1)+THETA(J+2)
 10   CONTINUE
      STORE2 =STORE2*DELZ/3.
      DIFF = STORE1 -STORE2
      PERCT=DABS(DIFF/STORE1*100.00)
      RETURN
      END
C
C*************************************************************************
```

APPENDIX B: DATA

Water table elevation

Date	Time	Water table elevation from soil surface (cm)
7-21-84	12:00	82.0
7-25-84	17:00	92.1
7-29-84	16:00	65.7
8:01-84	19:00	78.3

Soil water pressure head (cm)

Depth from soil surface (cm)	Date and time			
	7-21-84 12:00	7-25-84 17:00	7-29-84 15:30	8-01-84 19:00
150	68	63	82	73
130	48	42	58	51
110	28	21	33	35
90	8	5	15	12
70	-20	-21	-10	-7
50	-38	-42	-32	-26
30	-80	-104	-62	-52
10	-180	-156	-115	-105

Note: pressure head shows average of two replicates.

Rainfall

Date	Time		Amount (cm)
	From	To	
7-26-84	3:00	4:20	0.508
	4:20	4:40	1.016
	4:40	6:40	1.473
	total		2.997
7-27-84	13:30	13:40	0.914
	13:40	15:00	0.762
	15:00	16:40	0.152
	total		1.828
8-01-84	12:10	12:20	0.127
	total		0.127

Pan evaporation (cm)

Date	Pan evaporation	Date	Pan evaporation
7-21-84	0.94	7-27-84	0.56
7-22-84	0.97	7-28-84	0.43
7-23-84	0.76	7-29-84	0.64
7-24-84	0.79	7-30-84	0.69
7-25-84	0.53	7-31-84	0.58
7-26-84	0.61	8-01-84	0.58

Soil water retention data for a Webster silty clay loam (for main drying curve)

Pressure head (cm)	Water content
0	0.520*
-10	0.492
-30	0.476
-50	0.443*
-70	0.408
-100	0.380*
-150	0.343
-200	0.322*
-250	0.303
-300	0.294*
-350	0.286
-400	0.278*
-750	0.247
-1000	0.233*
-1500	0.218
-3000	0.195
-5000	0.187*
-10000	0.171
-15000	0.160*

*Laboratory data in this study.